PFC/RR-85-23 DOE/ET-51013-165
UC20G

Analytic Moment Method Calculations of the Drift Wave Spectrum

David R. Thayer* and Kim Molvig, M.I.T.

November, 1985

Plasma Fusion Center
Massachusetts Institute of Technology
Cambridge, Massachusetts 02139 USA

* present address: Institute for Fusion Studies. Austin, TX

Analytic Moment Method Calculations of the Drift Wave Spectrum

David R. Thayer and Kim Molvig, M. I. T.

ABSTRACT

A derivation and approximate solution of renormalized mode coupling equations describing the turbulent drift wave spectrum is presented. Arguments are given which indicate that a weak turbulence formulation of the spectrum equations fails for a system with negative dissipation. The inadequacy of the weak turbulence theory is circumvented by utilizing a renormalized formulation. An analytic moment method is developed to approximate the solution of the nonlinear spectrum integral equations. The solution method employs trial functions to reduce the integral equations to algebraic equations in basic parameters describing the spectrum. An approximate solution of the spectrum equations is first obtained for a model dissipation with known solution, and second for an electron dissipation in the NSA.

Analytic Moment Method Calculations of the Drift Wave Spectrum

I. Introduction

The low frequency drift wave induced turbulence in tokamaks is thought to be one of the dominant mechanisms driving the anomalous transport in tokamak devices. One of the fundamental ingredients of a complete turbulence transport theory is the difficult problem of developing a theory for the turbulence spectrum. The basic mechanism which we consider here that allows a steady state spectrum is nonlinear mode coupling. The negative electron drift wave dissipation drives the unstable modes, which then transfer energy to the stable modes through nonlinear mode coupling. Physically, the lowest order mode coupling process is a triplet interaction where two fluctuations beat together to produce a third fluctuation. Mathematically, this process is represented as a quadratic nonlinearity in the potential fluctuation equation.

In this article we treat two dimensional (k_x, k_y) stationary homogeneous electrostatic drift wave turbulence which obeys a potential fluctuation equation of the form,

$$\omega D_{\mathbf{k},\omega}\phi_{\mathbf{k},\omega} = \int d\mathbf{X} M_{\mathbf{k},\omega;\mathbf{k}',\omega';\mathbf{k}'',\omega''}\phi_{\mathbf{k}',\omega'}\phi_{\mathbf{k}'',\omega''}. \quad (1)$$

Here, $\phi_{\mathbf{k},\omega}$, is the frequency and wave number fourier transformed potential, and $d\mathbf{X} \equiv d\mathbf{k}'d\omega'd\mathbf{k}''d\omega''\delta(\mathbf{k}-\mathbf{k}'-\mathbf{k}'')\delta(\omega-\omega'-\omega'')$. It is convenient to isolate the linear dielectric term proportional to the frequency, ω, so that the dynamical mode coupling equation for the potential fluctuation is in general,

$$-i(\omega - \Omega_{\mathbf{k},\omega})\phi_{\mathbf{k},\omega} = \int d\mathbf{X} C_{\mathbf{k},\omega;\mathbf{k}',\omega';\mathbf{k}'',\omega''}\phi_{\mathbf{k}',\omega'}\phi_{\mathbf{k}'',\omega''}, \quad (2)$$

where $-i(\omega - \Omega_{\mathbf{k},\omega}) \equiv \omega D_{\mathbf{k},\omega}/[i\partial/\partial\omega(\omega D^R_{\mathbf{k},\omega})]$, the dielectric is $D = D^R + iD^I$, and the coupling coefficient is $C \equiv M/[i\partial/\partial\omega(\omega D^R_{\mathbf{k},\omega})]$. For the case of density gradient driven drift waves, with nonlinear polarization drift mode coupling dominant, the coupling coefficient is [1],

$$C_{\mathbf{k},\mathbf{k}',\mathbf{k}''} = \frac{1}{2}\Omega_i\frac{e}{T_e}\rho_s^4(k'_xk''_y - k'_yk''_x)(k''^2 - k'^2)/[1+(k\rho_s)^2], \quad (3)$$

and the complex frequency, $\Omega_{\mathbf{k},\omega}$, is

$$\Omega_{\mathbf{k},\omega} = \omega_{\mathbf{k}} + i\gamma_{\mathbf{k},\omega}, \omega_{\mathbf{k}} = \frac{\omega_e^*}{1+(k\rho_s)^2}, \gamma_{\mathbf{k},\omega} = \frac{-\omega D^I_{\mathbf{k},\omega}}{\frac{\partial}{\partial\omega}(\omega D^R_{\mathbf{k},\omega})}. \quad (4)$$

The diamagnetic drift frequency is $\omega_e^* \equiv \Omega_i(\rho_s/L_n)(\rho_s k_y)$, the ion gyrofrequency is $\Omega_i \equiv eB/m_i c$, the ion inertial scale length is $\rho_s \equiv c_s/\Omega_i$, and the ion sound speed is $c_s \equiv (T_e/m_i)^{1/2}$.

In Sec. II, two statistical closure schemes are analyzed in connection with the derivation of the spectrum equations. The mode coupling equation for the potential fluctuations, Eq. (2), is used as a starting point. Arguments are given which indicate that a weak turbulence formulation of the spectrum equations fails for a system with negative dissipation, such as the drift wave problem. The failure of the weak turbulence theory is shown to be directly related to the linear instability of the triplet correlation function. The nonlinear feedback effect from higher order correlations on the evolution of the triplet correlation is obtained by formulating a renormalized theory for the spectrum, using a scheme equivalent to the Direct Interaction Approximation, or DIA [2]. A set of renormalized nonlinear coupled integral equations for the wave number and frequency spectrum and nonlinear complex frequency are derived.

In Sec. III, an analytic moment method is developed to approximate the solution of the nonliner spectrum integral equations. The spectrum equations are reduced to wave number space by using either a Lorentzian or a Gaussian frequency trial function, and integrating out the frequency dependence. The wave number dependent nonlinear coupled integral equations which result are expressed in terms of a wave number spectrum, a nonlinear real frequency shift, and a nonlinear frequency width. It is noted that the Lorentzian frequency function is not applicable for frequency dependent growth rates, since the wave number reduced growth rate is a frequency averaged quantity, where the spectrum is a weighting function, and most moments of a Lorentzian do not exist. The wave number spectrum problem is solved to first order by using trial functions for the wave number spectrum and frequency width. The trial functions are dependent on physically relevant parameters, the total integrated amplitude, the spectral wave number width, and the spectral frequency width. Using the trial functions in the nonlinear integral equations, and taking select wave number moments, a corresponding set of nonlinear algebraic moment equations for the parameters are determined. The parameters are obtained by solving the nonlinear coupled algebraic equations, which is done in part numerically. Equations which determine the next order correction of the parameters are presented.

The selection of the wave number moments mentioned above can be formalized using a least squares method. The nonlinear integral equations are cast into a squared functional form which is then minimized with respect to the unknown spectrum parameters. The

"best" wave number moment algebraic equations are thus obtained in a least squares sense. Preliminary calculations using the least squares moment method which give little deviation from the results presented here have been done. A complete least squares calculation of the solution for the spectrum equations will be presented in a subsequent article.

The analytic moment method is tested by approximately solving the spectrum equations for a model dissipation proposed and numerically studied by Waltz [3]. This model wave number dependent growth rate exhibits damping for low and high wave numbers, with a narrow band of marginally positive growth rates between. The agreement between our approximate analytic moment method solution and the numerical solution of Waltz is excellent, both quantitatively and qualitatively. The average frequency width for this model problem is quite small, being much less than the average frequency. The analytic moment method is finally applied to the spectrum equations with a renormalized electron dissipation in the Normal Stochastic Approximation, or NSA [4]. The root mean square potential is found to be approximately, $e\phi_{rms}/T_e \approx 10^{-2}$, and the radial diffusion coefficient is found to be approximately, $\overline{D} \approx 1.8\Omega_i(\rho_s/L_n)\rho_s^2$. The results also indicate a large average spectral frequency width which is approximately equal to the average frequency. The saturation amplitude and large frequency widths are then in rough agreement with experimental observations in tokamaks. The two models indicate a large difference in frequency width solutions. In order to understand what causes the large frequency width for the electron dissipation in the NSA, we analyze the differences in dissipation for the two models. A comparison between the model problem growth rate and the growth rate derived from the electron dissipation in the NSA is then presented, with emphasis on the resultant spectral widths. A growth rate rescaling analysis is used to verify that such a trivial adjustment in the drive cannot account for the difference in frequency width to frequency ratio for the two spectrum solutions. The spectrum solution found after rescaling the growth rate derived in the NSA can be used to show that the frequency width as well as the frequency itself are roughly linearly proportional to the rescalings. Consequently, the ratio of the frequency width to the frequency is approximately independent of the rescaling. A characteristic of the model problem growth rate is that there are few unstable triplets to drive up the noneigenmode frequency spectrum which result in a small frequency width. However, the electron dissipation in the NSA results in large spectral frequency widths, since there are many unstable triplets which drive up and populate the noneigenmode frequency spectrum.

II. Derivation of Spectrum Equations: Renormalization

A renormalized nonlinear integral equation for the turbulent spectrum is derived in this section. The fluid-like (frequency independent) limit is taken in order to clearly demonstrate the failure of the weak turbulence formulation in a dissipative regime. The shortcoming of the weak turbulence theory is due to the associated linear instability of the triplet potential correlation function. The time asymptotic response of the linear propagator for the triplet correlation function is unbounded, when the sum of the three linear growth rates of the potential fluctuations interacting in the triplet is greater than zero. To resolve the inadequacy of the weak turbulence (linear propagator) treatment, one must include the effect of higher order correlations on the response of the triplet correlation. To this end, a renormalized theory is developed where the propagator obeys a nonlinear equation. The nonlinear feedback mechanism produces a damping which inhibits the divergence of the propagator found in the weak turbulence theory approach. This section ends with a detailed derivation of the renormalized nonlinear frequency and wave number spectrum integral equations for a general frequency and wave number dependent dissipation.

The usual derivation of the mode coupling equation follows from an expansion about the linear eigenfunction with a slow time separation employed [5]. The eigenmode expansion implies a narrow frequency spectral width of the form $S_{\mathbf{k},\omega} \approx S_{\mathbf{k}}\delta(\omega - \omega_{\mathbf{k}})$. If the theory is extended to a noneigenmode expansion, while keeping a slow time expansion, the spectral quantity $S_{\mathbf{k},\omega}(t) = \langle \phi_{\mathbf{k},\omega}(t)\phi^*_{\mathbf{k},\omega}(t)\rangle$ would appear, where the frequency, ω, is the Fourier transform of the fast time dependence while the explicit time dependence, t, is the slow time. Using this formulation the identification of the frequency width is difficult since a part is attributed to the explicit frequency dependence, ω, and another part to the time dependence, t. Also, a slow time expansion would be suspect in a chaotic regime. Consequently, the validity of the usual mode coupling theory is doubtful for the drift wave problem in tokamaks where there is some experimental evidence suggesting that the plasma is in a highly turbulent state exhibiting a broad frequency, as well as wave number, spectrum [6].

A. Spectrum Integral Equation - Frequency Independent Dissipation

The majority of research on the drift wave spectrum problem has dealt with a fluid–like version of the mode coupling equation where the growth rate, $\gamma_{\mathbf{k},\omega}$, is independent of frequency, ω. In these treatments the linear frequency, $\omega_{\mathbf{k}}$, is derived from the fluid equations while the growth rate, $\gamma_{\mathbf{k}}$, is usually modeled after the electron–ion dissipation found from a complete plasma kinetic theory derivation. In order to make contact with this fluid–like treatment of the spectrum problem in this section, the limit of the general mode coupling equation, Eq. (2), to frequency independent parameters, $\Omega_{\mathbf{k},\omega} \rightarrow \Omega_{\mathbf{k}}$ and $C_{\mathbf{k},\omega;\mathbf{k}',\omega';\mathbf{k}'',\omega''} \rightarrow C_{\mathbf{k},\mathbf{k}',\mathbf{k}''}$, is used to characterize the fluid limit. This limit produces a mode coupling equation formally equivalent to the mode coupling equation derived by a fluid mechanics approach. In the following section, Sec. B, the spectrum integral equation is derived with the complete plasma kinetic theory mode coupling equation, where the complex frequency, $\Omega_{\mathbf{k},\omega}$, is a general function of wave number and frequency.

The fluid limit of the mode coupling equation in the wave number, $\mathbf{k}$, time, t, domain is

$$\left(\frac{\partial}{t} + i\Omega_{\mathbf{k}}\right)\phi_{\mathbf{k}}(t) = \int dX C_{\mathbf{k},\mathbf{k}',\mathbf{k}''}\phi_{\mathbf{k}'}(t)\phi_{\mathbf{k}''}(t). \tag{5}$$

For a homogeneous system the wave number selection rule is,

$$\langle \phi_{\mathbf{k}}(t)\phi^*_{\mathbf{k}'}(t')\rangle = \delta(\mathbf{k}-\mathbf{k}')S_{\mathbf{k}}(t,t'), \tag{6}$$

so that,

$$\langle \phi_{\mathbf{k}}(t)\phi^*_{\mathbf{k}}(t')\rangle = S_{\mathbf{k}}(t,t'),$$

where, $<\quad>$, is an ensemble average and the infinite normalization is deleted for simplicity of presentation. Multiplying Eq. (5) by $\phi^*_{\mathbf{k}}(t')$ and using Eq. (6) results in the equation for the wave number spectral two time correlation function, $S_{\mathbf{k}}(t,t')$,

$$\left(\frac{}{\partial t} + i\Omega_{\mathbf{k}}\right)S_{\mathbf{k}}(t,t') = \int dX C_{\mathbf{k},\mathbf{k}',\mathbf{k}''}\langle \phi^*_{\mathbf{k}}(t')\phi_{\mathbf{k}'}(t)\phi_{\mathbf{k}''}(t)\rangle, \tag{7}$$

while the equation for the one time or energy wave number spectrum, $S_{\mathbf{k}}(t,t)$, is

$$\left(\frac{\partial}{\partial t} - 2\gamma_{\mathbf{k}}\right)S_{\mathbf{k}}(t,t) = \int dX C_{\mathbf{k},\mathbf{k}',\mathbf{k}''}\langle \phi^*_{\mathbf{k}}(t)\phi_{\mathbf{k}'}(t)\phi_{\mathbf{k}''}(t)\rangle + c.c.. \tag{8}$$

In order to obtain a completely closed equation for the spectrum, a relation for the triplet correlation function, $\langle \phi^* \phi \phi \rangle$, in terms of the spectrum must be obtained. Two closure schemes will be discussed. First, the closure scheme will be achieved using a weak turbulence theory [7] which employs the random phase approximation, or RPA [8]. The weak turbulence theory is then shown to be inadequate for systems with negative dissipation since the triplet correlation is linearly unstable in this theory, so that the time asymptotic limit of the triplet propagator is infinite. The need for renormalization is then motivated, so that higher order correlations can nonlinearly feedback on the response of the triplet correlation. The feature of the renormalized equations for the spectrum, which eliminates the linear instability associated with the weak turbulence theory, is the inclusion of nonlinear damping in the propagator of potential fluctuations. Second, closure will be derived using the Direct Interaction Approximation, or DIA [2]. A resolution of the problem found with weak turbulence theory is achieved since the final equations are a set of fully nonlinear coupled equations for the spectrum as well as the propagator. The DIA renormalization of the fluid–like mode coupling equation is derived in order to demonstrate its equivalence with the renormalization scheme used in Sec. B on the complete plasma kinetic theory mode coupling equation taken in the fluid limit.

1. Weak Turbulence Formulation

Using the potential fluctuation equation, Eq. (5), an equation for the triplet, $\langle \phi^*_{\mathbf{k}}(t)\phi_{\mathbf{k}'}(t)\phi_{\mathbf{k}''}(t)\rangle$, is found by differentiation and averaging,

$$\begin{aligned}
&\left[\frac{\partial}{\partial t} - i(\Omega^*_{\mathbf{k}} - \Omega_{\mathbf{k}'} - \Omega_{\mathbf{k}''})\right]\langle \phi_{\mathbf{k}}(t)\phi_{\mathbf{k}'}(t)\phi_{\mathbf{k}''}(t)\rangle \\
&= \int d\mathbf{k}_1 d\mathbf{k}_2 \Big[\delta(\mathbf{k}-\mathbf{k}_1-\mathbf{k}_2) C_{\mathbf{k},\mathbf{k}_1,\mathbf{k}_2}\langle \phi^*_{\mathbf{k}_1}(t)\phi^*_{\mathbf{k}_2}(t)\phi_{\mathbf{k}'}(t)\phi_{\mathbf{k}''}(t)\rangle \\
&\quad + \delta(\mathbf{k}'-\mathbf{k}_1-\mathbf{k}_2) C_{\mathbf{k}',\mathbf{k}_1,\mathbf{k}_2}\langle \phi^*_{\mathbf{k}}(t)\phi_{\mathbf{k}_1}(t)\phi_{\mathbf{k}_2}(t)\phi_{\mathbf{k}''}(t)\rangle \\
&\quad + \delta(\mathbf{k}''-\mathbf{k}_1-\mathbf{k}_2) C_{\mathbf{k}'',\mathbf{k}_1,\mathbf{k}_2}\langle \phi^*_{\mathbf{k}}(t)\phi_{\mathbf{k}'}(t)\phi_{\mathbf{k}_1}(t)\phi_{\mathbf{k}_2}(t)\rangle\Big]. \qquad (9)
\end{aligned}$$

In a highly turbulent (random) state the ensemble average potential fluctuation is zero, $\langle \phi \rangle = 0$, and the quartic correlation can be exactly expressed as a sum of all possible products of paired correlations plus an irreducible correlation, Q,

$$\langle \phi_1\phi_2\phi_2\phi_4\rangle = \langle \phi_1\phi_2\rangle\langle \phi_3\phi_4\rangle + \langle \phi_1\phi_3\rangle\langle \phi_2\phi_4\rangle + \langle \phi_1\phi_4\rangle\langle \phi_2\phi_3\rangle + Q. \qquad (10)$$

In this cumulant expansion it is postulated that the irreducible correlation, Q, is much smaller than the product of paired correlations, $Q/\langle\phi\phi\rangle\langle\phi\phi\rangle \ll 1$. The leading order quartic expansion is obtained by setting the irreducible correlation to zero, $Q \to 0$. This can be motivated by considering the relevant stochastic regime, where it is physically reasonable to treat the potential fluctuations as normally distributed. In fact, this is equivalent to the RPA where only the lowest order (paired) terms in the cumulant expansion are kept, while dropping the irreducible correlation, Q.

After using the wave number selection rule, Eq. (6), and the RPA for the cumulant expansion of the quartic in Eq. (9), the equation for the triplet correlation is

$$\begin{aligned}
&\left[\frac{\partial}{\partial t} - i(\Omega_{\mathbf{k}}^* - \Omega_{\mathbf{k}'} - \Omega_{\mathbf{k}''})\right]\langle\phi_{\mathbf{k}}^*(t)\phi_{\mathbf{k}'}(t)\phi_{\mathbf{k}''}(t)\rangle \\
&= 2[C_{\mathbf{k},\mathbf{k}',\mathbf{k}''}S_{\mathbf{k}'}(t,t)S_{\mathbf{k}''}(t,t) + C_{\mathbf{k}',-\mathbf{k}'',\mathbf{k}}S_{\mathbf{k}}(t,t)S_{\mathbf{k}''}(t,t) \\
&\quad + C_{\mathbf{k}'',-\mathbf{k}',\mathbf{k}}S_{\mathbf{k}}(t,t)S_{\mathbf{k}'}(t,t)], \qquad (11)
\end{aligned}$$

where the symmetry $C_{\mathbf{k}_1,\mathbf{k}_2,\mathbf{k}_3} = C_{\mathbf{k}_1,\mathbf{k}_3,\mathbf{k}_2}$ and reality condition $C = C^*$ have been used. The triplet equation can be solved formally in terms of a triplet propagator or Green's function, $G_{\mathbf{k}}^T(t,t')$, as follows,

$$\left[\frac{\partial}{\partial t} - i(\Omega_{\mathbf{k}}^* - \Omega_{\mathbf{k}'} - \Omega_{\mathbf{k}''})\right]G_{\mathbf{k}}^T(t,t') = \delta(t-t'), \qquad (12)$$

so that

$$G_{\mathbf{k}}^T(t,t') = \begin{cases} \exp[i(\Omega_{\mathbf{k}}^* - \Omega_{\mathbf{k}'} - \Omega_{\mathbf{k}''})(t-t')], & t \geq t' \\ 0, & t < t' \end{cases}, \qquad (13)$$

and the solution is

$$\begin{aligned}
\langle\phi_{\mathbf{k}}^*(t)\phi_{\mathbf{k}'}(t)\phi_{\mathbf{k}''}(t)\rangle &= \langle\phi_{\mathbf{k}}^*(0)\phi_{\mathbf{k}'}(0)\phi_{\mathbf{k}''}(0)\rangle G_{\mathbf{k}}^T(t,0) \\
&\quad + \int_0^\infty dt' G_{\mathbf{k}}^T(t,t')2[C_{\mathbf{k},\mathbf{k}',\mathbf{k}''}S_{\mathbf{k}'}(t',t')S_{\mathbf{k}''}(t',t') \\
&\quad + C_{\mathbf{k}',-\mathbf{k}'',\mathbf{k}}S_{\mathbf{k}}(t',t')S_{\mathbf{k}''}(t',t') \\
&\quad + C_{\mathbf{k}'',-\mathbf{k}',\mathbf{k}}S_{\mathbf{k}}(t',t')S_{\mathbf{k}'}(t',t')]. \qquad (14)
\end{aligned}$$

If the triplet propagator is well behaved in the time asymptotic limit, $\lim_{t\to\infty} G^T_{\mathbf{k}}(t,0) = 0$, then the initial triplet correlation will not contribute so that the final equation for the spectrum, $S_{\mathbf{k}}(t,t)$, is obtained by substituting Eq. (14) in Eq. (8),

$$\left(\frac{\partial}{\partial t} - 2\gamma_{\mathbf{k}}\right) S_{\mathbf{k}}(t,t) = \int dX \left[\int_0^t dt' G^T_{\mathbf{k}}(t,t') + c.c.\right]$$
$$\cdot 2[C^2_{\mathbf{k},\mathbf{k}',\mathbf{k}''} S_{\mathbf{k}'}(t',t') S_{\mathbf{k}''}(t',t')$$
$$- 2C_{\mathbf{k},\mathbf{k}',\mathbf{k}''} C_{\mathbf{k}',\mathbf{k}'',\mathbf{k}} S_{\mathbf{k}}(t',t') S_{\mathbf{k}''}(t',t')], \tag{15}$$

where the symmetry $C_{\mathbf{k}',-\mathbf{k}'',\mathbf{k}} = -C_{\mathbf{k}',\mathbf{k}'',\mathbf{k}}$ was used.

The steady state spectrum, $S_{\mathbf{k}}$, is obtained from Eq. (15) by taking the time asymptotic limit. With the resonance function defined by

$$ReI_{\mathbf{k},\mathbf{k}',\mathbf{k}''} \equiv \frac{1}{2\pi} \lim_{t\to\infty} \left[\int_0^t dt' G^T_{\mathbf{k}}(t,t') + c.c.\right], \tag{16}$$

the nonlinear integral equation for the spectrum is

$$-2\gamma_{\mathbf{k}} S_{\mathbf{k}} = \int dX 4\pi ReI_{\mathbf{k},\mathbf{k}',\mathbf{k}''} [C^2_{\mathbf{k},\mathbf{k}',\mathbf{k}''} S_{\mathbf{k}'} S_{\mathbf{k}''} - 2C_{\mathbf{k},\mathbf{k}',\mathbf{k}''} C_{\mathbf{k}',\mathbf{k}'',\mathbf{k}} S_{\mathbf{k}''} S_{\mathbf{k}}]. \tag{17}$$

In the steady state $\partial/\partial t S_{\mathbf{k}} = 0$, and after doing the resonance function time integral

$$ReI_{\mathbf{k},\mathbf{k}',\mathbf{k}''} = \frac{1}{\pi} \frac{-\gamma_T}{\gamma_T^2 + \Delta\omega^2}, \tag{18}$$

where

$$\gamma_T \equiv \gamma_{\mathbf{k}} + \gamma_{\mathbf{k}'} + \gamma_{\mathbf{k}''}, \quad \text{and} \quad \Delta\omega \equiv \omega_{\mathbf{k}} - \omega_{\mathbf{k}'} - \omega_{\mathbf{k}''}. \tag{19}$$

The major restriction on the above calculation is that the time asymptotic limit of the linearly propagated initial triplet correlation must be zero, $\lim_{t\to\infty} e^{\gamma_T t} = 0$. This is the same restriction for the resonance function Eq. (16) to exist. In fact, for a system with negative dissipation, $\gamma_{\mathbf{k}} > 0$, there may be positive triplet growth rates, $\gamma_T > 0$, so that the three wave interaction time or resonance function is infinite due to the linear instability of the triplet correlation.

For the case of zero dissipation, $\gamma_T \to 0$, the resonance function becomes a linear eigenfunction selection rule in frequency,

$$\lim_{\gamma_T \to 0} ReI_{\mathbf{k},\mathbf{k}',\mathbf{k}''} = \delta(\omega_{\mathbf{k}} - \omega_{\mathbf{k}'} - \omega_{\mathbf{k}''}), \tag{20}$$

so that the spectrum equation becomes the familiar nonlinear mode coupling spectral evolution equation (introducing $\partial/\partial t S_{\mathbf{k}}$ for slow time evolution) with an expansion about eigenmodes [7],

$$\left(\frac{\partial}{\partial t} - 2\gamma_{\mathbf{k}}\right) S_{\mathbf{k}} = 4\pi \int d\mathbf{k}' d\mathbf{k}'' \delta(\mathbf{k} - \mathbf{k}' - \mathbf{k}'') \delta(\omega_{\mathbf{k}} - \omega_{\mathbf{k}'} - \omega_{\mathbf{k}''})$$
$$\times [C^2_{\mathbf{k},\mathbf{k}',\mathbf{k}''} S_{\mathbf{k}'} S_{\mathbf{k}''} - 2C_{\mathbf{k},\mathbf{k}',\mathbf{k}''} C_{\mathbf{k}',\mathbf{k}'',\mathbf{k}} S_{\mathbf{k}''} S_{\mathbf{k}}]. \tag{21}$$

The failure of the weak turbulence theory for systems enjoying negative dissipation (such as the drift wave problem) can be traced back to the inadequacy of the propagator. In general, the spectrum problem is fully nonlinear; however, in weak turbulence theory the propagator, G^T, is determined by the linear frequency, $\omega_{\mathbf{k}}$, and growth rate, $\gamma_{\mathbf{k}}$. The final spectrum equation found in weak turbulence theory is quadratically nonlinear in the spectrum, S, but the resonance function has a linear character so that it is not valid for positive linear growth rates. The resolution of this problem is to include the effect of higher order correlations on the propagation of the triplet correlation, by renormalizing the propagator so that it will behave nonlinearly. The renormalized spectrum problem is formulated in terms of a set of coupled nonlinear equations for the spectrum, S, and propagator, G. Physically a bare triplet correlation can interact with numerous higher order correlations which contain a triplet character. By including this feedback from higher order correlations, the triplet will respond nonlinearly and damp, so that the linear instability of the triplet found in weak turbulence theory will be avoided.

2. DIA Renormalized Formulation

A short derivation of Kraichnan's DIA [2,9] is presented here so that it can be compared with the fluid limit of the renormalized spectrum equations for the plasma kinetic theory drift wave problem, Sec. B.

The linear propagator, $G^0_{\mathbf{k}}(t,t')$, for the mode coupling equation, Eq. (5), is defined by the expression

$$\left(\frac{\partial}{\partial t}+i\Omega_{\mathbf{k}}\right)G^0_{\mathbf{k}}(t,t')=\delta(t-t');\quad G^0_{\mathbf{k}}(t,t')=0,\quad t<t'. \tag{22}$$

The formal solution of the mode coupling equation is

$$\phi_{\mathbf{k}}(t)=\phi^0_{\mathbf{k}}(t)+\int dt' G^0_{\mathbf{k}}(t,t')\int dX C_{\mathbf{k},\mathbf{k}',\mathbf{k}''}\phi_{\mathbf{k}'}(t')\phi_{\mathbf{k}''}(t'), \tag{23}$$

where the zeroth order solution is $\phi^0_{\mathbf{k}}(t)=\phi_{\mathbf{k}}(0)G^0_{\mathbf{k}}(t,0)$. The infinitesimal response function, or propagator, is

$$G_{\mathbf{k}}(t,t')\equiv\langle\frac{\delta\phi_{\mathbf{k}}(t)}{\delta f_{\mathbf{k}}(t')}\rangle, \tag{24}$$

where $\phi_{\mathbf{k}}\rightarrow\phi_{\mathbf{k}}+\delta\phi_{\mathbf{k}}$, and $\delta f_{\mathbf{k}}$ is a forcing function added to the right hand side of the mode coupling equation, Eq. (5). Making the above substitution and taking the variational derivative with respect to $\delta f_{\mathbf{k}}$ results in the equation for the propagator, $G_{\mathbf{k}}(t,t')$,

$$\left(\frac{\partial}{\partial t}+i\Omega_{\mathbf{k}}\right)G_{\mathbf{k}}(t,t')=2\int dX C_{\mathbf{k},\mathbf{k}',\mathbf{k}''}\langle\phi_{\mathbf{k}'}(t)\frac{\delta\phi_{\mathbf{k}''}(t)}{\delta f_{\mathbf{k}}(t')}\rangle+\delta(t-t'). \tag{25}$$

The renormalization prescription is to expand the triplet, $\langle\phi^*\phi\phi\rangle$, in Eq. (7) and $\langle\phi(\delta\phi/\delta f)\rangle$ in Eq. (25), using the solution for $\phi_{\mathbf{k}}(t)$ in terms of the zeroth order quantities $\phi^0_{\mathbf{k}}(t)$ and $G^0_{\mathbf{k}}(t,t')$, up to the lowest order, and renormalize the spectrum and propagator by the substitution

$$S^0_{\mathbf{k}}(t,t')\rightarrow S_{\mathbf{k}}(t,t')\quad\text{and}\quad G^0_{\mathbf{k}}(t,t')\rightarrow G_{\mathbf{k}}(t,t'). \tag{26}$$

The renormalization procedure is equivalent to an infinite summation of a particular class of terms containing the zeroth order spectrum, $S^0_{\mathbf{k}}(t,t')$, and propagator, $G^0_{\mathbf{k}}(t,t')$. The result of the above analysis is a set of coupled nonlinear equations for the two time spectral correlation function, $S_{\mathbf{k}}(t,t')$, and propagator, $G_{\mathbf{k}}(t,t')$,

$$\left(\frac{\partial}{\partial t}+i\Omega_{\mathbf{k}}\right)S_{\mathbf{k}}(t,t')=\int dX\int dt''2[C^2_{\mathbf{k},\mathbf{k}',\mathbf{k}''}G^*_{\mathbf{k}}(t',t'')S_{\mathbf{k}}(t,t'')S_{\mathbf{k}''}(t,t'')$$
$$-2C_{\mathbf{k},\mathbf{k}',\mathbf{k}''}C_{\mathbf{k}',\mathbf{k}'',\mathbf{k}}G_{\mathbf{k}'}(t,t'')S^*_{\mathbf{k}}(t',t'')S_{\mathbf{k}''}(t,t'')], \tag{27}$$

and

$$\left(\frac{\partial}{\partial t} + i\Omega_{\mathbf{k}}\right) G_{\mathbf{k}}(t,t') = -\int dX \int dt'' 4C_{\mathbf{k},\mathbf{k}',\mathbf{k}''} C_{\mathbf{k}',\mathbf{k}'',\mathbf{k}} G_{\mathbf{k}}(t'',t') G_{\mathbf{k}'}(t,t'') S_{\mathbf{k}''}(t,t'') + \delta(t-t'). \tag{28}$$

For stationary turbulence, $S_{\mathbf{k}}(t,t') = S_{\mathbf{k}}(t-t') = S_{\mathbf{k}}(\tau)$ and $G_{\mathbf{k}}(t,t') = G_{\mathbf{k}}(t-t') = G_{\mathbf{k}}(\tau)$, the above equations become

$$\left(\frac{\partial}{\partial \tau} + i\Omega_{\mathbf{k}}\right) S_{\mathbf{k}} = \int dX \int d\tau' 2[C^2_{\mathbf{k},\mathbf{k}',\mathbf{k}''} G^*_{\mathbf{k}}(\tau'-\tau) S_{\mathbf{k}'}(\tau') S_{\mathbf{k}''}(\tau') - 2C_{\mathbf{k},\mathbf{k}',\mathbf{k}''} C_{\mathbf{k}',\mathbf{k}'',\mathbf{k}} S_{\mathbf{k}}(\tau-\tau') G_{\mathbf{k}'}(\tau') S_{\mathbf{k}''}(\tau')], \tag{29}$$

and

$$\left(\frac{\partial}{\partial \tau} + i\Omega_{\mathbf{k}}\right) G_{\mathbf{k}}(\tau) = -\int dX \int d\tau' 4C_{\mathbf{k},\mathbf{k}',\mathbf{k}''} C_{\mathbf{k}',\mathbf{k}'',\mathbf{k}} G_{\mathbf{k}}(\tau-\tau') G_{\mathbf{k}'}(\tau') S_{\mathbf{k}}(\tau') + \delta(\tau). \tag{30}$$

It is clear now that the propagator, G, is on equal ground with the spectrum, S, since they both obey a coupled set of nonlinear equations in this renormalized formulation of the spectrum problem.

The derivation of the DIA equations can proceed by expanding to infinite order in the zeroth order quantities and then resumming a particular set of infinite terms which renormalize and close the set of equations for the spectrum, S, and the propagator,G [10]. Weak turbulence theory can also be derived as a renormalization of the spectrum, S, using the initial statistical assumption of RPA on the zeroth order quantities, instead of applying the RPA statistical assumption on the fourth order cumulant for all times. However, it is clear that the propagator in weak turbulence theory is not renormalized, which leads to the problem that the propagator and resonance function do not behave nonlinearly, which results in a catastrophe for the negative dissipation regime of drift wave turbulence theory. The above demonstration should be ample impetus to explore a renormalized theory for the plasma drift wave frequency - wave number spectrum equations.

B. Spectrum Integral Equations - General Dissipation

The derivation of the renormalized nonlinear spectrum equations presented here follows that of Kadomtsev [11]. This calculation begins by adding an as yet unknown complex frequency shift, $\delta\eta_{\mathbf{k},\omega}$, to both sides of the general mode coupling equation, Eq. (2),

$$-i(\omega - \Omega_{\mathbf{k},\omega} - \delta\eta_{\mathbf{k},\omega})\phi_{\mathbf{k},\omega} = i\delta\eta_{\mathbf{k},\omega}\phi_{\mathbf{k},\omega} + \int dXC_{\mathbf{k},\mathbf{k}',\mathbf{k}''}\phi_{\mathbf{k}',\omega'}\phi_{\mathbf{k}'',\omega''}. \tag{31}$$

At this point the introduction of the complex frequency shift, $\delta\eta_{\mathbf{k},\omega}$, is exact. Physically, the frequency shift, $\delta\eta_{\mathbf{k},\omega}$, is isolated because the resultant spectrum equation will contain a nonlinear complex frequency shift term proportional to $S_{\mathbf{k},\omega}$, which can then be identified as $\delta\eta_{\mathbf{k},\omega}$. In effect, the propagator of potential fluctuations, Eq. (31), has been renormalized at the start by giving it a nonlinear piece $\delta\eta_{\mathbf{k},\omega}$,

$$G_{\mathbf{k},\omega} = \frac{1}{2\pi}\frac{1}{-i(\omega - \eta_{\mathbf{k},\omega})}, \quad \eta_{\mathbf{k},\omega} \equiv \Omega_{\mathbf{k},\omega} + \delta\eta_{\mathbf{k},\omega}. \tag{32}$$

By renormalizing the propagator and thus forcing it to have a nonlinear complex frequency character it is expected that the problem of the weak turbulence theory linear propagator will be corrected in this formulation of the spectrum equation.

Using the propagator, Eq. (32), the solution, $\phi_{\mathbf{k},\omega}$, of Eq. (31) is readily solved for,

$$\phi_{\mathbf{k},\omega} = \frac{i\delta\eta_{\mathbf{k},\omega}}{-i(\omega - \eta_{\mathbf{k},\omega})}\phi_{\mathbf{k},\omega} + \frac{1}{-i(\omega - \eta_{\mathbf{k},\omega})}\int dXC_{\mathbf{k},\mathbf{k}',\mathbf{k}''}\phi_{\mathbf{k}',\omega'}\phi_{\mathbf{k}'',\omega''}. \tag{33}$$

For homogeneous stationary turbulence the spectrum is $S_{\mathbf{k},\omega} = \langle|\phi_{\mathbf{k},\omega}|^2\rangle$, where, as stated previously, the infinite normalization is deleted for simplicity of presentation. The exact equation for the spectrum is obtained from Eq. (31), by multiplying it by $\phi^*_{\mathbf{k},\omega}$ and ensemble averaging,

$$-i(\omega - \eta_{\mathbf{k},\omega})S_{\mathbf{k},\omega} = i\delta\eta_{\mathbf{k},\omega}S_{\mathbf{k},\omega} + \int dXC_{\mathbf{k},\mathbf{k}',\mathbf{k}''}\langle\phi^*_{\mathbf{k},\omega}\phi_{\mathbf{k}',\omega'}\phi_{\mathbf{k}'',\omega''}\rangle. \tag{34}$$

Following the procedure used in the weak turbulence section, it is necessary to derive an equation for the triplet so that the spectrum equation, Eq. (34), can be written entirely in terms of spectral quantities. Using the potential, Eq. (33), for each term in the triplet, $\langle\phi^*\phi\phi\rangle$, results in an equation for the triplet,

$$\langle \phi^*_{\mathbf{k},\omega}\phi_{\mathbf{k}',\omega'}\phi_{\mathbf{k}'',\omega''}\rangle$$

$$= \left\{\left[\frac{i\delta\eta_{\mathbf{k},\omega}}{-i(\omega-\eta_{\mathbf{k},\omega})}\right]^* + \left[\frac{i\delta\eta_{\mathbf{k}',\omega'}}{-i(\omega'-\eta_{\mathbf{k}',\omega'})}\right] + \left[\frac{i\delta\eta_{\mathbf{k}'',\omega''}}{-i(\omega''-\eta_{\mathbf{k}'',\omega''})}\right]\right\}\langle \phi^*_{\mathbf{k},\omega}\phi_{\mathbf{k}',\omega'}\phi_{\mathbf{k}'',\omega''}\rangle$$

$$+ \int dX \left\{ C_{\mathbf{k},\mathbf{k}_1,\mathbf{k}_2}\left[\frac{1}{-i(\omega-\eta_{\mathbf{k},\omega})}\right]^* \langle \phi^*_{\mathbf{k}_1,\omega_1}\phi^*_{\mathbf{k}_2,\omega_2}\phi_{\mathbf{k}',\omega'}\phi_{\mathbf{k}'',\omega''}\rangle \right.$$

$$+ C_{\mathbf{k}',\mathbf{k}_1,\mathbf{k}_2}\left[\frac{1}{-i(\omega'-\eta_{\mathbf{k}',\omega'})}\right]\langle \phi^*_{\mathbf{k},\omega}\phi_{\mathbf{k}_1,\omega_1}\phi_{\mathbf{k}_2,\omega_2}\phi_{\mathbf{k}'',\omega''}\rangle$$

$$\left. + C_{\mathbf{k}'',\mathbf{k}_1,\mathbf{k}_2}\left[\frac{1}{-i(\omega''-\eta_{\mathbf{k}'',\omega''})}\right]\langle \phi^*_{\mathbf{k},\omega}\phi_{\mathbf{k}',\omega'}\phi_{\mathbf{k}_1,\omega_1}\phi_{\mathbf{k}_2,\omega_2}\rangle \right\}. \qquad (35)$$

As was done during the derivation of the weak turbulence equations, for a highly turbulent state, it is physically reasonable to treat the potential fluctuations as normally distributed. The normality assumption is equivalent to the RPA, so that closure is obtained by expressing the quartic correlations, on the right hand side of Eq. (35), as a sum of all possible products of paired correlations, and dropping the triplet correlation term, which corresponds to dropping the propagated initial triplet correlation in the time domain. Using the wave number–frequency selection rules, the equation for the triplet expressed in terms of spectral quantities is

$$\langle \phi^*_{\mathbf{k},\omega}\phi_{\mathbf{k}',\omega'}\phi_{\mathbf{k}'',\omega''}\rangle = 2\left\{ C_{\mathbf{k},\mathbf{k}',\mathbf{k}''}\left[\frac{1}{-i(\omega-\eta_{\mathbf{k},\omega})}\right] S_{\mathbf{k}',\omega'}S_{\mathbf{k}'',\omega''} \right.$$

$$+ C_{\mathbf{k}',-\mathbf{k}'',\mathbf{k}}\left[\frac{1}{-i(\omega'-\eta_{\mathbf{k}',\omega'})}\right] S_{\mathbf{k},\omega}S_{\mathbf{k}'',\omega''}$$

$$\left. + C_{\mathbf{k}'',-\mathbf{k}',\mathbf{k}}\left[\frac{1}{-i(\omega''-\eta_{\mathbf{k}'',\omega''})}\right] S_{\mathbf{k},\omega}S_{\mathbf{k}',\omega'} \right\} . \qquad (36)$$

Finally, using this expression for the triplet, Eq. (36), in the spectrum equation, Eq. (34), while using the coupling coefficient symmetries, $C_{\mathbf{k}_1,\mathbf{k}_2,\mathbf{k}_3} = C_{\mathbf{k}_1,\mathbf{k}_3,\mathbf{k}_2}$, $C_{\mathbf{k}_1,-\mathbf{k}_2,\mathbf{k}_3} = -C_{\mathbf{k}_1,\mathbf{k}_2,\mathbf{k}_3}$, and $C = C^*$, results in the spectrum equation,

$$-i(\omega-\eta_{\mathbf{k},\omega})S_{\mathbf{k},\omega} = i\delta\eta_{\mathbf{k},\omega}S_{\mathbf{k},\omega} + 2\int dX \left\{ C^2_{\mathbf{k},\mathbf{k}',\mathbf{k}''}S_{\mathbf{k}',\omega'}S_{\mathbf{k}'',\omega''}\left[\frac{1}{-i(\omega-\eta_{\mathbf{k},\omega})}\right]^* \right.$$

$$\left. - 2C_{\mathbf{k},\mathbf{k}',\mathbf{k}''}C_{\mathbf{k}',\mathbf{k}'',\mathbf{k}}S_{\mathbf{k},\omega}S_{\mathbf{k}'',\omega''}\frac{1}{-i(\omega'-\eta_{\mathbf{k}',\omega'})} \right\}. \qquad (37)$$

The complex frequency shift, $\delta\eta_{\mathbf{k},\omega}$, in Eq. (37) appears to be arbitrary; however, it was set up at the outset to represent the nonlinear complex frequency shift of the potential fluctuation. In fact, the frequency shift is contained in the propagator, $1/2\pi[-i(\omega-\eta_{\mathbf{k},\omega})]$, on the right hand side of Eq. (37). To the extent that the spectrum propagator is similar to the fluctuation propagator, it is reasonable in Eq. (37) to equate the frequency shift term, $\delta\eta_{\mathbf{k},\omega}S_{\mathbf{k},\omega}$, with the mode coupling term on the right hand side of Eq. (37) proportional to the spectrum, $S_{\mathbf{k},\omega}$. The equation for the nonlinear complex frequency shift, $\delta\eta_{\mathbf{k},\omega}$, is then

$$\delta\eta_{\mathbf{k},\omega} = -i\int dX4C_{\mathbf{k},\mathbf{k}',\mathbf{k}''}C_{\mathbf{k}',\mathbf{k}'',\mathbf{k}}\frac{1}{-i(\omega'-\eta_{\mathbf{k}',\omega'})}S_{\mathbf{k}'',\omega''}. \tag{38}$$

The result of the above separation is a coupled set of nonlinear equations for the spectrum, $S_{\mathbf{k},\omega}$, and the nonlinear complex frequency, $\eta_{\mathbf{k},\omega}$,

$$-i(\omega-\eta_{\mathbf{k},\omega})S_{\mathbf{k},\omega} = \int dX2C^2_{\mathbf{k},\mathbf{k}',\mathbf{k}''}\left[\frac{1}{-i(\omega-\eta_{\mathbf{k},\omega})}\right]^* S_{\mathbf{k}',\omega'}S_{\mathbf{k}'',\omega''}, \tag{39}$$

and

$$\eta_{\mathbf{k},\omega} = \Omega_{\mathbf{k},\omega} - i\int dX4C_{\mathbf{k},\mathbf{k}',\mathbf{k}''}C_{\mathbf{k}',\mathbf{k}'',\mathbf{k}}\left[\frac{1}{-i(\omega'-\eta_{\mathbf{k}',\omega'})}\right]S_{\mathbf{k}'',\omega''}. \tag{40}$$

It should be realized that a critical assumption in the derivation of the renormalized spectrum, Eqs. (39) and (40), is the addition of the nonlinear complex frequency shift, $\delta\eta_{\mathbf{k},\omega}$, in the fluctuation equation for $\phi_{\mathbf{k},\omega}$. After the spectrum equation for $S_{\mathbf{k},\omega}$ is derived, $\delta\eta_{\mathbf{k},\omega}$ is set up to be equal to the nonlinear frequency shift term proportional to $S_{\mathbf{k},\omega}$. It is clear that $\delta\eta_{\mathbf{k},\omega}$ represents the complex nonlinear frequency shift for the spectral evolution equation; however, it then has been assumed that this same nonlinear complex frequency shift, $\delta\eta_{\mathbf{k},\omega}$, appears in the fluctuation equation for $\phi_{\mathbf{k},\omega}$, since it was introduced in the propagator at the outset. The resultant approximation in this renormalized theory for the spectrum is that the nonlinear complex frequency shift, $\delta\eta_{\mathbf{k},\omega}$, which is defined as the nonlinear frequency shift in the spectrum equation, is also a good approximation for the fluctuation equation. Physically, it does seem reasonable that if the fluctuation equation for $\phi_{\mathbf{k},\omega}$ is used solely to derive the average evolution of the spectrum, $S_{\mathbf{k},\omega}$, then the complex frequency shift, $\delta\eta_{\mathbf{k},\omega}$, found in the spectrum equation, might be a good model to use in the fluctuation propagator, $G_{\mathbf{k},\omega}$.

It should be noted, as was noted for the DIA renormalization section, that instead of using the RPA on the potential fluctuations, $\phi_{\mathbf{k},\omega}$, the equations for the spectrum, S, and propagator, G, could have been obtained by expanding in terms of the zeroth order quantities, S^0 and G^0, and finally renormalizing to S and G. This suggests that the Kraichnan DIA coupled set of nonlinear spectrum and propagator equations can be obtained by taking the fluid-like frequency independent limit of Eqs. (39) and (40) for the spectrum and nonlinear complex frequency, where the linear complex frequency is $\Omega_{\mathbf{k}} = \omega_{\mathbf{k}} + i\gamma_{\mathbf{k}}$.

The demonstration that the DIA Eqs. (29) and (30) are identical to the fluid limit of the above renormalized Eqs. (39) and (40) follows by first writing out the equation for the propagator, $G_{\mathbf{k},\omega}$, from its definition, Eq. (32),

$$-i(\omega - \Omega_{\mathbf{k}})G_{\mathbf{k},\omega} = \frac{1}{2\pi}\frac{-i(\omega - \Omega_{\mathbf{k}})}{-i(\omega - \Omega_{\mathbf{k}} - \delta\eta_{\mathbf{k},\omega})} = \frac{1}{2\pi}\frac{-i(\omega - \Omega_{\mathbf{k}} - \delta\eta_{\mathbf{k},\omega}) - i\delta\eta_{\mathbf{k},\omega}}{-i(\omega - \Omega_{\mathbf{k}} - \delta\eta_{\mathbf{k},\omega})}. \quad (41)$$

Using Eq. (38) for the frequency shift, $\delta\eta_{\mathbf{k},\omega}$, in Eq. (41), along with the definition of $G_{\mathbf{k},\omega}$, results in the propagator equation,

$$-i(\omega - \Omega_{\mathbf{k}})G_{\mathbf{k},\omega} = -\int dX 4C_{\mathbf{k},\mathbf{k}',\mathbf{k}''}C_{\mathbf{k}',\mathbf{k}'',\mathbf{k}}2\pi G_{\mathbf{k},\omega}G_{\mathbf{k}',\omega'}S_{\mathbf{k}'',\omega''} + \frac{1}{2\pi}. \quad (42)$$

After taking the inverse frequency Fourier transform of the propagator, Eq. (42), while using the formula for the inverse transform of a product times a convolution,

$$\int d\omega e^{-i\omega\tau}G_{\mathbf{k},\omega}\int d\omega' G_{\mathbf{k}',\omega'}S_{\mathbf{k}'',\omega-\omega'} = \frac{1}{2\pi}\int d\tau' G_{\mathbf{k}}(\tau - \tau')G_{\mathbf{k}'}(\tau')S_{\mathbf{k}''}(\tau'), \quad (43)$$

the equation for the time evolution of the propagator, $G_{\mathbf{k}}(\tau)$, is

$$\left(\frac{\partial}{\partial\tau} + i\Omega_{\mathbf{k}}\right)G_{\mathbf{k}}(\tau) = -\int dX 4C_{\mathbf{k},\mathbf{k}',\mathbf{k}''}C_{\mathbf{k}',\mathbf{k}'',\mathbf{k}}\int d\tau' G_{\mathbf{k}}(\tau - \tau')G_{\mathbf{k}'}(\tau')S_{\mathbf{k}''}(\tau') + \delta(\tau). \quad (44)$$

The spectrum equation, Eq. (37), can be rewritten in terms of $G_{\mathbf{k},\omega}$ as

$$-i(\omega - \Omega_{\mathbf{k}})S_{\mathbf{k},\omega} = \int dX\Big[2C^2_{\mathbf{k},\mathbf{k}',\mathbf{k}''}2\pi G^*_{\mathbf{k},\omega}S_{\mathbf{k}',\omega'}S_{\mathbf{k}'',\omega''} - 4C_{\mathbf{k},\mathbf{k}',\mathbf{k}''}C_{\mathbf{k}',\mathbf{k}'',\mathbf{k}}2\pi S_{\mathbf{k},\omega}G_{\mathbf{k}',\omega'}S_{\mathbf{k}'',\omega''}\Big]. \quad (45)$$

This can be inversed Fourier transformed, using the convolution rule, Eq. (43), and the transform property $\int d\omega e^{-i\omega\tau} f_\omega^* = f^*(-\tau)$, to obtain the evolution equation of the spectrum, $S_{\mathbf{k}}(\tau)$,

$$\left(\frac{\partial}{\partial\tau} + i\Omega_{\mathbf{k}}\right) S_{\mathbf{k}}(\tau) = \int dX \Big[2C^2_{\mathbf{k},\mathbf{k}',\mathbf{k}''} \int d\tau' G^*_{\mathbf{k}}(\tau'-\tau) S_{\mathbf{k}'}(\tau') S_{\mathbf{k}''}(\tau') - 4C_{\mathbf{k},\mathbf{k}',\mathbf{k}''} C_{\mathbf{k}',\mathbf{k}'',\mathbf{k}} \int d\tau' S_{\mathbf{k}}(\tau-\tau') G_{\mathbf{k}'}(\tau') S_{\mathbf{k}''}(\tau') \Big]. \quad (46)$$

The Eqs. (44) and (46) for the propagator, $G_{\mathbf{k}}(\tau)$, and the spectrum, $S_{\mathbf{k}}(\tau)$, are exactly the DIA Eqs. (29) and (30) previously derived.

The starting point for the derivation of the renormalized spectrum equations was the general mode coupling equation, Eq. (2), for the potential fluctuations, $\phi_{\mathbf{k},\omega}$. It should be noted that a more consistent approach would be to attack the Vlasov–Poisson system of equations directly with a renormalization scheme, since they comprise a set of coupled nonlinear equations for the potential fluctuations, ϕ, and distribution, f. The upshot is that the nonlinear spectrum equations are similar to the results obtained here, with the additional feature that the kinetic resonance function under the velocity integral for the coupling coefficient, C, is also renormalized as $1/(\omega - \mathbf{k}\cdot\mathbf{v}) \to 1/(\omega - \mathbf{k}\cdot\mathbf{v} - \delta\eta_{\mathbf{k},\omega})$ [11].

III. Solution of Nonlinear Spectrum Integral Equation

The result of the preceding section is a set of coupled nonlinear integral equations, Eqs. (39) and (40), for the spectrum, $S_{\mathbf{k},\omega}$, and the nonlinear complex frequency, $\eta_{\mathbf{k},\omega}$. The objective of this section is to formulate an analytic technique to approximate the solution of nonlinear integral equations of this type, and then to apply the technique to the spectrum equations for various models of dissipation.

The solution of nonlinear integral equations is one of the major problems addressed by applied mathematics research at the present time. There are no general analytic solution techniques for these equations. Numerical solutions of nonlinear integral equations require very lengthy computation times, even for a coarse discretization of the spectrum, using few spectral modes. In fact, the solution of the spectrum equation, reduced to just wave number space, involves hours of Cray time [3]. Perturbation methods for the solution of nonlinear equations, where the solution is built up by summing the solutions for a series of related linearized problems, in many cases will not converge to the actual solution. Consequently, it is advantageous to try and obtain a solution directly without employing a linearization. To this end, as a first order approximation, a moment method is developed to approximate the solution of the coupled set of nonlinear integral equations for the spectrum. The method begins by selecting appropriate trial functions which are dependent on a set of physically relevant parameters. Similar to a variational method, the trial functions are used as a first order approximation to the solution of the nonlinear integral equations, where the functional form of the trial functions are determined with the aid of experimental evidence and physical insight. By using the trial functions in the nonlinear integral equations, a corresponding set of nonlinear algebraic moment equations for the parameters are determined. The nonlinear algebraic equations are then solved for the unknown parameters. These parameters are the leading order approximations to the corresponding physically relevant parameters of the true solution. Based on this first order solution, equations are systematically derived which determine the next order correction to the solution. The equations governing these next order corrections to the solution functions can be solved, so that the solution functions are then known to second order, which enables the calculation of the parameters to second order. In principle, this procedure can be iterated to determine higher order corrections to the solution of the coupled set of nonlinear integral equations. In this article, we will be concerned only with the first step.

Alternatively, the parameters of the theory could be solved to second order by using a nonlinear variational approach [12]. Briefly, the variational method guarantees by con-

struct that the resultant parameters will be good to second order if the trial functions are known to first order. However, as usual, one rarely gets something for nothing. The nonlinear variational calculation is quite difficult, and in many ways parallels the additional work needed to calculate next order corrections to the first order parameters, as presented in this section.

In Sec. A., the spectrum problem is reduced to wave number space by choosing a spectral trial function in frequency space and integrating out the frequency dependence of the spectrum equation. In Sec. 1., a Lorentzian spectral function in frequency is used to derive a spectrum equation in wave number space for fluid–like systems. The Lorentzian is shown to be incompatible with the more general plasma problem, where the linear growth rate is a function of wave number as well as frequency. The difficulty arises since the spectrum problem reduced to wave number space incorporates frequency averaged quantities, such as the growth rate, where the spectrum is a weighting function. However, most of the frequency moments of the Lorentzian are singular. In Sec. 2., in order to handle general frequency dependent growth rates such as the realistic electron drift wave dissipation in the NSA, a Gaussian spectral trial function in frequency is used to produce a spectrum equation in wave number space. The Gaussian function does not have the drawback associated with the Lorentzian function since all moments of the Gaussian exist.

Section B. contains the final solution of the spectrum equations. This is obtained by choosing a wave number spectral trial function which is a function of several important parameters, the total integrated spectral amplitude, the spectral wave number width, and the spectral frequency width. The parameters are determined by solving a set of independent nonlinear algebraic equations derived by taking select wave number moments of the wave number spectrum equations. It should be noted that the selection of the wave number moments can be formalized by using an optimizing least squares method. This procedure utilitizes a squared funcitonal form of the nonlinear integral equations which results in the "best" moment equations in the least squares sense. Our analysis of the spectrum equations using the least squares method will be reported later. In Sec. 1., the general moment method procedure is described in detail for the case of the spectrum equations. In Sec. 2., equations governing the next order correction to the first order solution are formally derived, so that in principle the solution parameters can be obtained to second order accuracy. In Sec. 3., in order to test this analytic moment technique for solving the nonlinear spectrum integral equation, a Lorentzian frequency function along with a Gaussian wave number function is used to solve the fluid limit spectrum equa-

tions for a model dissipation studied by Waltz [3]. A comparison is made between these analytic results and those obtained numerically by Waltz. It is found that there is both good qualitative and quantitative agreement between our analytic spectrum results and the numerical results of Waltz. The root mean square potential, obtained by this analytic moment method, in dimensionless normalized units, is $\phi_{rms} = 1.6$. This is in almost perfect agreement with the quoted numerical results, and is on the order of the experimental values. In dimensionless normalized units, the average frequency width, $\langle -\eta^I \rangle \approx .02$, found by this moment technique, is much less than the average frequency, $\langle \omega \rangle \approx .3$. This is also in agreement with the numerical results of Waltz, but, of course, quite a bit different from the broad frequency spectral widths observed experimentally. Finally, in Sec. 4., a Gaussian frequency function along with a Gaussian wave number function is used to solve the spectrum equation for a model of electron drift wave dissipation derived in the NSA [4]. Using the approximate analytic moment method of solution, in dimensionless normalized units, the root mean square potential is $\phi_{rms} = 3.1$. Also, in dimensionless normalized units, the average frequency width, $\langle -\eta^I \rangle \approx .3$, is on the order of the average frequency, $\langle \omega \rangle \approx .3$. A comparison is made between the model dissipation of Waltz and the electron dissipation in the NSA with emphasis on the resulting spectral frequency widths. It should be noted that the frequency width to frequency ratio is roughly independent of a growth rate rescaling for the electron dissipation in the NSA. Therefore, the difference in frequency widths for the two dissipation models cannot simply be attributed to a rescaling of the growth rate. Consequently, a more detailed analysis of differences in the growth rate structure for the two models must be considered. The basic point is that the wave number dependent growth rate for the model problem of Waltz contains a narrow wave number region with small positive growth rates. Almost any two unstable linear eigenmodes which beat together form a third nonlinear mode which is stable, where the triplet growth rate is also stable. Since there are very few unstable triplets to drive up the noneigenmode frequency spectrum, the resultant spectral frequency widths are small. For the case of the growth rates derived from this model of electron dissipation in the NSA, every eigenmode, $\omega = \omega_{\mathbf{k}}$, is unstable. Any two eigenmodes with positive y components of the wave vectors which beat together form a third nonlinear mode which is also unstable. There are many unstable triplets that drive up and populate the noneigenmode frequencies. It is then anticipated that the solution of the spectrum equations dependent on the electron dissipation in the NSA will result in large frequency spectral widths. The spectrum results for this dissipation model, being $e\phi_{rms}/T_e \approx 10^{-2}$ and an average frequency width on the order of the average frequency, are in rough agreement with the experimental observations in

tokamaks.

A. Spectral Trial Function: Frequency

In a linear eigenmode theory the effective frequency spectrum, for any fixed wave number, is centered about the linear eigenfrequency, $\omega_{\mathbf{k}}$, with negligible frequency width. In general, however, the spectrum equation is nonlinear so that one expects the frequency spectrum to be centered about a nonlinear frequency, $\eta_{\mathbf{k}}^R \equiv \omega_{\mathbf{k}} + \delta\eta_{\mathbf{k}}^R$ ($\delta\eta_{\mathbf{k}}^R$ is the nonlinear frequency shift), with the frequency width being $\eta_{\mathbf{k}}^I \equiv \gamma_{\mathbf{k}} + \delta\eta_{\mathbf{k}}^I$ ($\delta\eta_{\mathbf{k}}^I$ is the nonlinear growth rate shift). Employing these two general physical features of the frequency spectrum, two particular frequency spectral shapes are chosen (the Lorentzian and Gaussian) for the trial functions. This leads to a reduction of the spectrum problem to wave number space.

1. Lorentzian Line Shape

One possibility for the spectral frequency trial function is the very common Lorentzian model. In fact, the Lorentzian frequency function appears to occur naturally in the spectrum equation. Actually, it will be demonstrated that this is due to the method of renormalization used to derive the spectrum equations, where the nonlinear complex frequency, $\eta_{\mathbf{k},\omega}$, was introduced. Although superficially there seems to be only one reasonable choice for the frequency trial function (the Lorentzian), it is shown that general choices are possible by changing representation of the spectrum problem from the calculation of a nonlinear complex frequency, $\eta_{\mathbf{k},\omega}$, and a spectrum, $S_{\mathbf{k},\omega}$, to the calculation of a propagator, $G_{\mathbf{k},\omega}$, and a spectrum, $S_{\mathbf{k},\omega}$. The use of this alternate representation will not lead to any practical restriction on the form the frequency spectral trial function may assume. In this section, the representation employing the nonlinear complex frequency, $\eta_{\mathbf{k},\omega}$, is used. In the following section, we will develop the other representation.

The spectrum problem [via Eqs. (39) and (40)] is that of calculating the spectrum, $S_{\mathbf{k},\omega}$, and the nonlinear complex frequency, $\eta_{\mathbf{k},\omega}$. The equation for the spectrum is analyzed first, followed by that of the nonlinear complex frequency. The starting point is Eq. (39) for the spectrum, where definition (40) has been used,

$$-i(\omega - \Omega_{\mathbf{k},\omega})S_{\mathbf{k},\omega} = \int dX \left\{ 2C^2_{\mathbf{k},\mathbf{k}',\mathbf{k}''} S_{\mathbf{k}',\omega'} S_{\mathbf{k}'',\omega''} \left[\frac{1}{-i(\omega - \eta_{\mathbf{k},\omega})}\right]^* \right.$$
$$\left. - 4C_{\mathbf{k},\mathbf{k}',\mathbf{k}''} C_{\mathbf{k}',\mathbf{k}'',\mathbf{k}} S_{\mathbf{k},\omega} S_{\mathbf{k}'',\omega''} \left[\frac{1}{-i(\omega' - \eta_{\mathbf{k}',\omega'})}\right] \right\}. \qquad (47)$$

Taking the real part of Eq. (47), with the definition $\eta_{\mathbf{k},\omega} = \eta_{\mathbf{k},\omega}^R + i\eta_{\mathbf{k},\omega}^I$, results in

$$-2\gamma_{\mathbf{k},\omega}S_{\mathbf{k},\omega} = \int dX \left[4\pi C^2_{\mathbf{k},\mathbf{k}',\mathbf{k}''} \frac{1}{\pi} \frac{-\eta^I_{\mathbf{k},\omega}}{(\omega - \eta^R_{\mathbf{k},\omega})^2 + (\eta^I_{\mathbf{k},\omega})^2} S_{\mathbf{k}',\omega'} S_{\mathbf{k}'',\omega''} \right.$$

$$\left. - 8\pi C_{\mathbf{k},\mathbf{k}',\mathbf{k}''} C_{\mathbf{k}',\mathbf{k}'',\mathbf{k}} S_{\mathbf{k},\omega} \frac{1}{\pi} \frac{-\eta^I_{\mathbf{k}',\omega'}}{(\omega' - \eta^R_{\mathbf{k}',\omega'})^2 + (\eta^I_{\mathbf{k}',\omega'})^2} S_{\mathbf{k}'',\omega''} \right]. \qquad (48)$$

It is interesting to note that the real part of the propagator,

$$R_{\mathbf{k},\omega} \equiv G_{\mathbf{k},\omega} + G^*_{\mathbf{k},\omega} = \frac{1}{\pi} \frac{-\eta^I_{\mathbf{k},\omega}}{(\omega - \eta^R_{\mathbf{k},\omega})^2 + (\eta^I_{\mathbf{k},\omega})^2}, \qquad (49)$$

will take on a Lorentzian form in frequency, if $\eta_{\mathbf{k},\omega} \to \eta_{\mathbf{k}}$.

In reference to Eq. (48), it should be noted that the right hand side driving terms each contain two spectrum factors, S, and one real propagator factor, R. It will be found that the equation for the nonlinear complex frequency will have a triplet driving term containing two real propagator factors, R, and one spectrum factor, S. This symmetry will be even more clear when we examine the alternate representation utilizing the propagator, $G_{\mathbf{k},\omega}$, and the spectrum, $S_{\mathbf{k},\omega}$. The three factors in each equation physically represent the fundamental triplet interaction found in mode–mode coupling. Parenthetically, in order to integrate the spectrum equation, Eq. (48), over frequency to obtain a wave number spectrum equation, the frequency convolution integrals for the triplet interaction must be obtained. If the spectrum, $S_{\mathbf{k},\omega}$, is taken to be proportional to the real part of the propagator, $R_{\mathbf{k},\omega}$, then the resultant convolution integrals in frequency will combine in such a way that the derived resonance function or interaction time, $I_{\mathbf{k},\mathbf{k}',\mathbf{k}''}$, will contain elements of the nonlinear complex frequency, symmetrically for all three waves in a triplet, similar to that found in weak turbulence theory. Consequently, in view of the above arguments, it is a useful simplifying assumption to make an ansatz such that the spectrum is proportional to the real part of the propagator,

$$S_{\mathbf{k},\omega} \to S_{\mathbf{k}} R_{\mathbf{k},\omega}, \qquad (50)$$

where the real part of the propagator is normalized to one, $\int d\omega R_{\mathbf{k},\omega} = 1$.

The spectrum problem is thereby reduced to the evaluation of the normalized spectrum, $R_{\mathbf{k},\omega}$, and the nonlinear complex frequency, $\eta_{\mathbf{k},\omega}$, with the subsidiary condition that

Eq. (49) is satisfied. In view of Eq. (49) for the general form of the normalized spectrum, $R_{\mathbf{k},\omega}$, a possible choice for the normalized spectral frequency trial function is the Lorentzian,

$$R_{\mathbf{k},\omega} \rightarrow \frac{1}{\pi} \frac{-\eta_{\mathbf{k}}^I}{(\omega - \eta_{\mathbf{k}}^R)^2 + (\eta_{\mathbf{k}}^I)^2}, \quad \eta_{\mathbf{k},\omega} \rightarrow \eta_{\mathbf{k}}. \tag{51}$$

Inverse Fourier transforming the normalized spectrum, $R_{\mathbf{k},\omega}$, gives

$$R_{\mathbf{k}}(\tau) = e^{-i\eta_{\mathbf{k}}^R \tau + \eta_{\mathbf{k}}^I |\tau|}, \tag{52)}$$

where $R_{\mathbf{k}}(\tau)$ is the spectral correlation function. The propagator, $G_{\mathbf{k},\omega}$, and its inverse Fourier transform are

$$G_{\mathbf{k},\omega} = \frac{1}{2\pi} \frac{1}{-i(\omega - \eta_{\mathbf{k}})}, \quad \text{and} \quad G_{\mathbf{k}}(\tau) = \begin{cases} e^{-i\eta_{\mathbf{k}}\tau}, & \tau > 0 \\ 0, & \tau < 0 \end{cases}, \tag{53}$$

where the imaginary part of the nonlinear frequency is assumed to be less than zero, $Im\eta_{\mathbf{k}} \equiv \eta_{\mathbf{k}}^I < 0$.

The time asymptotic steady state wave number spectrum, $S_{\mathbf{k}}$, can be obtained by integrating the wave number frequency spectrum, $S_{\mathbf{k},\omega}$, over frequency,

$$\begin{aligned} \int d\omega S_{\mathbf{k},\omega} &= \int d\omega \frac{1}{(2\pi)^2} \int dy d\tau e^{-i(\mathbf{k}\cdot\mathbf{y} - \omega\tau)} \langle \phi(\mathbf{x}+\mathbf{y}, t+\tau)\phi(\mathbf{x},t)\rangle \\ &= \frac{1}{2\pi} \int dy e^{-i\mathbf{k}\cdot\mathbf{y}} \langle \phi(\mathbf{x}+\mathbf{y},t)\phi(\mathbf{x},t)\rangle = S_{\mathbf{k}}. \end{aligned} \tag{54}$$

The wave number spectrum, $S_{\mathbf{k}}$, is independent of time for a stationary turbulent state, which is assumed to exist. The steady state spectral equation in wave number space is then derived by introducing the frequency spectral trial function, Eq. (51), in the spectrum Eq. (48) and integrating over frequency,

$$\begin{aligned} &-2 \int d\omega \gamma_{\mathbf{k},\omega} S_{\mathbf{k},\omega} \\ &= \int d\mathbf{k}' d\mathbf{k}'' \delta(\mathbf{k} - \mathbf{k}' - \mathbf{k}'') [4\pi C_{\mathbf{k},\mathbf{k}',\mathbf{k}''}^2 S_{\mathbf{k}'} S_{\mathbf{k}''} \int d\omega R_{\mathbf{k},\omega} \int d\omega' R_{\mathbf{k}',\omega'} R_{\mathbf{k}'',\omega-\omega'} \\ &- 8\pi C_{\mathbf{k},\mathbf{k}',\mathbf{k}''} C_{\mathbf{k}',\mathbf{k}'',\mathbf{k}} S_{\mathbf{k}} S_{\mathbf{k}''} \int d\omega R_{\mathbf{k},\omega} \int d\omega' R_{\mathbf{k}',\omega'} R_{\mathbf{k}'',\omega-\omega'}]. \end{aligned} \tag{55}$$

The triplet resonance function is

$$ReI_{\mathbf{k},\mathbf{k}',\mathbf{k}''} \equiv \int d\omega R_{\mathbf{k},\omega} \int d\omega' R_{\mathbf{k}',\omega'} R_{\mathbf{k}'',\omega-\omega'} = \frac{1}{\pi} \frac{-n_T^I}{(\Delta n^R)^2 + (n_T^I)^2}, \tag{56}$$

where $\eta_T^I \equiv \eta_{\mathbf{k}}^I + \eta_{\mathbf{k}'}^I + \eta_{\mathbf{k}''}^I$, $\Delta\eta^R \equiv \eta_{\mathbf{k}}^R - \eta_{\mathbf{k}'}^R - \eta_{\mathbf{k}''}^R$, and use has been made of Parseval's power theorem, $\int d\omega f_\omega g_\omega = (1/2\pi) \int dt f(-t) g(t)$, and the inverse transform of a convolution, $\int d\omega e^{-i\omega t} \int d\omega' f_{\omega'} g_{\omega-\omega'} = f(t)g(t)$.

The spectral equation in wave number space can now be written in a familiar form,

$$-2\gamma_{\mathbf{k}} S_{\mathbf{k}} = \int dX 4\pi ReI_{\mathbf{k},\mathbf{k}',\mathbf{k}''} [C^2_{\mathbf{k},\mathbf{k}',\mathbf{k}''} S_{\mathbf{k}'} S_{\mathbf{k}''} - 2C_{\mathbf{k},\mathbf{k}',\mathbf{k}''} C_{\mathbf{k}',\mathbf{k}'',\mathbf{k}} S_{\mathbf{k}} S_{\mathbf{k}''}], \tag{57}$$

where the integrated growth rate is defined as

$$\gamma_{\mathbf{k}} \equiv \int d\omega \gamma_{\mathbf{k},\omega} R_{\mathbf{k},\omega}, \tag{58}$$

and $\int dX \equiv \int d\mathbf{k} \delta(\mathbf{k} - \mathbf{k}' - \mathbf{k}'')$.

In order to complete the coupled set of nonlinear integral equations describing the spectrum in wave number space, the equation for the nonlinear complex frequency, $\eta_{\mathbf{k}}$, must be derived. This is obtained by multiplying Eq. (40) for the nonlinear complex frequency, $\eta_{\mathbf{k}}$, by the normalized spectrum, $R_{\mathbf{k},\omega}$, to give,

$$\eta_{\mathbf{k}} R_{\mathbf{k},\omega} = \Omega_{\mathbf{k},\omega} R_{\mathbf{k},\omega} - i \int dX 4 C_{\mathbf{k},\mathbf{k}',\mathbf{k}''} C_{\mathbf{k}',\mathbf{k}'',\mathbf{k}} 2\pi R_{\mathbf{k},\omega} \int d\omega' G_{\mathbf{k}',\omega'} S_{\mathbf{k}'',\omega-\omega'}. \tag{59}$$

Then integrating Eq. (59) over frequency, which corresponds to the step used in deriving the wave number spectrum equation, results in

$$\eta_{\mathbf{k}} = \int d\omega \Omega_{\mathbf{k},\omega} R_{\mathbf{k},\omega} - i \int dX 4\pi C_{\mathbf{k},\mathbf{k}',\mathbf{k}''} C_{\mathbf{k}',\mathbf{k}'',\mathbf{k}} S_{\mathbf{k}''} 2 \int d\omega R_{\mathbf{k},\omega} \int d\omega' G_{\mathbf{k}',\omega'} R_{\mathbf{k}'',\omega-\omega'}. \tag{60}$$

Defining the complex resonance function, $I_{\mathbf{k},\mathbf{k}',\mathbf{k}''}$, from the term on the right hand side of Eq. (60) and performing the frequency integrals which are similar to those done in obtaining Eq. (56), results in

$$I_{\mathbf{k},\mathbf{k}',\mathbf{k}''} \equiv 2 \int d\omega R_{\mathbf{k},\omega} \int d\omega' G_{\mathbf{k}',\omega'} R_{\mathbf{k}'',\omega-\omega'}, \tag{61}$$

so that the complex resonance function is

$$I_{\mathbf{k},\mathbf{k}',\mathbf{k}''} = \frac{1}{\pi} \frac{-1}{i\Delta\eta^R + \eta_T^I}, \quad ReI_{\mathbf{k},\mathbf{k}',\mathbf{k}''} = \frac{1}{\pi} \frac{-\eta_T^I}{(\Delta\eta^R)^2 + (\eta_T^I)^2},$$

$$ImI_{\mathbf{k},\mathbf{k}',\mathbf{k}''} = \frac{1}{\pi} \frac{\Delta\eta^R}{(\Delta\eta^R)^2 + (\eta_T^I)^2}. \tag{62}$$

Finally, the equation for the nonlinear complex frequency is

$$\eta_{\mathbf{k}} = \Omega_{\mathbf{k}} - i \int dX 4\pi I_{\mathbf{k},\mathbf{k}',\mathbf{k}''} C_{\mathbf{k},\mathbf{k}',\mathbf{k}''} C_{\mathbf{k}',\mathbf{k}'',\mathbf{k}} S_{\mathbf{k}''}, \tag{63}$$

so that the nonlinear growth rate is

$$\eta_{\mathbf{k}}^I = \gamma_{\mathbf{k}} - \int dX 4\pi ReI_{\mathbf{k},\mathbf{k}',\mathbf{k}''} C_{\mathbf{k},\mathbf{k}',\mathbf{k}''} C_{\mathbf{k}',\mathbf{k}'',\mathbf{k}} S_{\mathbf{k}''}, \tag{64}$$

and the nonlinear frequency is

$$\eta_{\mathbf{k}}^R = \omega_{\mathbf{k}} + \int dX 4\pi ImI_{\mathbf{k},\mathbf{k}',\mathbf{k}''} C_{\mathbf{k},\mathbf{k}',\mathbf{k}''} C_{\mathbf{k}',\mathbf{k}'',\mathbf{k}} S_{\mathbf{k}''}, \tag{65}$$

where we have defined the spectral averaged complex frequency as

$$\Omega_{\mathbf{k}} \equiv \int d\omega \Omega_{\mathbf{k},\omega} R_{\mathbf{k},\omega}, \quad \text{and} \quad \omega_{\mathbf{k}} \equiv \int d\omega \omega_{\mathbf{k},\omega} R_{\mathbf{k},\omega}. \tag{66}$$

Using the nonlinear growth rate Eq. (64) in the spectrum Eq. (57), yields a convenient equation for the spectrum,

$$-2\eta_{\mathbf{k}}^I S_{\mathbf{k}} = \int dX 4\pi ReI_{\mathbf{k},\mathbf{k}',\mathbf{k}''} C_{\mathbf{k},\mathbf{k}',\mathbf{k}''}^2 S_{\mathbf{k}'} S_{\mathbf{k}''}. \tag{67}$$

This last equation, Eq. (67), demonstrates the physical picture that, in the steady state, the spectrum, $S_{\mathbf{k}}$, is proportional to the ratio of nonlinear drive (via the $S_{\mathbf{k}'} S_{\mathbf{k}''}$ term) to nonlinear damping, $\eta_{\mathbf{k}}^I$. The nonlinear drive is due to the three wave process where a spectral quanta at $\mathbf{k}'$ interacts with one at $\mathbf{k}''$ to produce one at $\mathbf{k}$. The nonlinear damping

is a result of linear wave particle interaction plus nonlinear wave–wave interaction, where a spectral quanta at $\mathbf{k}$ interacts with a second quanta to produce a third quanta.

If this spectrum problem had been formulated without renormalizing the propagator, as demonstrated in the weak turbulence section, then it would not be possible to integrate for the interaction time, $ReI_{\mathbf{k},\mathbf{k}',\mathbf{k}''}$, of the triplets. Some of the triplets are linearly unstable ($\gamma_T = \gamma_{\mathbf{k}} + \gamma_{\mathbf{k}'} + \gamma_{\mathbf{k}''} > 0$), so that the integral would diverge. However, when the resonance function is defined in this renormalized version of the spectrum problem, the nonlinear growth rates, $\eta^I_{\mathbf{k}}$, are nonlinearly coupled to the spectrum [Eqs. (64) and (67)] and can adjust to become negative, $\eta^I_{\mathbf{k}} < 0$. In the limit that the nonlinear damping rate is zero, $\eta^I_{\mathbf{k}} \to 0$, so that there is no width in the frequency spectrum, the resonance function implies a nonlinear frequency, $\eta^R_{\mathbf{k}}$, selection rule, since $ReI_{\mathbf{k},\mathbf{k}',\mathbf{k}''} \mid_{\eta^I_T \to 0} \to \delta(\Delta\eta^R) = \delta(\eta^R_{\mathbf{k}} - \eta^R_{\mathbf{k}'} - \eta^R_{\mathbf{k}''})$. This produces an expansion about spectra of nonlinear real frequency that satisfy the above selection rule, and is similar to the linear real frequency expansion found in weak turbulence theory.

An equation similar to Eq. (63), for the nonlinear complex frequency, was derived by Kraichnan [13] while searching for an approximate solution of the wave number spectrum, by using the time domain DIA equations in the fluid turbulence limit ($\Omega_{\mathbf{k},\omega} \to \Omega_{\mathbf{k}}$). At first, Kraichnan [13] did not obtain the three wave symmetric resonance function, Eq. (12). However, by using a Fokker–Planck type formulation of the spectrum problem, Edwards [14] obtained this symmetric result. Later, Kraichnan [15] developed a revised version of the DIA, which employed a semi–Lagrangian–Eulerian formulation, and produced the symmetric resonance function, Eq. (62).

In the above reduction of the spectrum problem to wave number space, the derived wave number dependent linear complex frequencies, $\Omega_{\mathbf{k}}$, involve frequency moments over the spectrum, $\Omega_{\mathbf{k}} \equiv \int d\omega \Omega_{\mathbf{k},\omega} R_{\mathbf{k},\omega}$. For the fluid limit of the spectrum problem, the linear frequency, $\omega_{\mathbf{k}}$, and growth rate, $\gamma_{\mathbf{k}}$, are unchanged in the wave number reduced spectrum problem, since $\int d\omega R_{\mathbf{k},\omega} = 1$. For the general plasma spectrum problem, where the drift wave growth rate is a function of frequency as well as wave number, the frequency moment integral presents a problem if the Lorentzian frequency function is used. The width of a Lorentzian function is usually defined as the width at half maximum, $R_{\mathbf{k},\eta^R_{\mathbf{k}} \pm \text{width}} \equiv 1/2 R_{\mathbf{k},\eta^R_{\mathbf{k}}} \to \text{width} = \eta^I_{\mathbf{k}}$, although the variance or higher moments of the Lorentzian are not convergent, $\int d\omega \omega^2 R_{\mathbf{k},\omega} \to \infty$.

The problem associated with the Lorentzian can be traced back to the original renormalization prescription of the potential fluctuation equation, where the nonlinear complex

frequency shift, $\delta\eta_{\mathbf{k},\omega}$, was formally added to the propagator. The propagator then had the form

$$G_{\mathbf{k},\omega} = \frac{1}{2\pi}\frac{1}{-i(\omega - \eta_{\mathbf{k},\omega})},$$

where

$$G_{\mathbf{k},\omega} + G^*_{\mathbf{k},\omega} = \frac{1}{\pi}\frac{-\eta^I_{\mathbf{k},\omega}}{(\eta^R_{\mathbf{k},\omega})^2 + (\eta^I_{\mathbf{k},\omega})^2}$$

is a Lorentzian function if $\eta_{\mathbf{k},\omega} \to \eta_{\mathbf{k}}$. This led to a seemingly natural choice for the spectrum, $S_{\mathbf{k},\omega}$, of the Lorentzian form with $\eta_{\mathbf{k},\omega} \to \eta_{\mathbf{k}}$. However, when the nonlinear complex frequency, $\eta_{\mathbf{k},\omega}$, is generally dependent on frequency, ω, the real part of the propagator, $G_{\mathbf{k},\omega}+G^*_{\mathbf{k},\omega}$, is not at all of a Lorentzian form. The formulation of the spectrum equations is general so that other choices of trial solutions can be made. The renormalized equations describing the spectrum can be written in terms of a propagator, $G_{\mathbf{k},\omega}$, and a spectrum, $S_{\mathbf{k},\omega}$, instead of a nonlinear complex frequency, $\eta_{\mathbf{k},\omega}$, and a spectrum. By doing this it is clear that there is freedom to choose any trial functions for the spectrum, $S_{\mathbf{k},\omega}$, and the propagator, $G_{\mathbf{k},\omega}$. In fact, if a Gaussian is chosen, the problem encountered with the Lorentzian will not occur, since the Gaussian function has the property that all moments exist.

2. Gaussian Line Shape

Let us now reexamine the spectrum choice, by starting with the nonlinear coupled set of integral equations expressed in terms of the propagator, $G_{\mathbf{k},\omega}$, and the spectrum, $S_{\mathbf{k},\omega}$, as opposed to the nonlinear complex frequency, $\eta_{\mathbf{k},\omega}$, and the spectrum, $S_{\mathbf{k},\omega}$. Here we are looking for a representation of the spectrum problem which permits, in a simple manner, the use of general choices for the frequency spectrum trial functions. Using the definition of the propagator, Eq. (32), in Eq. (47) produces the equation for the spectrum,

$$\begin{aligned} -i(\omega - \Omega_{\mathbf{k},\omega})S_{\mathbf{k},\omega} = \int dX[&4\pi C^2_{\mathbf{k},\mathbf{k}',\mathbf{k}''}G^*_{\mathbf{k},\omega}S_{\mathbf{k}',\omega'}S_{\mathbf{k}'',\omega''} \\ &- 8\pi C_{\mathbf{k},\mathbf{k}',\mathbf{k}''}C_{\mathbf{k}',\mathbf{k}'',\mathbf{k}}S_{\mathbf{k},\omega}G_{\mathbf{k}',\omega'}S_{\mathbf{k}'',\omega''}]. \end{aligned} \tag{68}$$

The propagator equation is obtained from Eq. (42) by letting $\Omega_{\mathbf{k}} \to \Omega_{\mathbf{k},\omega}$,

$$-i(\omega - \Omega_{\mathbf{k},\omega})G_{\mathbf{k},\omega} = -\int dX 4\pi C_{\mathbf{k},\mathbf{k}',\mathbf{k}''}C_{\mathbf{k}',\mathbf{k}'',\mathbf{k}}2G_{\mathbf{k},\omega}G_{\mathbf{k}',\omega'}S_{\mathbf{k}'',\omega''} + \frac{1}{2\pi}. \tag{69}$$

By taking the real part of Eq. (68), the equation for the spectral energy follows,

$$-2\gamma_{\mathbf{k},\omega}S_{\mathbf{k},\omega} = \int dX[4\pi C^2_{\mathbf{k},\mathbf{k}',\mathbf{k}''}(G_{\mathbf{k},\omega} + G^*_{\mathbf{k},\omega})S_{\mathbf{k}',\omega'}S_{\mathbf{k}'',\omega''}$$
$$- 8\pi C_{\mathbf{k},\mathbf{k}',\mathbf{k}''}C_{\mathbf{k}',\mathbf{k}'',\mathbf{k}}S_{\mathbf{k},\omega}(G_{\mathbf{k}',\omega'} + G^*_{\mathbf{k}',\omega'})S_{\mathbf{k}'',\omega''}]. \tag{70}$$

There is a symmetry among the triplet driving terms for the spectrum and propagator equations, Eqs. (68) and (69), displayed by interchanging $S_{\mathbf{k},\omega}$ and $G_{\mathbf{k},\omega}$. This is the same symmetry, noted in the previous section, between the real part of the propagator, $R_{\mathbf{k},\omega} \equiv G_{\mathbf{k},\omega} + G^*_{\mathbf{k},\omega}$, and the spectrum, $S_{\mathbf{k},\omega}$, for the energy equation, Eq. (70), and the real part of the propagator equation, to be derived. It should also be realized that the spectrum, $S_{\mathbf{k},\omega}$, may be proportional to the real part of the propagator, $R_{\mathbf{k},\omega}$, but not simply to the propagator, $G_{\mathbf{k},\omega}$, since $S_{\mathbf{k}}(\tau)$ and $R_{\mathbf{k}}(\tau)$ are both two sided Fourier inverse time functions, but $G_{\mathbf{k}}(\tau)$ is one sided. Consequently, as was done in the previous section, it is a useful simplifying assumption to make an ansatz such that the spectrum is proportional to the real part of the propagator,

$$S_{\mathbf{k},\omega} \rightarrow S_{\mathbf{k}}R_{\mathbf{k},\omega}, \tag{71}$$

where the real part of the propagator is normalized to one, $\int d\omega R_{\mathbf{k},\omega} = 1$.

The spectrum problem has been reduced to the evaluation of the normalized spectrum, $R_{\mathbf{k},\omega}$. An appealing choice for the normalized spectral frequency trial function is a Gaussian,

$$R_{\mathbf{k},\omega} \rightarrow \frac{1}{\pi^{1/2}|\eta^I_{\mathbf{k}}|}exp[-(\frac{\omega - \eta^R_{\mathbf{k}}}{\eta^I_{\mathbf{k}}})^2], \tag{72}$$

since it has the same type of characteristics as the Lorentzian with a well defined real frequency centroid, $\eta^R_{\mathbf{k}}$, and a spectral frequency width, $\eta^I_{\mathbf{k}}$, for each wave number. However, unlike the Lorentzian, the Gaussian has the property that all frequency moments are well defined. Inverse Fourier transforming the normalized spectrum, $R_{\mathbf{k},\omega}$, gives

$$R_{\mathbf{k}}(\tau) = exp[-i\eta^R_{\mathbf{k}}\tau - \frac{1}{4}(\eta^I_{\mathbf{k}}\tau)]^2, \tag{73}$$

where $R_{\mathbf{k}}(\tau)$ is the spectral correlation function. The inverse Fourier transform of the propagator, $G_{\mathbf{k},\omega}$, is

$$G_{\mathbf{k}}(\tau) = \begin{cases} R_{\mathbf{k}}(\tau), & \tau > 0 \\ 0, & \tau < 0 \end{cases} = \begin{cases} \exp[-i\eta^R_{\mathbf{k}}\tau - \frac{1}{4}(\eta^I_{\mathbf{k}}\tau)^2], & \tau > 0 \\ 0, & \tau < 0 \end{cases} \tag{74}$$

It should be noted that the spectrum problem posed in terms of $S_{\mathbf{k},\omega}$ and $G_{\mathbf{k},\omega}$ is just as general as that in terms of $S_{\mathbf{k},\omega}$ and $\eta_{\mathbf{k},\omega}$. The normalized spectrum

$$R_{\mathbf{k},\omega} = \frac{1}{\pi} \frac{-\eta^I_{\mathbf{k},\omega}}{(\omega - \eta^R_{\mathbf{k},\omega})^2 + (\eta^I_{\mathbf{k},\omega})^2},$$

looks like a Lorentzian frequency function only when $\eta_{\mathbf{k},\omega} \rightarrow \eta_{\mathbf{k}}$, and in general there is no simple relation between $\eta_{\mathbf{k}}$, used as a parameter, and the original $\eta_{\mathbf{k},\omega}$. This can be made quite clear if the relation between $\eta_{\mathbf{k}}$ and $\eta_{\mathbf{k},\omega}$ is explicitly written out for the Gaussian trial function,

$$R_{\mathbf{k},\omega} \equiv \frac{1}{\pi} \frac{-\eta^I_{\mathbf{k},\omega}}{(\omega - \eta^R_{\mathbf{k},\omega})^2 + (\eta^I_{\mathbf{k},\omega})^2} \rightarrow \frac{1}{\pi^{1/2}|\eta^I_{\mathbf{k}}|} \exp\left[-\left(\frac{\omega - \eta^R_{\mathbf{k}}}{\eta^I_{\mathbf{k}}}\right)^2\right].$$

The above equation demonstrates that if the Gaussian trial function choice is used for the normalized spectrum, $R_{\mathbf{k},\omega}$, then for the other representation, in order to produce the same Gaussian choice, the choice of the nonlinear complex frequency, $\eta_{\mathbf{k},\omega}$, would have to be a complicated expression. In this case, the choice for $\eta_{\mathbf{k},\omega}$, picked to fit the Gaussian, and the $\eta_{\mathbf{k}}$ used as a parameter for the Gaussian, would be drastically different functions.

As in the previous section, the equation for the wave number spectrum, $S_{\mathbf{k}}$, is derived by integrating Eq. (70) for the spectrum, $S_{\mathbf{k},\omega}$, over frequency and using the Gaussian trial function

$$-2\gamma_{\mathbf{k}} S_{\mathbf{k}} = \int dX 4\pi Re I_{\mathbf{k},\mathbf{k}',\mathbf{k}''} \left[C^2_{\mathbf{k},\mathbf{k}',\mathbf{k}''} S_{\mathbf{k}'} S_{\mathbf{k}''} - 2C_{\mathbf{k},\mathbf{k}',\mathbf{k}''} C_{\mathbf{k}',\mathbf{k}'',\mathbf{k}} S_{\mathbf{k}} S_{\mathbf{k}''}\right], \tag{75}$$

where the frequency integrated growth rate is $\gamma_{\mathbf{k}} \equiv \int d\omega \gamma_{\mathbf{k},\omega} R_{\mathbf{k},\omega}$. The resonance function, $Re I_{\mathbf{k},\mathbf{k}',\mathbf{k}''}$, is obtained by doing a contour integral,

$$ReI_{\mathbf{k},\mathbf{k}',\mathbf{k}''} \equiv \int d\omega R_{\mathbf{k},\omega} \int d\omega\prime R_{\mathbf{k}\prime,\omega\prime} R_{\mathbf{k}\prime\prime,\omega-\omega\prime\prime} = \frac{1}{\pi^{1/2}|\eta_T^I|} \exp\left[-(\Delta\eta^R/\eta_T^I)^2\right], \qquad (76)$$

where the triplet nonlinear frequency mismatch, $\Delta\eta^R$, and the triplet nonlinear growth rate sum, η_T^I is

$$\Delta\eta^R \equiv \eta_{\mathbf{k}}^R - \eta_{\mathbf{k}\prime}^R - \eta_{\mathbf{k}\prime\prime}^R$$

and

$$\eta_T^I \equiv \left[(\eta_{\mathbf{k}}^I)^2 + (\eta_{\mathbf{k}\prime}^I)^2 + (\eta_{\mathbf{k}\prime\prime}^I)^2\right]^{1/2}. \qquad (77)$$

This Gaussian resonance function has the same structure as the Lorentzian resonance function Eq. (56), with the same limit of zero nonlinear damping rate,

$$ReI_{\mathbf{k},\mathbf{k}',\mathbf{k}''} \Big|_{\eta_T^I \to 0} \to \delta(\Delta\eta^R) = \delta(\eta_{\mathbf{k}}^R - \eta_{\mathbf{k}\prime}^R - \eta_{\mathbf{k}\prime\prime}^R),$$

resulting in a nonlinear real frequency selection rule in Eq. (75) for the spectrum.

Equation (69) for the propagator is used to construct an equation for the nonlinear complex frequency, $\eta_{\mathbf{k}}$. Prior to this derivation it is necessary to obtain the complete complex form of the propagator, $G_{\mathbf{k},\omega}$, so that the complex frequency, $\eta_{\mathbf{k}}$, can be determined. The propagator, $G_{\mathbf{k},\omega}$, is obtained by taking the frequency Fourier transform of Eq. (74), after performing a contour integral, the result is

$$G_{\mathbf{k},\omega} = \frac{1}{2\pi^{1/2}|\eta_{\mathbf{k}}^I|} \exp\left[-\left(\frac{\omega - \eta_{\mathbf{k}}^R}{\eta_{\mathbf{k}}^I}\right)^2\right]\left[1 + erf\left(i\frac{\omega - \eta_{\mathbf{k}}^R}{|\eta_{\mathbf{k}}^I|}\right)\right]. \qquad (77)$$

Here, erf(ix) is the well known error function of imaginary argument. Note that the propagator satisfies, as it must, the defining relation,

$$G_{\mathbf{k},\omega} + G_{\mathbf{k},\omega}^{\wedge} = \frac{1}{\pi^{1/2}|\eta_{\mathbf{k}}^I|} exp[-(\frac{\omega - \eta_{\mathbf{k}}^R}{\eta_{\mathbf{k}}^I})^2] = R_{\mathbf{k},\omega}.$$

To form a closed coupled set of equations describing the spectrum, an equation for the nonlinear complex frequency, $\eta_{\mathbf{k}}$, must be derived. This is obtained by forming an equation for the normalized spectrum, $R_{\mathbf{k},\omega}$, similar to Eq. (59) for the Lorentzian approximation, where multiplying the propagator Eq. (69) by $R_{\mathbf{k},\omega}/G_{\mathbf{k},\omega}$, produces the result,

$$-i(\omega - \Omega_{\mathbf{k},\omega})R_{\mathbf{k},\omega} = -\int dX 4\pi C_{\mathbf{k},\mathbf{k}',\mathbf{k}''}C_{\mathbf{k}',\mathbf{k}'',\mathbf{k}}2R_{\mathbf{k},\omega}G_{\mathbf{k}',\omega'}S_{\mathbf{k}'',\omega''} + \frac{1}{2\pi}\frac{R_{\mathbf{k},\omega}}{G_{\mathbf{k},\omega}}. \quad (78)$$

Integrating the correlation Eq. (78) over frequency produces the equation for the nonlinear complex frequency, $\eta_{\mathbf{k}}$,

$$\int d\omega(-i\omega R_{\mathbf{k},\omega}) + i\int d\omega\Omega_{\mathbf{k},\omega}R_{\mathbf{k},\omega} = -\int dX 4\pi C_{\mathbf{k},\mathbf{k}',\mathbf{k}''}C_{\mathbf{k}',\mathbf{k}'',\mathbf{k}}S_{\mathbf{k}''}$$
$$\times 2\int d\omega R_{\mathbf{k},\omega}\int d\omega' G_{\mathbf{k}',\omega'}R_{\mathbf{k}'',\omega-\omega'} + \frac{1}{2\pi}\int d\omega\frac{R_{\mathbf{k},\omega}}{G_{\mathbf{k},\omega}}. \quad (79)$$

The integrals on the left hand side of Eq. (79) are straightforward,

$$\int d\omega(-i\omega R_{\mathbf{k},\omega}) = \frac{d}{dt}R_{\mathbf{k}}(t)\ \Big|_{t=0} = -i\eta^R_{\mathbf{k}} - \frac{1}{2}(\eta^I_{\mathbf{k}})^2 t\ \Big|_{t=0} = -i\eta^R_{\mathbf{k}}, \quad (80)$$

and

$$\int d\omega\Omega_{\mathbf{k},\omega}R_{\mathbf{k},\omega} \equiv \omega_{\mathbf{k}} + i\gamma_{\mathbf{k}}. \quad (81)$$

The resonance function integral on the right hand side of Eq. (79) is calculated similar to Eq. (62), where the contour integral is evaluated exactly like the derivation of Eq. (78), and the result is

$$I_{\mathbf{k},\mathbf{k}',\mathbf{k}''} = \frac{1}{\pi^{1/2}|\eta^I_T|}\exp\left[-(\Delta\eta^R/\eta^I_T)^2\right]\left[1 + erf\left(i\frac{\Delta\eta^R}{|\eta^I_T|}\right)\right]. \quad (82)$$

The final integral on the right hand side of Eq. (79) is

$$\frac{1}{2\pi}\int d\omega\frac{R_{\mathbf{k},\omega}}{G_{\mathbf{k},\omega}} = \frac{1}{\pi}\int d\omega\frac{1}{1 + erf\left(i\frac{\omega-\eta^R_{\mathbf{k}}}{|\eta^I_{\mathbf{k}}|}\right)} = \frac{1}{\pi}\int d\omega\frac{1}{1 + erf\left(i\frac{\omega}{|\eta^I_{\mathbf{k}}|}\right)}.$$

With the use of the parity of $erf(ix)$, $erf(ix) = -erf(-ix)$, the final expression is

$$\frac{1}{2\pi}\int d\omega\frac{R_{\mathbf{k},\omega}}{G_{\mathbf{k},\omega}} = \frac{1}{\pi}\int d\omega\frac{1}{1 + \left|erf\left(i\frac{\omega}{|\eta^I_{\mathbf{k}}|}\right)\right|^2} = F\left|\eta^I_{\mathbf{k}}\right|, \quad (83)$$

where

$$F \equiv \frac{1}{\pi}\int_{-\infty}^{\infty} dx \frac{1}{1+|erf(ix)|^2} = \frac{2}{\pi}\int_{0}^{\infty} dx \frac{1}{1+\frac{4}{\pi}(\int_0^x dt e^{t^2})^2} \approx .49. \tag{84}$$

The value for F is obtained by numerical integration. Finally, using Eqs. (80), (81), (82), and (83) in Eq. (79), with $-\eta_{\mathbf{k}}^I > 0$, results in the equation for the nonlinear complex frequency, $\eta_{\mathbf{k}}$,

$$-i\eta_{\mathbf{k}}^R + i(\omega_{\mathbf{k}} + i\gamma_{\mathbf{k}}) = -\int dX 4\pi I_{\mathbf{k},\mathbf{k}',\mathbf{k}''} C_{\mathbf{k},\mathbf{k}',\mathbf{k}''} C_{\mathbf{k}',\mathbf{k}'',\mathbf{k}} S_{\mathbf{k}''} - F\eta_{\mathbf{k}}^I,$$

or multiplying by i gives

$$\eta_{\mathbf{k}}^R + iF\eta_{\mathbf{k}}^I = \Omega_{\mathbf{k}} - i\int dX 4\pi I_{\mathbf{k},\mathbf{k}',\mathbf{k}''} C_{\mathbf{k},\mathbf{k}',\mathbf{k}''} C_{\mathbf{k}',\mathbf{k}'',\mathbf{k}} S_{\mathbf{k}''}. \tag{85}$$

This equation is identical to Eq. (63) derived for the Lorentzian approximation except for the factor F in front of the $\eta_{\mathbf{k}}^I$ term. Taking the real part of Eq. (85) produces the equation for the nonlinear frequency, $\eta_{\mathbf{k}}^R$,

$$\eta_{\mathbf{k}}^R = \omega_{\mathbf{k}} + \int dX 4\pi ImI_{\mathbf{k},\mathbf{k}',\mathbf{k}''} C_{\mathbf{k},\mathbf{k}',\mathbf{k}''} C_{\mathbf{k}',\mathbf{k}'',\mathbf{k}} S_{\mathbf{k}''}, \tag{86}$$

and taking the imaginary part produces the equation for the nonlinear frequency width or growth rate, $\eta_{\mathbf{k}}^I$,

$$F\eta_{\mathbf{k}}^I = \gamma_{\mathbf{k}} - \int dX 4\pi ReI_{\mathbf{k},\mathbf{k}',\mathbf{k}''} C_{\mathbf{k},\mathbf{k}',\mathbf{k}''} C_{\mathbf{k}',\mathbf{k}'',\mathbf{k}} S_{\mathbf{k}''}. \tag{87}$$

A convenient equation for the spectrum is obtained by combining Eqs. (75) and (87),

$$-2F\eta_{\mathbf{k}}^I S_{\mathbf{k}} = \int dX 4\pi ReI_{\mathbf{k},\mathbf{k}',\mathbf{k}''} C_{\mathbf{k},\mathbf{k}',\mathbf{k}''}^2 S_{\mathbf{k}'} S_{\mathbf{k}''}. \tag{88}$$

The form of the final equations describing the spectrum for this Gaussian trial function are identical to those for the Lorentzian, except for the numerical factor F. It does seem reasonable that there should be a slight numerical difference between the two models in taking moments, since the parameter $\eta_{\mathbf{k}}^I$ has somewhat different meanings in the two models. The main virtue of the Gaussian frequency function is that the spectral weighted average of the complex frequency, $\Omega_{\mathbf{k}} = \omega_{\mathbf{k}} + i\gamma_{\mathbf{k}} = \int d\omega \Omega_{\mathbf{k},\omega} R_{\mathbf{k},\omega}$, is well defined for a general frequency dependent growth rate, $\gamma_{\mathbf{k},\omega}$.

B. Spectral Trial Function: Wave Number

The set of nonlinear coupled integral equations for the wave number spectrum, $S_{\mathbf{k}}$, and frequency width, $\eta_{\mathbf{k}}^I$, are solved to first order by choosing a spectral wave number trial function dependent on a set of basic parameters describing the spectrum (E – the total integrated spectral amplitude, Δk – the wave number width, and W – the average spectral frequency width). By taking wave number moments of the integral equations, a coupled set of nonlinear algebraic equations for the unknown first order parameters is obtained. The parameters are then determined, which results in the approximate analytic solution of the spectrum.

The analytic technique for solving the nonlinear spectrum equations might be of interest for application to other problems. This formulation of the spectrum solution is based on obtaining three parameters describing the spectrum. However, the solution technique is easily generalized to more parameters.

In Sec. 1., the moment equation method is presented. In Sec. 2., the equations describing the next order correction to the first order solution are formally obtained, which enable a calculation of the parameters to second order accuracy. As mentioned previously, the parameters of the theory may be obtained to second order by an alternate nonlinear variational calculation, which may or may not be easier to implement than the present method. In Sec. 3., the solution technique is applied to a model problem studied by Waltz [3], and the results are compared with the numerical solution. Finally, in Sec. 4., the saturated state drift wave spectrum is obtained for the renormalized electron dissipation model derived in the NSA [16]. The spectrum for this final drift wave problem is solved self–consistently. The renormalized electron dissipation is a functional of the spectrum, as a consequence of the broadened resonance theory. This additional nonlinear dependence is included while solving the spectrum equation. An iterative procedure is employed to yield the spectrum saturation level consistent with the electron dissipation used to drive this spectrum.

The following analysis is done in terms of scaled dimensionless variables. The unit of length is ρ_S so that the wave number transforms as $\rho_S k \rightarrow k$. The unit of time is $1/\Omega_i(\rho_s/L_n)$ so that the frequencies transform as $[\omega_{\mathbf{k}}, \gamma_{\mathbf{k}}, \eta_{\mathbf{k}}]/\Omega_i(\rho_S/L_n) \rightarrow [\omega_{\mathbf{k}}, \gamma_{\mathbf{k}}, \eta_{\mathbf{k}}]$. The transformation to a dimensionless potential being $(e/T_e)(\rho_S/L_n)^{-1}\phi \rightarrow \phi$ indicates that the spectrum transformation is $(e/T_e)^2(\rho_S/L_n)^{-2}S \rightarrow S$. The linear frequency and

coupling coefficient are

$$\omega_{\mathbf{k}} = k_y/(1+k^2) and C_{\mathbf{k},\mathbf{k}',\mathbf{k}''} = \frac{1}{2}(k'_x k''_y - k'_y k''_z)(k''^2 - k'^2)/(1+k^2),$$

where $\omega_e^* = k_y$.

1. Moment Equation Method

The moment equation technique can either be applied to the wave number integral equations obtained by using the Lorentz or Gaussian spectral frequency trial functions. The following calculations for the spectrum are made with the approximation that the nonlinear frequency shift is small compared to the linear frequency so that $\eta_{\mathbf{k}}^R \approx \omega_{\mathbf{k}}$. This approximation is consistent with Eq. (86) for the nonlinear frequency, $\eta_{\mathbf{k}}^R$, where $ImI_{\mathbf{k},\mathbf{k}',\mathbf{k}''}$, Eq. (62) or Eq. (82), tends to zero for $\Delta\omega \equiv \omega_{\mathbf{k}} - \omega_{\mathbf{k}'} - \omega_{\mathbf{k}''}$ tending to zero, which is a good approximation for many triplet interactions. The equations to be solved are Eqs. (75) and (88), and for simplicity of solution the equation obtained by subtracting one half of Eq. (75) from one half of Eq. (88) is also used,

$$(\gamma_{\mathbf{k}} - F\eta_{\mathbf{k}}^I)S_{\mathbf{k}} = \int dX 4\pi ReI_{\mathbf{k},\mathbf{k}',\mathbf{k}''} C_{\mathbf{k},\mathbf{k}',\mathbf{k}''} C_{\mathbf{k}',\mathbf{k}'',\mathbf{k}} S_{\mathbf{k}''} S_{\mathbf{k}}. \tag{90}$$

The Lorentzian frequency trial function corresponds to $F = 1$, and the Gaussian to $F = .49$, where the appropriate functions are Eq. (51) and Eq. (72), respectively.

An approximate solution for the wave number spectrum, $S_{\mathbf{k}}$, is obtaind by using a wave number trial function dependent on two parameters, the total integrated amplitude, $E \equiv \int d\mathbf{k} S_{\mathbf{k}}$, and the wave number width, $\Delta k \equiv (E^{-1}\int d\mathbf{k} k^2 S_{\mathbf{k}})^{1/2}$. The set of equations describing the total spectrum problem, entails two equations in two unknowns, the spectrum, $S_{\mathbf{k}}$, and the frequency width, $\eta_{\mathbf{k}}^I$. The trial form for $\eta_{\mathbf{k}}^I$ is taken to be a function of wave number and a third parameter, the average frequency width, $W \equiv 1/E\int d\mathbf{k}\eta_{\mathbf{k}}^I S_{\mathbf{k}}$. These trial functions are substituted into the spectrum equations and a set of three independent moment equations for the three unknown parameters are obtained by applying the moments $M_i = \int d\mathbf{k} H_{i_{\mathbf{k}}}[i^{th} Eq.]$, $i = 1,2,3$, one to each of the Eqs. (75), (88), and (90). The $H_{i_{\mathbf{k}}}$ are selected weighting functions. The parameters in the nonlinear algebraic moment equations are the leading order approximations to the corresponding parameters of the true solution.

The first moment equation, obtained by applying M_1 to Eq. (75), is an energy conservation dissipative constraint. The nonlinear polarization drift mode coupling satisfies

energy conservation. The mode coupling for the renormalized spectrum equation also conserves energy, as it should. Energy conservation arguments applied to the spectrum equation, Eq. (75), are given below, where the total wave energy density using scaled dimensionless variables is

$$\mathcal{W} = \int d\mathbf{k}d\omega \frac{\partial}{\partial\omega}(\omega D^R_{\mathbf{k},\omega})\mathcal{E}_{\mathbf{k},\omega} = \int d\mathbf{k}d\omega \frac{\partial}{\partial\omega}(\omega D^R_{\mathbf{k},\omega})\frac{k^2}{8\pi}S_{\mathbf{k},\omega} = \int d\mathbf{k}\frac{\rho_s^2}{8\pi\lambda_e^2}[1+k^2]S_{\mathbf{k}}. \tag{91}$$

By taking the weighting function $H_{1_{\mathbf{k}}} \equiv 1 + k^2$, and applying this to Eq. (75), the rate of change of the wave energy density can be determined. The right hand side of the energy moment equation is then evaluated as follows,

$$M_1 = \int d\mathbf{k}d\mathbf{k}'d\mathbf{k}''\delta(\mathbf{k}-\mathbf{k}'-\mathbf{k}'')4\pi ReI_{\mathbf{k},\mathbf{k}',\mathbf{k}''}(1+k^2)$$
$$\times C_{\mathbf{k},\mathbf{k}',\mathbf{k}''}[C_{\mathbf{k},\mathbf{k}',\mathbf{k}''}S_{\mathbf{k}'}S_{\mathbf{k}''} - C_{\mathbf{k}',\mathbf{k}'',\mathbf{k}}S_{\mathbf{k}''}S_{\mathbf{k}} - C_{\mathbf{k}'',\mathbf{k}',\mathbf{k}}S_{\mathbf{k}'}S_{\mathbf{k}}], \tag{92}$$

where the coupling symmetry, $C_{\mathbf{k},\mathbf{k}',\mathbf{k}''} = C_{\mathbf{k},\mathbf{k}'',\mathbf{k}'}$, was used to write out the last two coupling terms. Using the definition of the coupling coefficient, $C_{\mathbf{k},\mathbf{k}',\mathbf{k}''} = (1/2)(k'_x k''_y - k'_y k''_x)(k''^2 - k'^2)/(1+k^2)$, and making the change of variables $\mathbf{k}' \to \mathbf{k}''$, $\mathbf{k}'' \to \mathbf{k}'$, $\mathbf{k} \to \mathbf{k}$, the resonance function and spectrum are unchanged, so that the following replacement can be made, $(1+k^2)C_{\mathbf{k},\mathbf{k}',\mathbf{k}''} \to (k'_x k''_y - k'_y k''_x)k''^2$. Using the delta function, the result is $(k'_x k_y - k'_y k_x)k''^2$. The M_1 moment is then

$$M_1 = \int d\mathbf{k}d\mathbf{k}'d\mathbf{k}''\delta(\mathbf{k}-\mathbf{k}'-\mathbf{k}'')4\pi ReI_{\mathbf{k},\mathbf{k}',\mathbf{k}''}(k'_x k_y - k'_y k_x)k''^2$$
$$\times [C_{\mathbf{k},\mathbf{k}',\mathbf{k}''}S_{\mathbf{k}'}S_{\mathbf{k}''} - C_{\mathbf{k}',\mathbf{k}'',\mathbf{k}}S_{\mathbf{k}''}S_{\mathbf{k}} - C_{\mathbf{k}'',\mathbf{k}',\mathbf{k}}S_{\mathbf{k}'}S_{\mathbf{k}}]. \tag{93}$$

Making the final change of variables $\mathbf{k} \to \mathbf{k}'$, $\mathbf{k}' \to \mathbf{k}$, $\mathbf{k}'' \to -\mathbf{k}''$ in the first term results in $k'_x k_y \to k_x k'_y$. With this transformation the delta function is unchanged due to its even parity. The mode coupling terms interchange among themselves so that there is no net change due to the coupling symmetries, $C_{\mathbf{k},\mathbf{k}',\mathbf{k}''} = C_{\mathbf{k},\mathbf{k}'',\mathbf{k}'} = -C_{\mathbf{k},\mathbf{k}',-\mathbf{k}''}$, and the spectrum reality condition, $S_{\mathbf{k}} = S_{-\mathbf{k}}$. The resonance function is also unchanged due to the frequency and growth rate reality conditions, $\eta^R_{\mathbf{k}} = -\eta^R_{-\mathbf{k}}$ and $\eta^I_{\mathbf{k}} = \eta^I_{-\mathbf{k}}$. The M_1 moment result is

$$M_1 = \int d\mathbf{k}d\mathbf{k}'d\mathbf{k}''\delta(\mathbf{k}-\mathbf{k}'-\mathbf{k}'')4\pi ReI_{\mathbf{k},\mathbf{k}',\mathbf{k}''}(k_xk'_y - k_xk'_y)k''^2$$
$$\times [C_{\mathbf{k},\mathbf{k}',\mathbf{k}''}S_{\mathbf{k}'}S_{\mathbf{k}''} - C_{\mathbf{k}',\mathbf{k}'',\mathbf{k}}S_{\mathbf{k}''}S_{\mathbf{k}} - C_{\mathbf{k}'',\mathbf{k}',\mathbf{k}}S_{\mathbf{k}'}S_{\mathbf{k}}] = 0. \quad (94)$$

Consequently, the energy moment, M_1, annihilates the right hand side of Eq. (75) to give the dissipative constraint for the steady state spectrum,

$$M_1 = \int d\mathbf{k}(1+k^2)\gamma_{\mathbf{k}}S_{\mathbf{k}} = 0. \quad (95)$$

The dissipative constraint, Eq. (95), demonstrates that the negative dissipation, unstable regions in wave number space must balance the positive dissipation, or damped, regions. The energy conservation of the mode coupling terms indicate that the coupling does not create or destroy energy but simply transfers, or mode couples, energy from sources to sinks. For the spectrum to satisfy this dissipative constraint, the parameters must adjust so that, in some sense, there is equal positive and negative dissipation averaged over the spectrum. The first moment equation, which utilizes M_1, produces an equation for the wave number width, or for the wave number width and the frequency width parameters, depending on the form of the dissipation. The total amplitude, E, factors out of this moment equation.

The second moment equation, which utilizes M_2, is obtained by selecting a weighting function, $H_{2_{\mathbf{k}}}$, and integrating over Eq. (88),

$$M_2 = \int d\mathbf{k}H_{2_{\mathbf{k}}}[-2F\eta^I_{\mathbf{k}}S_{\mathbf{k}}]$$
$$= \int d\mathbf{k}d\mathbf{k}'d\mathbf{k}''\delta(\mathbf{k}-\mathbf{k}'-\mathbf{k}'')4\pi ReI_{\mathbf{k},\mathbf{k}',\mathbf{k}''}H_{2_{\mathbf{k}}}C^2_{\mathbf{k},\mathbf{k}',\mathbf{k}''}S_{\mathbf{k}'}S_{\mathbf{k}''}. \quad (96)$$

This moment equation gives a condition for the total amplitude, E, in terms of the two other parameters. The third moment equation, which utilizes M_3, is also obtained by selecting a weighting function, $H_{3_{\mathbf{k}}}$, and integrating over Eq. (90),

$$M_3 = \int d\mathbf{k}H_{3_{\mathbf{k}}}(\gamma_{\mathbf{k}} - \eta^I_{\mathbf{k}})S_{\mathbf{k}}$$
$$= \int d\mathbf{k}d\mathbf{k}'d\mathbf{k}''\delta(\mathbf{k}-\mathbf{k}'-\mathbf{k}'')4\pi ReI_{\mathbf{k},\mathbf{k}',\mathbf{k}''}H_{3_{\mathbf{k}}}C_{\mathbf{k},\mathbf{k}',\mathbf{k}''}C_{\mathbf{k}',\mathbf{k}'',\mathbf{k}}S_{\mathbf{k}''}S_{\mathbf{k}}. \quad (97)$$

This final moment equation gives another condition for the total amplitude, E, in terms of the two other parameters.

The three nonlinear algebraic equations, obtained by applying the moments M_1, M_2, and M_3, are easily manipulated into the problem of solving one nonlinear algebraic equation in one unknown. This is due to the general structure of the spectrum integral equations and this particular simple choice of parameters and moment equations. In general, the three moment equations are of the form $P_i(E, \Delta k^2, W) = 0$, $i = 1, 2, 3$. However, in this case, the first moment gives a condition $P_1(\Delta k^2, W) = 0$, while the second and third moments can be written as the conditions $E = P_2(\Delta k^2, W)$ and $E = P_3(\Delta k^2, W)$. The final equation to be solved is then of the form $1 = P_3(\Delta k^2, W)/P_2(\Delta k^2, W)$, with the subsidiary condition $P_1(\Delta k^2, W) = 0$. Either the wave number width squared, Δk^2, or the average frequency width, W, can be used as the unknown parameter for which a solution search is carried out. If W is chosen, then the P_1 equation produces a Δk^2 for each W which is then used in the P_3/P_2 ratio equation. A search in the parameter W is made until the ratio, P_3/P_2, is one; the points at which this occurs are the solutions. In general, there may be a multiplicity of solutions, some of which can be ruled out on physical grounds.

2. Next Order Correction

The main objective in this section is a formal calculation of the next order corrections to the first order solution parameters. The equations governing the correction of the first order spectrum functions are derived. Given the solution of these equations, the parameter corrections can be determined.

The first order parameters are leading order approximations to the corresponding parameters of the true solution. The true parameters are defined in terms of the true solution functions, the spectrum, $S_{\mathbf{k}}$, and the frequency width, $\eta^I_{\mathbf{k}}$. The exact integrated amplitude, wave number spectral width squared, and frequency spectral width are $E \equiv \int d\mathbf{k} S_{\mathbf{k}}$, $\Delta k^2 \equiv (1/E) \int d\mathbf{k} k^2 S_{\mathbf{k}}$, and $W \equiv (1/E) \int d\mathbf{k} \eta^I_{\mathbf{k}} S_{\mathbf{k}}$, respectively. Equations are derived here, which give the next order approximation of these true solution parameters.

The solutions for the spectrum, $S_{\mathbf{k}}$, and frequency width, $\eta^I_{\mathbf{k}}$, are expressed as a sum of the first order solutions, $S^0_{\mathbf{k}}$ and $\eta^{I_0}_{\mathbf{k}}$, plus the correction solutions, $S^1_{\mathbf{k}}$ and $\eta^{I_1}_{\mathbf{k}}$,

$$S_{\mathbf{k}} = S^0_{\mathbf{k}} + S^1_{\mathbf{k}}, \quad \eta^I_{\mathbf{k}} = \eta^{I_0}_{\mathbf{k}} + \eta^{I_1}_{\mathbf{k}}. \tag{98}$$

The above solution separation, Eq. (98), is substituted into the spectrum integral Eqs. (75) and (88) in order to derive a set of equations for the correction functions. With the

assumption that the corrections are of second order compared to the first order solutions, which can be checked aposteriori, the Eqs. (75) and (88) are solved by separating out the first order equations, for $S^0_{\mathbf{k}}$ and $\eta^{I_o}_{\mathbf{k}}$, from the linearized equations for $S^1_{\mathbf{k}}$ and $\eta^{I_1}_{\mathbf{k}}$. The two sets of equations are

$$-2\gamma_{\mathbf{k}} S^0_{\mathbf{k}} = \int dX 4\pi ReI_{\mathbf{k},\mathbf{k}',\mathbf{k}''}[\eta_T^{I0}][C^2_{\mathbf{k},\mathbf{k}',\mathbf{k}''} S^0_{\mathbf{k}'} S^0_{\mathbf{k}''} - 2C_{\mathbf{k},\mathbf{k}',\mathbf{k}''} C_{\mathbf{k}',\mathbf{k}'',\mathbf{k}} S^0_{\mathbf{k}''} S^0_{\mathbf{k}}] - F_{\mathbf{k}}, \tag{99}$$

$$-2F\eta_T^{I0} S^0_{\mathbf{k}} = \int dX 4\pi ReI_{\mathbf{k},\mathbf{k}',\mathbf{k}''}[\eta_T^{I0}] C^2_{\mathbf{k},\mathbf{k}',\mathbf{k}''} S^0_{\mathbf{k}'} S^0_{\mathbf{k}''} - G_{\mathbf{k}}, \tag{100}$$

and

$$\begin{aligned} -2\gamma_{\mathbf{k}} S^1_{\mathbf{k}} = \int dX \Bigg\{ & \eta_T^{I_1} \frac{\partial}{\partial \eta_T^{I_o}} \left(4\pi ReI_{\mathbf{k},\mathbf{k}',\mathbf{k}''}[\eta_T^{I_o}] \right) \Big[C^2_{\mathbf{k},\mathbf{k}',\mathbf{k}''} S^o_{\mathbf{k}'} S^o_{\mathbf{k}''} \\ & - 2C_{\mathbf{k},\mathbf{k}',\mathbf{k}''} C_{\mathbf{k},\mathbf{k}',\mathbf{k}''} S^o_{\mathbf{k}''} S^o_{\mathbf{k}} \Big] \\ & + 4\pi ReI_{\mathbf{k},\mathbf{k}',\mathbf{k}''} \left[\eta^{I_o}_{\mathbf{k}} \right] \Big[C^2_{\mathbf{k},\mathbf{k}',\mathbf{k}''} (S^o_{\mathbf{k}'} S^1_{\mathbf{k}''} + S^1_{\mathbf{k}'} S^o_{\mathbf{k}''}) \\ & - 2C_{\mathbf{k},\mathbf{k}',\mathbf{k}''} C_{\mathbf{k},\mathbf{k}',\mathbf{k}''} (S^1_{\mathbf{k}''} S^o_{\mathbf{k}} + S^o_{\mathbf{k}''} S^1_{\mathbf{k}}) \Bigg\} + F_{\mathbf{k}} \end{aligned} \tag{101}$$

$$\begin{aligned} -2F(\eta^{I_o}_{\mathbf{k}} S^1_{\mathbf{k}} + \eta^{I_1}_{\mathbf{k}} S^o_{\mathbf{k}}) = \int dX \Bigg\{ & \eta_T^{I_o} \frac{\partial}{\partial \eta_T^{I_o}} \left(4\pi ReI_{\mathbf{k},\mathbf{k}',\mathbf{k}''}[\eta_T^{I_o}] \right) C^2_{\mathbf{k},\mathbf{k}',\mathbf{k}''} S^o_{\mathbf{k}'} S^o_{\mathbf{k}''} \\ & + 4\pi ReI_{\mathbf{k},\mathbf{k}',\mathbf{k}''}[\eta_T^{I_o}] C^2_{\mathbf{k},\mathbf{k}',\mathbf{k}''} (S^o_{\mathbf{k}'} S^1_{\mathbf{k}''} + S^1_{\mathbf{k}'} S^o_{\mathbf{k}''}) \Bigg\} + G_{\mathbf{k}}. \end{aligned} \tag{102}$$

The errors in the solutions of Eqs. (99) and (100) are expressed by $F_{\mathbf{k}}$ and $G_{\mathbf{k}}$.

The first order parameters, E^0, Δk^{0^2}, and W^0 are determined by the algebraic moment equations,

$$P_i(E^0, \Delta k^{0^2}, W^0) = 0, \quad i = 1, 2, 3 \tag{103}$$

derived by taking moments, $M_i = \int d\mathbf{k} H_{i_\mathbf{k}}[\ \ ]$, of Eqs. (99) and (100). Since the first order solutions, $S^0_\mathbf{k}$ and $\eta^0_\mathbf{k}$, are forced to be exact solutions of the moment equations, this imposes integral conditions on the errors, $F_\mathbf{k}$ and $G_\mathbf{k}$,

$$\int d\mathbf{k} H_1 F_\mathbf{k} = 0, \quad \int d\mathbf{k} H_2 G_\mathbf{k} = 0, \quad \int d\mathbf{k} H_3 (F_\mathbf{k} - G_\mathbf{k}) = 0. \tag{104}$$

The first order solutions, $S^0_\mathbf{k}$ and $\eta^{I_0}_\mathbf{k}$, when substituted in Eqs. (99) and (100), produce the error functions, $F_\mathbf{k}$ and $G_\mathbf{k}$. By substituting the known first order solutions and the error functions into Eqs. (101) and (102), a set of linear equations for the solution corrections, $S^1_\mathbf{k}$ and $\eta^{I_1}_\mathbf{k}$, are obtained of the form

$$\mathcal{L}_1[S^1_\mathbf{k}, \eta^{I_1}_\mathbf{k}] = F_\mathbf{k}, \quad \mathcal{L}_2[S^1_\mathbf{k}, \eta^{I_1}_\mathbf{k}] = G_\mathbf{k}. \tag{105}$$

The solution of these linear integral equations give the corrections to the first order solutions. Given these correction functions, $S^1_\mathbf{k}$ and $\eta^{I_1}_\mathbf{k}$, the parameter corrections can be obtained.

The exact integrated amplitude is $E \equiv \int d\mathbf{k} S_\mathbf{k}$. Using Eq. (98) this is $E = \int d\mathbf{k} S^0_\mathbf{k} + \int d\mathbf{k} S^1_\mathbf{k}$. With the definition for the first order integrated amplitude, $E^0 \equiv \int d\mathbf{k} S^0_\mathbf{k}$, and the amplitude correction, $E \equiv E^0 + E^1$, the equation for the correction of integrated amplitude is

$$E^1 = \int d\mathbf{k} S^1_\mathbf{k}. \tag{106}$$

For known $S^1_\mathbf{k}$, by solving Eq. (105), the amplitude correction is determined by Eq. (106).

The exact wave number spectral width squared is $\Delta k^2 \equiv 1/E \int d\mathbf{k} k^2 S_\mathbf{k}$. With the definition of the first order wave number spectral width squared, $\Delta k^{0^2} \equiv 1/E^0 \int d\mathbf{k} k^2 S^0_\mathbf{k}$, and the correction to the wave number width squared, $\Delta k^2 \equiv \Delta k^{0^2} \pm \Delta k^{1^2}$, the lowest order correction in wave number width number squared is

$$\pm \Delta k^{1^2} = \frac{1}{E^0} \int d\mathbf{k} k^2 S^1_\mathbf{k} - \left(\frac{E^1}{E^0} \right) \Delta k^{0^2}. \tag{107}$$

For known $S^1_\mathbf{k}$, the correction in wave number spectral width is obtained from Eqs. (106) and (107).

The exact average frequency spectral width is defined as $W \equiv 1/E \int d\mathbf{k} \eta_{\mathbf{k}}^{I} S_{\mathbf{k}}$. With the definition of the first order average frequency width, $W^0 \equiv 1/E^0 \int d\mathbf{k} \eta_{\mathbf{k}}^{I_0} S_{\mathbf{k}}^0$, and the correction in average frequency width, $W \equiv W^0 + W^1$, the lowest order correction in average frequency width is

$$W^1 = \frac{1}{E^0} \int d\mathbf{k} \eta_{\mathbf{k}}^{I_0} S_{\mathbf{k}}^1 + \frac{1}{E^0} \int d\mathbf{k} \eta_{\mathbf{k}}^{I_1} S_{\mathbf{k}}^0 - \left(\frac{E^1}{E^0} \right) W^0. \tag{108}$$

For known $S_{\mathbf{k}}^1$ and $\eta_{\mathbf{k}}^{I_1}$, the correction in average frequency spectral width is obtained from Eqs. (106) and (108). The parameter corrections, Eqs. (106), (107), and (108), are of the same order as the solution corrections, so that the parameters can then be obtained to second order accuracy. The above procedure can be iterated to determine higher order corrections to the solution of the coupled set of nonlinear integral equations.

3. Spectrum Solution of Model Problem

Presented in this section is an approximate analytic solution of the spectrum, which utilizes the moment technique, for a model dissipation problem proposed and solved numerically by Waltz [3]. In Ref. 3, numerical results are given for the solution of the renormalized spectrum equations for the Lorentzian frequency approximation, Eqs. (57), (64), and (65), as well as the solution of the original potential fluctuation equation, Eq. (5), for the fluid limit. The numerical study uses the approximation of analyzing 11×11 modes, ranging from -1 to $+1$ in k_x and k_y with a spacing of .2 between modes. Actually, there are only approximately one fourth this number of distinct modes. This is due to a combination of two spectral symmetries. The first is a consequence of the reality condition, $S_{\mathbf{k}} = S_{-\mathbf{k}}$, which reduces the number of distinct modes by one half. The second, a feature of the drift wave problem, is due to the k_x symmetry, $S_{k_x,k_y} = S_{-k_x,k_y}$, which finally reduces the number of distinct modes to one fourth the total number of modes.

Both numerical solutions of the spectrum, obtained by Waltz [3], agree reasonably well. The root mean square potentials, $\phi_{rms} \equiv (E)^{1/2}$, for the two numerical solutions, agree to within thirty percent, where $\phi_{rms} = 1.0$ for the integration of the dynamical potential equation, and $\phi_{rms} = 1.3$ for the numerical solution of the renormalized spectrum equations. The k_x averaged potential,

$$|\phi_{rms}|_{k_y} \equiv (S_{k_y})^{1/2}, \quad S_{k_y} \equiv \int dk_x S_{\mathbf{k}}, \tag{109}$$

and the spectral weighted k_x averaged frequency width, growth rate, and frequency,

$$\langle \begin{pmatrix} -\eta^I \\ \gamma \\ \omega \end{pmatrix} \rangle_{k_y} \equiv \int dk_x \begin{pmatrix} -\eta^I \\ \gamma \\ \omega \end{pmatrix} S_{\mathbf{k}} / S_{k_y}, \tag{110}$$

have very similar structures to the corresponding quantities for the two numerical solutions. However, there is quite a significant deviation, as much as a factor of two or three, between results on a mode by mode basis. Qualitative agreement is also obtained for a numerical solution of the spectrum, calculated by Terry and Horton [17], using the dynamical potential equation with a different model dissipation for the case of just twenty modes. The renormalized spectrum equations in the Lorentzian approximation seem to give a reasonably good description of the spectrum governed by the dynamical potential fluctuation equation. The analytic solution of the renormalized spectrum equations, using the moment method, derived in this section, is compared with the numerical solution ob-

tained by Waltz [3], and is shown to have very close agreement. This lends some credence to the accuracy of the moment method, even when carried out only to leading order.

The growth rate in Waltz's model is

$$\gamma_{\mathbf{k}} \rightarrow .06\left[1 - .5\left(\frac{|k_x| - .5}{.5}\right)^2 - .5\left(\frac{|k_y| - .5}{.5}\right)^2\right] - .05$$

$$= -.12k^2 + .12(|k_x| + |k_y|) - .05. \tag{111}$$

The main features of this growth rate are that it has a maximum drive, at $k_x = \pm.5$ and $k_y = \pm.5$, of $\gamma = .01$, and a maximum damping, at $k_x = k_y = 0$, or $k_x = \pm 1$ and $k_y = \pm 1$, of $\gamma = -.05$, for the k_x, k_y range [-1,1]. For $k_x = 0$ or $k_y = 0$ there is damping, $\gamma < 0$.

The Lorentzian frequency trial function,

$$S_{\mathbf{k},\omega} = \frac{1}{\pi}\frac{-\eta^I_{\mathbf{k}}}{(\omega - \omega_{\mathbf{k}})^2 + (\eta^I_{\mathbf{k}})^2} S_{\mathbf{k}}, \tag{112}$$

applied to the spectrum problem results in the coupled nonlinear integral Eqs. (75), (88), and (90) for the wave number spectrum, $S_{\mathbf{k}}$, and the wave number dependent frequency width, $\eta^I_{\mathbf{k}}$. Besides the features of the growth rate and spectrum symmetries, the boundary conditions on the spectrum and width functions help determine the best trial function. From Eq. (64) for the nonlinear growth rate or spectral width, $\eta^I_{\mathbf{k}}$, the condition at $k = 0$ is

$$\eta^I_0 = \gamma_0, \tag{113}$$

where use has been made of the coupling condition

$$C_{0,\mathbf{k}',-\mathbf{k}'} = 0. \tag{114}$$

Using Eq. (114) again gives the $k = 0$ limit of Eq. (67),

$$\eta^I_0 S_0 = 0. \tag{115}$$

The result obtained from Eqs. (113) and (115) is

$$S_0 = 0 \quad \text{and} \quad \eta_0^I = -.05. \tag{116}$$

In order that the spectrum have a finite integrated amplitude, E, the large k spectrum must be zero,

$$\lim_{k \to 0} S_{\mathbf{k}} = 0. \tag{117}$$

Taking into account the indicated features of the growth rate, the spectrum symmetries, and the boundary conditions, the trial function for the wave number spectrum is chosen to be a Gaussian times a quadratic in k_x and k_y,

$$S_{\mathbf{k}} \to \frac{4E}{\pi \Delta k^2} \left(\frac{k_x}{\Delta k} \right)^2 \left(\frac{k_y}{\Delta k} \right)^2 exp[-(k/\Delta k)^2]. \tag{118}$$

The spectrum is normalized to E,

$$E = \int d\mathbf{k} S_{\mathbf{k}}, \tag{119}$$

and has a maximum at $k_x = \pm \Delta k$ and $k_y = \pm \Delta k$. The frequency width trial function is chosen as a quadratic form, which is modeled after the growth rate, and which has maxima in the center of the k_x, k_y quadrants similar to the spectrum trial function structure,

$$\begin{aligned} \eta_{\mathbf{k}}^I &\to -.025 \left[\left(\frac{|k_x|}{k_0} - 1 \right)^2 + \left(\frac{|k_y|}{k_0} - 1 \right)^2 \right] \\ &= -\frac{.025}{A^2} \left[\left(\frac{|k_x|}{\Delta k} - A \right)^2 + \left(\frac{|k_y|}{\Delta k} - A \right)^2 \right] \end{aligned} \tag{120}$$

where $A \equiv k_0/\Delta k$. The boundary condition and symmetries are incorporated into the frequency width trial function, while the maximum value of zero is achieved at $k_x = \pm k_0$ and $k_y = \pm k_0$, which represents the marginally stable region of the spectrum. Using Eqs. (118) and (120) in the spectrum Eqs. (75), (88), and (90), along with the moment technique, the solution for the unknown parameters (E, Δk and k_0) can be obtained.

The dissipative constraint, Eq. (95), gives a condition for the wave number width, Δk,

$$M_1 = \int d\mathbf{k}(1+k^2)\gamma_{\mathbf{k}} S_{\mathbf{k}} = 0, \tag{121}$$

which is a quartic equation in Δk,

$$\Delta k^4 - \frac{7}{6\pi^{1/2}}\Delta k^3 + \frac{51}{144}\Delta k^2 - \frac{1}{3\pi^{1/2}}\Delta k + \frac{5}{144} = 0. \tag{122}$$

The real solutions of this quartic equation are

$$\Delta k = .31 \quad \text{or} \quad .41. \tag{123}$$

From the symmetry of the growth rate, $\gamma_{\mathbf{k}}$, and the spectrum trial function, $S_{\mathbf{k}}$, it is possible to have two solutions to the dissipative constraint condition. The $\Delta k = .31$ solution balances the damping near $k = 0$ with the growth rate in the central wave number region. The $\Delta k = .41$ solution balances the higher wave number damping with the growth rate in the central wave number region.

The choices for the second and third weighting functions, $W_{2_{\mathbf{k}}}$ and $W_{3_{\mathbf{k}}}$, are actually arbitrary, and give slightly different results for each choice. In general, the weighting functions depend on which exact constraints are desirable to impose on the approximate solution, obtained by this moment method. One criterion that was used to determine the weighting functions is to choose them so that the final equation, in one unknown parameter, has a large slope at the solution point, in order to reduce the error of the solution parameter. Just as with the weighting function used in the dissipative constraint, or energy moment, it is reasonable to choose low order wave number moments, $H_{\mathbf{k}} = k^n$, to represent exact constaints such as for the average frequency width ($H = 1$) or the average wave number width squared ($H = k^2$). After some trial and error, and noting that the solution did not vary much with weighting function choice, in order to satisfy the above criteria, the second and third weighting functions are chosen as one, $H_{2_{\mathbf{k}}} \rightarrow 1$ and $H_{3_{\mathbf{k}}} \rightarrow 1$.

Substituting this second weighting function, $H_{2_{\mathbf{k}}} \rightarrow 1$ in Eq. (96), results in the second moment equation,

$$M_2 = \int d\mathbf{k}[-2\eta^I_{\mathbf{k}} S_{\mathbf{k}}] = \int d\mathbf{k}d\mathbf{k}'d\mathbf{k}''\delta(\mathbf{k}-\mathbf{k}'-\mathbf{k}'')4\pi Re I_{\mathbf{k},\mathbf{k}',\mathbf{k}''} C^2_{\mathbf{k},\mathbf{k}',\mathbf{k}''} S_{\mathbf{k}'} S_{\mathbf{k}''}. \tag{124}$$

The left hand side of this equation can be readily evaluated,

$$M_2 = \frac{.4}{\pi A^2}\left(\frac{3}{8}\pi - \pi^{1/2}A + \frac{1}{4}A^2\right)E. \tag{125}$$

The integral on the right hand side of Eq. (124) is very complicated. It is useful to make the simplifying assumption that $(\Delta\omega)^2 \lesssim (\eta_T^I)^2$ for evaluation of the resonance function. This approximation is very well satisfied for most of the small wave number triplet interactions. In fact, some analysis with the complete resonance function was done as a check, and it was found that little variation in the solution resulted. The resonance function then takes on the approximate form

$$ReI_{\mathbf{k},\mathbf{k}',\mathbf{k}''} \approx \frac{1}{\pi}\frac{1}{-\eta_T^I}. \tag{126}$$

This approximation of the resonance function is consistent with the physical picture that a long interaction time, or large resonance function ($ReI_{\mathbf{k},\mathbf{k}',\mathbf{k}''}$), corresponds to a marginally stable nonlinear triplet, where the nonlinear growth rate sum, η_T^I, is small.

The evaluation of the integral on the right hand side of Eq. (124) proceeds as follows,

$$M_2 = \int d\mathbf{k}d\mathbf{k}'d\mathbf{k}''\delta(\mathbf{k}-\mathbf{k}'-\mathbf{k}'')\frac{4}{-\eta_T^I}C^2_{\mathbf{k},\mathbf{k}',\mathbf{k}''}S_{\mathbf{k}'}S_{\mathbf{k}''}, \tag{127}$$

and by using the delta function,

$$M_2 = \int d\mathbf{k}'d\mathbf{k}''\frac{-4}{\eta^I_{\mathbf{k}'+\mathbf{k}''}+\eta^I_{\mathbf{k}'}+\eta^I_{\mathbf{k}''}}C^2_{\mathbf{k}'+\mathbf{k}'',\mathbf{k}',\mathbf{k}''}S_{\mathbf{k}'}S_{\mathbf{k}''}. \tag{128}$$

Expressing the integral in polar coordinates,

$$\mathbf{k}' = k'(\cos\theta'\mathrm{Ax} + \sin\theta'\mathrm{Ay}), \quad \mathbf{k}'' = \mathrm{k}''(\cos\theta''\mathrm{Ax} + \sin\theta''\mathrm{Ay}), \tag{129}$$

while using the coupling coefficient, Eq. (89), the spectral and frequency width trial functions, Eqs. (118) and (120), and the change of variables in Eq. (128),

$$k' \equiv \Delta k x, \quad k'' \equiv \Delta k y, \tag{130}$$

results in

$$M_2 = \frac{16(40)A^2\Delta k^8 L_1(\Delta k, A)}{\pi^2} E^2, \tag{131}$$

where

$$L_1(\Delta k, A) \equiv \int_0^\infty dx \int_0^\infty dy \int_0^{2\pi} d\theta' \int_0^{2\pi} d\theta''$$

$$[\sin(\theta' - \theta'') \sin\theta' \sin\theta'' \cos\theta' \cos\theta'']^2 (xy)^7 (x^2 - y^2)^2 \exp[-(x^2 + y^2)]$$

$$\times [1 + \Delta k^2 (x^2 + y^2 + 2xy\cos(\theta' - \theta''))]^{-2}$$

$$\times [(x|\cos\theta'| - A)^2 + (x|\sin\theta'| - A)^2 + (y|\cos\theta''| - A)^2 + (y|\sin\theta''| - A)^2$$

$$+ (|x\cos\theta' + y\cos\theta''| - A)^2 + (|x\sin\theta' + y\sin\theta''| - A)^2]^{-1}. \tag{132}$$

Combining the two expressions for M_2, Eqs. (125) and (131), produces an equation for the total integrated amplitude,

$$E = \frac{\pi}{1600A^4\Delta k^8 L_1(\Delta k, A)} \left(\frac{3}{8}\pi - \pi^{1/2}A + \frac{1}{4}\pi A^2 \right). \tag{133}$$

The final expression which closes the system of nonlinear algebraic equations is obtained by using the third weighting function, $H_{3_{\mathbf{k}}} \rightarrow 1$, and inserting it in Eq. (97), which results in

$$M_3 = \int d\mathbf{k}(\gamma_{\mathbf{k}} - \eta^I_{\mathbf{k}}) S_{\mathbf{k}} = \int d\mathbf{k}d\mathbf{k}'d\mathbf{k}'' 4\pi Re I_{\mathbf{k},\mathbf{k}',\mathbf{k}''} C_{\mathbf{k},\mathbf{k}',\mathbf{k}''} C_{\mathbf{k}',\mathbf{k}'',\mathbf{k}} S_{\mathbf{k}''} S_{\mathbf{k}}. \tag{134}$$

The left hand side of Eq. (134) is readily evaluated to give,

$$M_3 = \frac{.2}{\pi A^2} \left[\frac{3}{8}\pi - \pi^{1/2}A + (2.4\pi^{1/2}\Delta k - 1.8\pi\Delta k^2) A^2 \right] E. \tag{135}$$

The integral on the right hand side of Eq. (134) is evaluated in a similar manner to Eq. (128),

$$M_3 = \int d\mathbf{k}d\mathbf{k}'d\mathbf{k}''\delta(\mathbf{k} - \mathbf{k}' - \mathbf{k}'') 4\pi Re I_{\mathbf{k},\mathbf{k}',\mathbf{k}''} C_{\mathbf{k},\mathbf{k}',\mathbf{k}''} C_{\mathbf{k}',\mathbf{k}'',\mathbf{k}} S_{\mathbf{k}''} S_{\mathbf{k}}, \tag{136}$$

and making the change of variables $\mathbf{k} \rightarrow -\mathbf{k}'$, $\mathbf{k}' \rightarrow -\mathbf{k}$, $\mathbf{k}'' \rightarrow \mathbf{k}''$,

$$M_3 = \int d\mathbf{k} d\mathbf{k}' d\mathbf{k}'' \delta(\mathbf{k} - \mathbf{k}' - \mathbf{k}'') 4\pi Re I_{\mathbf{k},\mathbf{k}',\mathbf{k}''} C_{-\mathbf{k}',-\mathbf{k},\mathbf{k}''} C_{-\mathbf{k},\mathbf{k}'',-\mathbf{k}'} S_{\mathbf{k}''} S_{\mathbf{k}'}, \qquad (137)$$

where use has been made of the delta function symmetry and the resonance function property

$$Re I_{-\mathbf{k}',-\mathbf{k},\mathbf{k}''} = Re I_{\mathbf{k},\mathbf{k}',\mathbf{k}''}. \qquad (138)$$

Using polar coordinates, Eq. (129), and the change of variables, Eq. (130), the Eq. (137) integral becomes

$$M_3 = \frac{16(40) A^2 \Delta k^8 L_2(\Delta k, A)}{\pi^2} E^2, \qquad (139)$$

where

$$L_2(\Delta k, A) \equiv \int_0^\infty dx \int_0^\infty dy \int_0^{2\pi} d\theta' \int_0^{2\pi} d\theta''$$

$$[\sin(\theta' - \theta'') \sin\theta' \sin\theta'' \cos\theta' \cos\theta'']^2 (xy)^7 (x^2 - y^2)[x^2 + 2xy\cos(\theta' - \theta'')] exp[-(x^2 + y^2)]$$

$$\times [1 + \Delta k^2 (x^2 + y^2 + 2xy\cos(\theta' - \theta''))]^{-1} [1 + \Delta k^2 x^2]^{-1}$$

$$\times [(x|\cos\theta'| - A)^2 + (x|\sin\theta'| - A)^2 + (y|\cos\theta''| - A)^2 + (y|\sin\theta''| - A)^2$$

$$+ (|x\cos\theta' + y\cos\theta''| - A)^2 + (|x\sin\theta' + y\sin\theta''| - A)^2]^{-1}. \qquad (140)$$

Combining the two expressions for M_3, Eqs. (135) and (139), produces another equation for the total integrated amplitude,

$$E = \frac{\pi}{3200 A^4 \Delta k^8 L_2(\Delta k, A)} \left[\frac{3}{8}\pi - \pi^{1/2} A + (2.4\pi^{1/2}\Delta k - 1.8\pi\Delta k^2) A^2 \right]. \qquad (141)$$

The equations determining the parameters are Eqs. (123), (133), and (141). To generate a numerical iteration procedure, the two equations for E, Eqs. (133) and (141),

can be combined as a ratio which is equal to one. The final equation for determining the parameters is then

$$R_1 \equiv \frac{[\frac{3}{8}\pi - \pi^{1/2}A + (2.4\pi^{1/2}\Delta k - 1.8\pi\Delta k^2)A^2]}{2[\frac{3}{8}\pi - \pi^{1/2}A + \frac{1}{4}\pi A^2]} \frac{L_1(\Delta k, A)}{L_2(\Delta k, A)}, \tag{142}$$

where the solution is found by solving

$$R_1 = 1. \tag{143}$$

Only two choices of the wave number width, Δk, are allowed by Eq. (123). For each choice of Δk, Eq. (143) is solved by choosing various values of A and iteratively searching for the solutions. The nonlinear integral equation problem has been reduced to the numerical evaluation of just two integrals $L_1(\Delta k, A)$, Eq. (132), and $L_2(\Delta k, A)$, Eq. (140).

The four dimensional integrals, Eq. (132) and (140), are computed using an extension of the Simpson's quadratic rule for one dimensional integrals. The total number of points the integrand is evaluated at is $(N+1)(M+1)(L+1)(P+1)$. The intervals

$$x : [0, 4], \quad y : [0, 4], \quad \theta' : [0, 2\pi], \quad \theta' : [0, 2\pi] \tag{144}$$

are found to be sufficiently accurate by comparison with larger intervals. A quick solution search was made using the number of steps as $N = M = L = P = 10$ on a hand held computer. The final accurate integrations were made using the MACSYMA system where $N = M = L = P = 20$ was used. It is interesting to note that the analytic moment method reduces the spectrum problem to a few hours of computation on a hand held computer as compared to hours of Cray time [3], a reduction of about a factor of 10^6 in computation steps.

One expects the solution to be in the regime where $A \equiv k_0/\Delta k \approx 1$, since the nonlinear marginally stable modes ($k_x = k_y \approx k_0$) should roughly correspond to the maximum amplitude modes ($k_x = k_y \approx \Delta k$). In this regime the search for a solution, using Eq. (143) for R_1, with $\Delta k = .41$ indicates that no solution exists. The ratio, R_1 for this wave number width is always greater than 1, $R_1 > 1$, which is shown in Fig. 1(a). The search for a solution using $\Delta k = .31$ is successful, with a solution found at $A = .97$. This is shown in Fig. 1(b). Using Eq. (133) for E, the solution parameters are

$$\Delta k = .31, \quad k_0 = .30, \quad \phi_{rms} = 1.6, \tag{145}$$

where $k_0 = A\Delta k$, and $\phi_{rms} = E^{1/2}$.

The spectrum results are presented graphically in Fig. 2 by averaging over k_x, where the root mean square potential, $|\phi_{rms}|_{k_y}$ as a function of k_y is defined by Eq. (109), and the spectral weighted k_x averaged frequency width, $\langle -\eta^I \rangle_{k_y}$, growth rate, $\langle \gamma \rangle_{k_y}$, and frequency, $\langle \omega \rangle_{k_y}$, are defined by Eq. (110). The k_x averaged potential is evaluated from the wave number spectral solution, Eq. (118). Using the solution parameters, $\Delta k = .31$ and $\phi_{rms} = 1.6$, the average potential,

$$|\phi_{rms}|_{k_y} = \frac{2^{1/2}(1.6)}{\pi^{1/4}(.31)^{1/2}} \left| \frac{k_y}{.31} \right| exp[-\frac{1}{2}(k_y/.31)^2], \quad (k_y)_{max} = .31, \tag{146}$$

is plotted in Fig. 2(a).

The spectrum weighted k_x average of the frequency width, $\langle -\eta^I \rangle_{k_y}$, is evaluated from the frequency width trial function, Eq. (120). Using the solution parameters, $\Delta k = .31$ and $A = .97$, the spectral weighted average of the frequency width,

$$\langle -\eta^I \rangle_{k_y} = \frac{.025}{(.97)^2} \left[\left(\frac{3}{2} - \frac{4}{\pi^{1/2}}(.97) + (.97)^2 \right) + \left(\frac{|k_y|}{.31} - .97 \right)^2 \right], \quad (k_y)_{min} = .30, \tag{147}$$

is also plotted in Fig. 2(a).

The spectral weighted k_x average of the growth rate, $\langle \gamma \rangle_{k_y}$, is evaluated from the expression for the growth rate, Eq. (111). Using the solution parameter, $\Delta k = .31$, the spectral weighted average growth rate,

$$\langle \gamma \rangle_{k_y} = -.12 \left[\left(\frac{3}{2}(.31)^2 - \frac{2}{\pi^{1/2}}(3.1) + \frac{1}{6} \right) + (|k_y| - .5)^2 \right], \quad (k_y)_{max} = .5, \tag{148}$$

is plotted in Fig. 2(b).

The spectral weighted k_x average of the frequency, $\langle \omega \rangle_{k_y}$, is evaluated from the expression for the frequency, Eq. (89). Using the solution parameter, $\Delta k = .31$, the spectral weighted average frequency,

$$\langle \omega \rangle_{k_y} = \frac{4}{\pi^{1/2}} \int_0^\infty dx \frac{x^2 e^{-x^2}}{1 + k_y^2 + (.31)^2 x^2} k_y, \tag{149}$$

is also plotted in Fig. 2(b).

The results presented here compare favorably with the numerical solution of the renormalized equations for the spectrum obtained by Waltz [3]. The integrated spectral amplitude or root mean square potential, $\phi_{rms} = 1.6$, derived from this analytic moment method, is in almost perfect agreement with the quoted numerical results for a system of 30×30 modes, $\phi_{rms}^{num} \approx 1.6$. The numerical study, in Ref. 3, dealt mainly with a system of 11×11 (or only $6 \times 6 = 36$ distinct) modes, for this case, $\phi_{rms}^{num} = 1.3$, there is about a twenty percent discrepancy with our results. However, the numerical study was based on a descretization of the spectrum, where a set of 11×11 modes is not sufficient. This is actually explored in the numerical study, where they have included a test for changes of the saturation amplitude while increasing the number of modes. It was found that approximately a system of 30×30 modes is necessary for an accurate saturation amplitude calculation. In this case, as stated above, we are in agreement.

There is also a good agreement between the potential spectrum obtained numerically and our analytic potential spectrum,

$$|\phi_{rms}|_{\mathbf{k}} \equiv S_{\mathbf{k}}^{1/2}. \tag{150}$$

From Eq. (118), the potential spectrum is

$$|\phi_{rms}|_{\mathbf{k}} = \frac{2\phi_{rms}}{\pi^{1/2}\Delta k}\left|\frac{k_x}{\Delta k}\right|\left|\frac{k_y}{\Delta k}\right| exp[-\frac{1}{2}(k/\Delta k)^2], \tag{151}$$

or using the solution parameters, this is

$$|\phi_{rms}|_{\mathbf{k}} = \frac{2(1.6)}{\pi^{1/2}(.31)}\left|\frac{k_x}{.31}\right|\left|\frac{k_y}{.31}\right| exp[-\frac{1}{2}(k/.31)^2]. \tag{152}$$

The results quoted in the numerical study have a different normalization than ours, due to their discretized approach. In all the following comparison of results, between our analytic solution and the numerical ones of Ref. 3, all values are presented with our normalization while incorporating a correction factor in the numerical ones. The details of this normalization difference are found in appendix A.

With the normalization correction factor utilized, there is reasonable agreement between the potential spectra of the analytic solution and the numerical solution on a mode by mode basis. The maximum analytic amplitude occurs at $k = \sqrt{2}\Delta k = .44$ and has the

value $|\phi_{rms}|_{max} = 2.2$, while the maximum numerical amplitude occurs at $k \approx .45$ and has the value $|\phi^{num}_{rms}|_{max} \approx 2.7$. The trial function property that $|\phi_{rms}| = 0$ for $k_x = 0$ or $k_y = 0$ is of course not in good agreement with the numerical solution since this is just a simplifying feature of the trial function.

The qualitative structure of the average analytic potential, Fig. 2(a), is very similar to that of the average numerical potential. Also, quantitatively the comparison is close, where the maximum analytic amplitude of the average potential occurs at $k = \Delta k = .31$ and has the value $|\phi_{rms}|_{k_y,max} = 1.9$, while the maximum numerical amplitude occurs at $k \approx .2$ and has the value $|\phi^{num}_{rms}|_{k_y,max} \approx 1.7$. The slight discrepancy between the position of the analytic maximum average amplitude and the numerical one might be understood by the fact that the numerical study allowed modes only up to a maximum of $k_{max} = 1$. The numerical study of the spectrum solution included a test for changes in the average spectrum with increases in the maximum wave number, $k_{max} > 1$. The case $k_{max} = 1.2$ was analyzed numerically with the result that the maximum average spectrum amplitude shifted to a slightly higher wave number, or closer to our analytic result.

The agreement between the analytic frequency width and the numerical frequency width is also very good. For both solutions the minimum of the frequency width and the k_x average frequency width occurs where the spectrum and k_x average spectrum reach a maximum. This is indicative of the fact that the marginal nonlinearly stable modes should be the largest amplitude modes. The dominant part of the spectrum naturally coincides with the most narrow frequency width region of the spectrum. The average analytic frequency width, Fig. 2(a), is both qualitatively and quantitatively similar to the average numerical frequency width up to $k_y \approx .8$. The simple quadratic frequency width trial function is not able to match the numerical results beyond $k_y \approx .8$; however, this is an unimportant region of the solution, physically, where the spectrum is insignificantly small. The average frequency width found for this model problem is quite small, $\langle -\eta^I \rangle \approx .02$, compared to the average frequency, $\langle \omega \rangle \approx .3$. This result is over a factor of ten different from the experimental indication that the frequency width is on the order of the frequency, $\langle -\eta^I \rangle / \langle \omega \rangle \sim 1$ [6].

There is also good agreement between the analytic and numerical results for the average growth rate and frequency, Fig. 2(b). It is interesting to note that the maximum drive of the average growth rate occurs at $k_y \approx .5$, while the maximum average potential amplitude occurs at $k_y \approx .31$. This is evidence of the nonlinear cascade of the spectrum to lower wave numbers than the maximum drive wave number. This can be understood

since it is found that for a system with no dissipation, $\gamma = 0$, the equilibrium is centered about $k = 0$ [18]. Physically, it is reasonable that if a system is driven near some finite wave number, that it would have a tendency to relax towards the equilibrium nearer to $k = 0$.

It is clear from this comparison of the analytic spectrum solution to the numerical solution that accurate results can be obtained using the analytic moment method. The useful feature of the moment method is that the important parameters of the solutions for the nonlinear spectrum integral equations can be obtained from quite trivial numerical integrations. The results give very accurate values for the important bulk parameters such as the saturation integrated amplitude, the wave number width, and the frequency width, when the trial functions can be made reasonably close, in shape, with the true solutions.

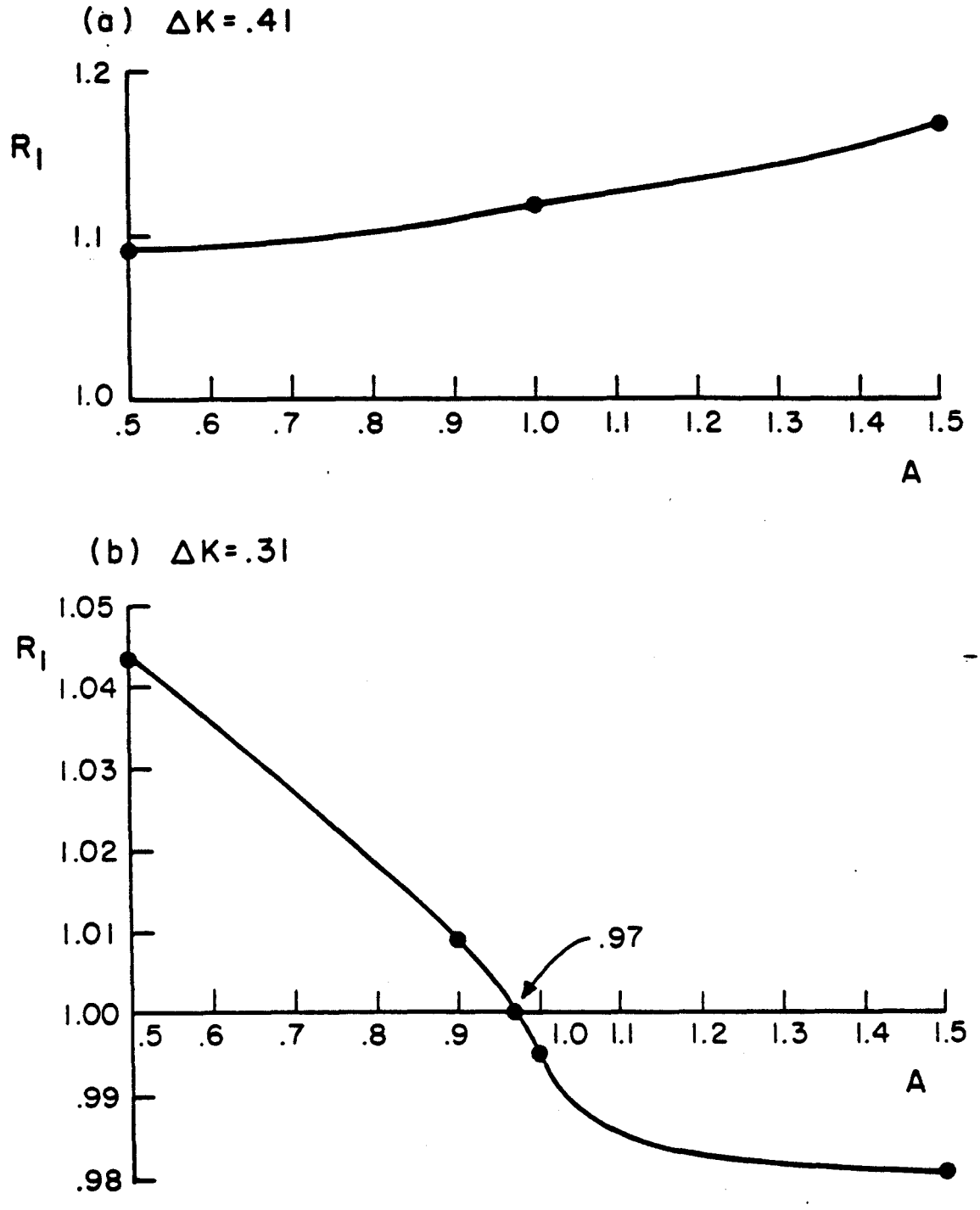

Figure 1: The spectrum solution parameters for the model problem are determined by the ratio equation, $R_1(\Delta k, A) = 1$, where the ratio, R_1, is defined by Eq. (142). The two allowed wave number width parameters ($\Delta k = .41, .31$) are used while varying the frequency width parameter, A. (a) For $\Delta k = .41$, no solution ($R_1 \neq 1$) exists. (b) For $\Delta k = .31$, a solution ($R_1 = 1$) is found at $A = .97$. All the points in the above graphs are from numerical computations.

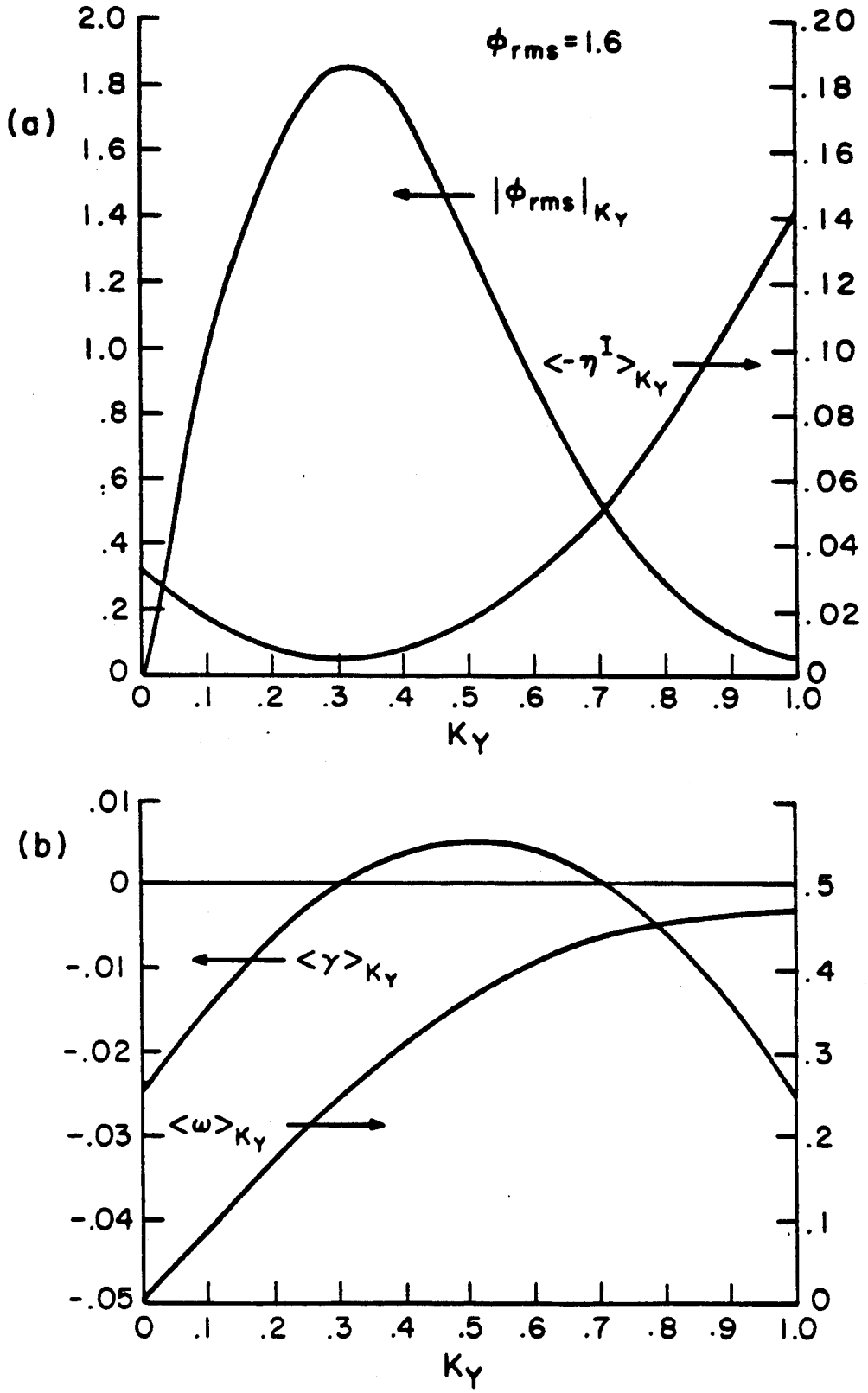

Figure 2: Spectrum results for the model problem are presented in terms of k_x-averaged quantities. (a) Root mean square potential, $|\phi_{rms}|_{k_y}$, and frequency width, $\langle -\eta^I \rangle_{k_y}$. (b) Growth rate, $\langle \gamma \rangle_{k_y}$, and frequency, $\langle \omega \rangle_{k_y}$.

4. Spectrum Solution of Self–Consistent Drift Wave Problem

In this section, the spectrum equations are solved for the drift wave electron dissipation computed in the NSA [4]. The renormalized electron dissipation in the NSA is a nonlinear analysis of the drift wave problem, where the important feature of stochastic electron diffusion, due to the resonance overlap condition being satisfied, is incorporated. The desire here is to calculate an accurate drift wave spectrum utilizing this realistic drift wave electron dissipation. Besides the general motivation to derive a turbulent spectrum needed for a transport theory, there is also the current question whether a good theory can predict the experimentally observed broad frequency spectrum.

The dissipation considered here is fundamentally different from that of the model problem, Sec. 3. The wave number dependent growth rate for the model problem exhibits very large damping for low and high wave numbers, with a narrow band of marginally unstable growth rates in between, $k_x \approx k_y \approx .5$. Almost any two unstable linear eigenmodes, $\omega = \omega_{\mathbf{k}}$, which beat together, satisfying the selection rule, $\mathbf{k} = \mathbf{k}' + \mathbf{k}''$, produce a nonlinear mode, $\omega \neq \omega_{\mathbf{k}}$, which is stable, where the triplet growth rate is negative. It is then found that there are very few unstable triplets. Since there is no drive to populate the noneigenmode spectral frequencies, it is expected that the spectral frequency width for this dissipation model would be small. This narrow frequency width assertion is in agreement with the results of the last section. In contrast, the growth rate derived from the electron dissipation in the NSA, which is obtained from Eq. (4) and Ref. 16,

$$\gamma_{\mathbf{k},\omega} = -\frac{\omega(\omega - \omega_e^*)T}{1 + k^2}, \tag{153}$$

indicates that all linear eigenmodes, $\omega = \omega_{\mathbf{k}}$, are unstable. Here, the parameter T is a correlation time. It is also found that any two linear eigenmodes with y components of the wave vectors, either both positive or both negative, produces a nonlinear mode which is also unstable. This property of the electron dissipation in the NSA can be ascertained by plotting the vector sum of any two eigenmodes in a two dimensional frequency, ω, and y component of wave vector, k_y, coordinate system. The growth rate from Eq. (153), $\gamma_{\mathbf{k},\omega}$, is proportional to $-\omega(\omega - \omega_e^*)$. The eigenmode frequency is $\omega = \omega_{\mathbf{k}} = \omega_e^*/(1 + k^2) = k_y/(1 + k^2)$. The beat waves must satisfy the selection rules, $\omega = \omega' + \omega''$, and $\mathbf{k} = \mathbf{k}' + \mathbf{k}''$. For positive y components of the wave vectors, k_y' and $k_y'' > 0$, it is clear that the beat wave frequency, $\omega' + \omega'' = [k_y'/(1 + k'^2)] + [k_y''/(1 + k''^2)]$, is less than the drift wave frequency, $\omega_e^* = k_y' + k_y''$. In this case the growth rate is positive, which is also true for y components

of the wave vectors both negative, k'_y and $k''_y < 0$. The above picture for the beat wave growth rate is also clearly represented by formally expressing the growth rate,

$$\gamma_{\mathbf{k}'+\mathbf{k}'',\omega'+\omega''} \quad \text{is proportional to} \quad \left(\frac{k'_y}{1+k'^2}+\frac{k''_y}{1+k''^2}\right)\left[k'_y+k''_y-\left(\frac{k'_y}{1+k'^2}+\frac{k''_y}{1+k''^2}\right)\right].$$

The beat wave growth rate is positive for k'_y, k''_y both positive or both negative. For this model of dissipation there are then many unstable triplets. The unstable triplets tend to drive up and populate the noneigenmode frequency spectrum, $\omega \neq \omega_{\mathbf{k}}$. In the spectrum problem reduced to wave number space, the noneigenmode frequencies are expressed in terms of a spectral frequency width. Consequently, it is anticipated that the spectral frequency widths will be large for the spectrum dependent on the electron dissipation in the NSA.

The Lorentzian frequency trial function is not appropriate for a frequency dependent growth rate such as Eq. (153). In order that the frequency moment integral of the growth rate converge, the Gaussian spectral frequency trial function is chosen,

$$S_{\mathbf{k},\omega} = \frac{1}{\pi^{1/2}|\eta^I_{\mathbf{k}}|} exp[-(\frac{\omega-\omega_{\mathbf{k}}}{\eta^I_{\mathbf{k}}})^2] S_{\mathbf{k}}. \tag{154}$$

The wave number spectrum integral equations to be solved now are Eqs. (75), (88), and (90). The moment technique is used to reduce the wave number integral equations to a set of nonlinear algebraic equations for the unknown parameters which are incorporated in the trial functions. This solution is dependent on the dissipation parameter, T, of Eq. (153). The parameter, T, is itself a functional of the spectrum level, via the diffusion coefficient,

$$T = \tau'_c \Omega_i \frac{\rho_s}{L_n} = 2.8\tau_c \Omega_i \frac{\rho_s}{L_n}, \quad \tau_c = \left[\frac{1}{3}\overline{D}(\overline{k}'_{\|}v_e)^2\right]^{-1/3}, \tag{155}$$

where the average diffusion coefficient, $\overline{D}$, is

$$\overline{D} = \int du \frac{1}{\pi^{1/2}v_e} \exp[-(u/v_e)^2] \int dk_y \frac{\pi R}{|u|}\left(\frac{ck_y}{B}\right)^2 S_{k_y}(x)\Big|_{x=\frac{L_s\overline{\omega}}{k_y u}}. \tag{156}$$

Here, $v_e \equiv (2T_e/m_e)^{1/2}$ is the electron thermal velocity, R is the tokamak major radius, L_s is the shear length, $\overline{\omega} = \Omega_i(\rho_s/L_n)\overline{k}_y, \overline{k}'_{\|} = \overline{k}_y/L_s$, and $\overline{k}_y$ is the spectral averaged wave

vector, k_y. The final spectrum solution is insured to be self-consistent by obtaining a new parameter, T, from the spectrum solution and iterating until a common solution for both the spectrum equation and the dissipation is found. Initially a value for the parameter, T, is chosen, the spectrum equations are then solved. The spectrum solution can be used to calculate a second parameter, T, using the diffusion coefficient, Eq. (156), and the equation for T, Eq. (155). This new value for T is used in the solution of the spectrum equations, and this implies a new T value. The feedback is found to be negative, so that when this iteration scheme is continued, the parameter, T, oscillates about a fixed point. In fact, the parameter, T, converges quite rapidly to a solution. This problem is fully nonlinear, having the nonlinear mode coupling saturation spectrum problem combined with the nonlinear electron dissipation.

Using the Gaussian frequency trial function, Eq. (154), the wave number growth rate moment integral is calculated using Eq. (81),

$$\gamma_{\mathbf{k}} = \frac{1}{1+k^2}\left[\omega_{\mathbf{k}}(\omega_e^* - \omega_{\mathbf{k}}) - \frac{1}{2}(\eta_{\mathbf{k}}^I)^2\right]T. \tag{157}$$

Note that the frequency averaged growth rate, $\gamma_{\mathbf{k}}$, has the nonlinear spectral width, $\eta_{\mathbf{k}}^I$, explicitly incorporated. The sources of negative and positive dissipation are clearly presented in Eq. (157) as a dichotomy. The $\omega < \omega_e^*$ portion of the spectrum produces the negative dissipation (positive growth rate), while the $\omega > \omega_e^*$ portion of the spectrum, arising because of the nonlinear frequency width, $\eta_{\mathbf{k}}^I$, produces the positive dissipation (negative growth rate).

Just as in the solution of the model problem, Sec. 3., the boundary conditions of $S_{\mathbf{k}}$ and $\eta_{\mathbf{k}}^I$ help to determine good trial function choices. The $k = 0$ limit of the frequency spectral width is found using Eq.(87),

$$F\eta_0^I = \gamma_0, \tag{158}$$

where use has been made of the coupling constraint Eq. (114). For the same reason, the $k = 0$ limit of Eq. (88) is

$$\eta_0^I S_0 = 0. \tag{159}$$

The growth rate Eq. (157) can be written as

$$\gamma_{\mathbf{k}} = \frac{T}{1+k^2}\left[\frac{k_y^2}{1+k^2}\left(1-\frac{1}{1+k^2}\right)-\frac{1}{2}(\eta_{\mathbf{k}}^I)^2\right], \tag{160}$$

where use has been made of the frequencies $\omega_e^* = k_y$ and $\omega_{\mathbf{k}} = k_y/(1+k^2)$. Combining Eq. (158) with Eq. (160) results in the condition for the $k = 0$ limit of the frequency width, η_0^I,

$$F\eta_0^I = -\frac{1}{2}T(\eta_0^I)^2, \tag{161}$$

so that there are two possibilities,

$$\eta_0^I = 0 \quad \text{or} \quad \eta_0^I = -\frac{2F}{T}. \tag{162}$$

The two solutions of the boundary conditions are $\eta_0^I = -2F/T$ with $S_0 = 0$, or $\eta_0^I = 0$ with any S_0. The choice taken here is to pick the latter condition so that a large amplitude of the frequency width, near the dominant part of the spectrum at $k = 0$, is not picked a priori. Also, the first boundary condition choice tends to produce a positive feedback loop for the self–consistency condition, where the parameter, T, is evaluated from the spectrum, S, and vice versa. This occurs since the average spectrum, S, is directly proportional to the average frequency width, η^I, which can be noted from Eq. (88). With use of this first boundary condition choice, where the frequency width is inversely proportional to T, it is clear that the spectrum and parameter, T, are inversely related for one half of the iteration loop. Using Eqs. (155) and (156) it can be noted that the parameter, T, is inversely proportional to the spectrum for the other half of the feedback loop. This indicates an overall positive feedback loop, so that there would tend to be no solution found using the iteration procedure and the first boundary condition choice.

In order to model the spectrum response after the region of negative dissipation (source) at some finite k position, the choice of the trial function for the wave number spectrum is a Gaussian times a quadratic in wave number,

$$S_{\mathbf{k}} \rightarrow \frac{E}{\pi\Delta k^2}\left(\frac{k}{\Delta k}\right)^2 exp[-(k/\Delta k)^2]. \tag{163}$$

The spectrum is normalized to E,

$$E = \int d\mathbf{k} S_{\mathbf{k}}, \tag{164}$$

and attains a maximum at $k = \Delta k$. The trial function for the frequency spectral width is chosen to be a quartic function,

$$\eta_{\mathbf{k}}^I \rightarrow -Gk^4. \tag{165}$$

A quadratic frequency width trial function was attempted but no solution for the spectrum problem could be found since the growth rate, Eq. (160), did not produce sufficient negative dissipation to balance the positive dissipation from the frequency width, $\eta_{\mathbf{k}}^I$, term. Consequently, one needs a trial function for the frequency width which would demonstrate a slower increase with wave number near $k = 0$. The growth rate, Eq. (160), is now

$$\gamma_{\mathbf{k}} = \frac{T}{1+k^2}\left[\frac{k_y^2}{1+k^2}\left(1 - \frac{1}{1+k^2}\right) - \frac{1}{2}G^2k^8\right]. \tag{166}$$

Using the trial function choices, Eqs. (163) and (165), in the spectrum Eqs. (75), (88), and (90), along with the moment technique, the solution for the unknown parameters ($\bar{E}$, Δk, and G) can be obtained.

The dissipation constraint, Eq. (95), gives a condition for the parameters Δk and G,

$$M_1 = \int d\mathbf{k}(1+k^2)\gamma_{\mathbf{k}} S_{\mathbf{k}} = 0, \tag{167}$$

Defining the functions,

$$I_1(\Delta k) \equiv \int_0^\infty dx \frac{x^5 e^{-x^2}}{1+\Delta k^2 x^2} \quad \text{and} \quad I_2 \equiv \int_0^\infty dx \frac{x^5 e^{-x^2}}{(1+\Delta k^2 x^2)^2}, \tag{168}$$

the equation for the parameter G is

$$G^2 = \frac{I_1(\Delta k) - I_2(\Delta k)}{60\Delta k^6}. \tag{169}$$

Given any value of the wave number width, Δk, the corresponding value of the frequency width parameter, G, is obtained from Eq. (169).

As noted in the previous section, the choices for the weighting functions depend on which exact constraints are desired to impose on the approximate solution. It was also noted that the weighting function choice can be used to satisfy the criterion that the slope near the solution point is large, when solving an equation equivalent to Eq. (143). After

some trial and error, the choices for the second and third weighting functions were found as, $H_{2_{\mathbf{k}}} \rightarrow 1+k^2$ and $H_{3_{\mathbf{k}}} \rightarrow k^2$. After inserting this second weighting function in Eq. (96), the second moment equation is,

$$M_2 = \int d\mathbf{k}(1+k^2)(-2F\eta^I_{\mathbf{k}})S_{\mathbf{k}}$$

$$= \int d\mathbf{k}d\mathbf{k}'d\mathbf{k}''\delta(\mathbf{k}-\mathbf{k}'-\mathbf{k}'')4\pi ReI_{\mathbf{k},\mathbf{k}',\mathbf{k}''}(1+k^2)C^2_{\mathbf{k},\mathbf{k}',\mathbf{k}''}S_{\mathbf{k}'}S_{\mathbf{k}''}. \qquad (170)$$

The left hand side of this equation can be readily evaluated,

$$M_2 = 12FG\Delta k^4(1+4\Delta k^2)E. \qquad (171)$$

The integral on the right hand side of Eq. (170) is obtained using the same approximation for the resonance function, that was used in solving the model problem,

$$ReI_{\mathbf{k},\mathbf{k}',\mathbf{k}''} \approx \frac{1}{\pi^{1/2}}\frac{1}{\eta^I_T}, \quad \eta^I_T = \sqrt{(\eta^I_{\mathbf{k}})^2+(\eta^I_{\mathbf{k}'})^2+(\eta^I_{\mathbf{k}''})^2}. \qquad (172)$$

The right hand side of Eq. (170) is then

$$M_2 = \int d\mathbf{k}'d\mathbf{k}''\frac{4\pi^{1/2}(1+k^2)}{[(\eta^I_{\mathbf{k}'+\mathbf{k}''})^2+(\eta^I_{\mathbf{k}'})^2+(\eta^I_{\mathbf{k}''})^2]^{1/2}}C^2_{\mathbf{k}'+\mathbf{k}'',\mathbf{k}',\mathbf{k}''}S_{\mathbf{k}'}S_{\mathbf{k}''}. \qquad (173)$$

Using polar coordinates, Eq. (129),and the change of variables, Eq. (130), the result for Eq. (173) is

$$M_2 = \frac{\Delta k^4 E^2}{\pi^{3/2}G}\int_0^\infty dx\int_0^\infty dy\int_0^{2\pi}d\theta'\int_0^{2\pi}d\theta'' \qquad (174)$$

$$\frac{\sin^2(\theta''-\theta')(xy)^5(x^2-y^2)^2 exp[-(x^2+y^2)]}{\{x^8+y^8+[x^2+y^2+2xy\cos(\theta''-\theta')]^4\}^{1/2}\{1+\Delta k^2|x^2+y^2+2xy\cos(\theta''-\theta')|\}}.$$

The final change of variables is obtained using the transformation

$$\phi = \theta''-\theta', \quad \phi' = \theta'+\theta'', \quad \theta' = \frac{1}{2}(\phi'-\phi), \quad \theta'' = \frac{1}{2}(\phi+\phi'), \qquad (175)$$

which gives the final expression for M_2,

$$M_2 = \frac{2\Delta k^4 L_3(\Delta k)}{\pi^{3/2} G} E^2, \tag{176}$$

where

$$L_3(\Delta k) \equiv \int_0^\infty dx \int_0^\infty dy \int_0^{2\pi} d\phi \tag{177}$$
$$\frac{\phi \sin^2\phi (xy)^5 (x^2-y^2)^2 exp[-(x^2+y^2)]}{[x^8+y^8+(x^2+y^2+2xy\cos\phi)^4]^{1/2}[1+\Delta k^2(x^2+y^2+2xy\cos\phi)]}.$$

Combining the two expression for M_2, Eqs. (171) and (176), produces an equation for the total integrated amplitude,

$$E = \frac{6\pi^{3/2} F G^2 (1+4\Delta k^2)}{L_3(\Delta k)}. \tag{178}$$

The final expression which closes the system of nonlinear algebraic equations is obtained by using the third weighting function, $H_{3_{\mathbf{k}}} \rightarrow k^2$, and inserting this in Eq. (97), where the result is

$$M_3 = \int d\mathbf{k} k^2 (\gamma_{\mathbf{k}} - F\eta^I_{\mathbf{k}}) S_{\mathbf{k}} = \int d\mathbf{k} d\mathbf{k}' d\mathbf{k}'' 4\pi Re I_{\mathbf{k},\mathbf{k}',\mathbf{k}''} k^2 C_{\mathbf{k},\mathbf{k}',\mathbf{k}''} C_{\mathbf{k}',\mathbf{k}'',\mathbf{k}} S_{\mathbf{k}''} S_{\mathbf{k}}. \tag{179}$$

The left hand side of Eq. (158) is readily evaluated, with

$$I_3(\Delta k) \equiv \int_0^\infty dx \frac{x^7 e^{-x^2}}{(1+\Delta k^2 x^2)^2}, \quad I_4(\Delta k) \equiv \int_0^\infty dx \frac{x^7 e^{-x^2}}{(1+\Delta k^2 x^2)^3},$$
$$I_5(\Delta k) \equiv \int_0^\infty dx \frac{x^{13} e^{-x^2}}{1+\Delta k^2 x^2}, \tag{180}$$

the result is

$$M_3 = 24 F G \Delta k^6 \left[1 + \frac{T}{24 F G \Delta k^2}[I_3(\Delta k) - I_4(\Delta k) - G^2 \Delta k^6 I_5(\Delta k)]\right] E. \tag{181}$$

The integral on the right hand side of Eq. (179) is evaluated in a similar manner to Eq. (176) and Eq. (137). Using the polar coordinates, Eq. (129), and the change of variables, Eq. (130), the result of Eq. (179) is

$$M_3 = \frac{2\Delta k^6 L_4(\Delta k)}{\pi^{3/2} G} E^2, \tag{182}$$

where

$$L_4(\Delta k) \equiv \int_0^\infty dx \int_0^\infty dy \int_0^{2\pi} d\phi \tag{183}$$
$$\frac{\phi \sin^2\phi (xy)^5 (x^2-y^2)(x^2+2xy\cos\phi)(x^2+y^2+2xy\cos\phi) exp[-(x^2+y^2)]}{[x^8+y^8+(x^2+y^2+2xy\cos\phi)^4]^{1/2}[1+\Delta k^2(x^2+y^2+2xy\cos\phi)][1+\Delta k^2 x^2]}.$$

Combining the M_3 Eqs. (181) and (182) produces another equation for the total integrated amplitude,

$$E = \frac{12\pi^{3/2} F G^2}{L_4(\Delta k)} \left[1 + \frac{T}{24 F G \Delta k^2} [I_3(\Delta k) - I_4(\Delta k) - G^2 \Delta k^6 I_5(\Delta k)]\right]. \tag{184}$$

The solution of the parameters is found from Eqs. (169), (178), and (184). The two equations for E, Eqs. (178) and (184), can be combined as a ratio which is equal to one. The final equation for determining the parameters is then

$$R_2 \equiv \frac{2\left[1 + \frac{T}{24FG\Delta k^2}[I_3(\Delta k) - I_4(\Delta k) - G^2\Delta k^6 I_5(\Delta k)]\right]}{[1+4\Delta k^2]} \frac{L_3(\Delta k)}{L_4(\Delta k)}, \tag{185}$$

where the solution is found by solving

$$R_2 = 1. \tag{186}$$

The solution of Eq. (186) is obtained by choosing various values of Δk^2, with the subsidiary condition for G, Eq. (169), and iteratively searching for a solution. The nonlinear integral equation problem has been reduced to the numerical evaluation of just two (three dimensional) integrals $L_3(\Delta k)$, Eq. (177), and $L_4(\Delta k)$, Eq. (183), and the simple numerical evaluation of five (one dimensional) integrals $I_1(\Delta k), \ldots, I_5(\Delta k)$. The three dimensional integrals, Eqs. (177) and (183), are computed using an extension of the Simpson's quadratic rule for one dimensional integrals. The integration domains

$$x : [0,4], \quad y : [0,4], \quad \phi : [0,2\pi], \tag{187}$$

were found to be sufficiently accurate. A quick solution search was made using the number of steps as $N = M = L = 10$ on a hand held computer. The final accurate integrations were made using the MACSYMA system where $N = M = L = 20$ was used. Similar to that found during the model problem computation, Sec. 3., the analytic moment method reduces the spectrum problem to a few hours of computation on a hand held computer as compared to hours of Cray time needed for the numerical solution of the spectrum integral equation. Just as noted in the previous section, this is different in speed by about 10^6.

In order that Eqs. (186) and (178) for E be self-consistently solved, the expression for the dissipation parameter, T, as a function of Δk and E must be known. The parameter, T, is found by using our spectrum trial function in the diffusion coefficient, Eq. (156), and substituting this in Eq. (155), where the result is evaluated in Appendix B,

$$T \approx \frac{2}{(\Delta k^4 E)^{1/3}}, \tag{188}$$

and typical parameters have been used ($m_i/m_e \approx 1836, L_s/L_n \approx 16, L_s/R \approx 3, \Delta k \approx .6$).

The search for a solution of Eq. (186) proceeds by choosing a Δk^2 value, computing G from Eq. (169), computing I_3, I_4, and I_5 from Eq. (180), computing L_3 and L_4 from Eqs. (177) and (183), computing E from Eq. (178), computing T from Eq. (188), and finally computing R_2 from Eq. (185). An iteration of this procedure is performed until Eq. (186), $R_2 = 1$, is solved. This iteration converged very rapidly, and as mentioned at the beginning of this section, the feedback is negative so that the solution is quite stable. A solution is found at $\Delta k^2 = .28$, as can be seen from Fig. 3. The solution parameters are found to be

$$\Delta k = .53, \quad G = .41, \quad T = 2.2, \quad \phi_{rms} = 3.1. \tag{189}$$

The spectrum results are presented graphically, Fig. 4, by averaging over k_x, as was done for the presentation of the model problem results, Sec. 3. The average root mean square potential, $|\phi_{rms}|_{k_y}$, is defined by Eq. (109), and the average spectral weighted average frequency width, $\langle -\eta^I \rangle_{k_y}$, growth rate, $\langle \gamma \rangle_{k_y}$, and frequency, $\langle \omega \rangle_{k_y}$, are defined by Eq. (110). The k_x average potential is evaluated from the wave number spectral

solution, Eq. (163). Using the solution parameters, $\Delta k = .53$ and $\phi_{rms} = 3.1$, the average potential,

$$|\phi_{rms}|_{k_y} = \frac{3.1}{2^{1/2}\pi^{1/4}(.53)^{1/2}}\left[1+2\left(\frac{k_y}{.53}\right)^2\right]^{1/2} exp[-\frac{1}{2}(k_y/.53)^2], \quad (k_y)_{max} = .37, \quad (190)$$

is plotted in Fig. 4(a).

The spectral weighted k_x average of the frequency width, $\langle -\eta^I \rangle_{k_y}$, is evaluated from the frequency width solution, Eq. (165). Using the solution parameters, $\Delta k = .53$ and G = .41, the spectral weighted average of the frequency width,

$$\langle -\eta^I \rangle_{k_y} = 2(.41)(.53)^4\left[\frac{15}{8}+\frac{9}{4}\left(\frac{k_y}{.53}\right)^2+\frac{3}{2}\left(\frac{k_y}{.53}\right)^4+\left(\frac{k_y}{.53}\right)^6\right]\Big/\left[1+2\left(\frac{k_y}{.53}\right)^2\right], \quad (k_y)_{min} = .29, \quad (191)$$

is also plotted in Fig. 4(a).

The spectral weighted k_x average of the growth rate, $\langle \gamma \rangle_{k_y}$, is evaluated from the expression for the growth rate, Eq. (166) Using the solution parameters, $\Delta k = .53$ and $G = .41$, the spectral weighted average growth rate,

$$\langle \gamma \rangle_{k_y} = \frac{4(2.2)}{\pi^{1/2}(.53)^3} \quad (192)$$

$$\times \frac{\int_0^\infty dx \frac{k_y^2+x^2}{1+k_y^2+x^2}\left[\frac{k_y^2}{1+k_y^2+x^2}\left(1-\frac{1}{1+k_y^2+x^2}\right)-\frac{1}{2}(.41)^2(k_y+x^2)^4\right]\exp\left[-(x/.53)^2\right]}{\left[1+2\left(\frac{k_y}{.53}\right)^2\right]},$$

is numerically integrated and plotted in Fig. 4(b), where the maximum value occurs at $(k_y)_{max} = .8$.

The spectral weighted k_x average of the frequency, $\langle \omega \rangle_{k_y}$, is evaluated from the expression for the frequency, Eq. (89). Using the solution parameter, $\Delta k = .53$, the spectral weighted average frequency,

$$\langle\omega\rangle_{k_y} = \frac{4}{\pi^{1/2}}(.53)\left(\frac{k_y}{.53}\right)\int_0^\infty dx \frac{\left(\frac{k_y}{.53}\right)^2 + x^2}{\frac{1}{(.53)^2} + \left(\frac{k_y}{.53}\right)^2 + x^2} e^{-x^2} \Big/ \left[1 + 2\left(\frac{k_y}{.53}\right)^2\right], \qquad (193)$$

is also numerically integrated and also plotted in Fig. 4(b).

The radial diffusion coefficient, $\overline{D}$, is computed by using the spectrum trial function, Eq. (163), in Eq. (156), which is evaluated in Appendix B,

$$\overline{D} = \left[\frac{\pi}{\sqrt{2}}\left(\frac{m_e}{m_i}\right)^{1/2}\left(\frac{R}{L_s}\right)\left(\frac{L_s}{L_n}\right)(I\Delta k^2 E)\right]\Omega_i \frac{\rho_s}{L_n}\rho_s^2, \qquad (194)$$

where,

$$I = \frac{2}{\pi}K_o(2M), \quad M = \frac{1}{2}\left(\frac{m_e}{2m_i}\right)^{1/2}\left(\frac{L_s}{L_n}\right)\Delta k, \qquad (195)$$

and K_o is the modified Bessel function. Using the spectrum solution, Eq. (189), and typical parameters ($m_i/m_e = 1836$, $L_s/L_n = 16$, $L_s/R = 3$), the diffusion coefficient is,

$$\overline{D} \approx 1.8\Omega_i \frac{\rho_s}{L_n}\rho_s^2. \qquad (196)$$

The physical parameters (L_s/L_n, m_i/m_e, L_s/R) were varied in order to determine the scaling of the diffusion coefficient on them. The results indicate that the diffusion coefficient is roughly independent of L_s/L_n and $(m_i/m_e)^{1/2}$, but it scales with $(R/L_s)^{1.5}$,

$$\overline{D} \approx \left[9.6\left(\frac{R}{L_s}\right)^{1.5}\right]\Omega_i \frac{\rho_s}{L_s}\rho_s^2. \qquad (197)$$

The diffusion coefficient scaling with R/L_s can be physically understood since R/L_s is proportional to the density of modes or mode rational surface points.

The integrated amplitude or root mean square potential result, $\phi_{rms} = 3.1$, and the radial diffusion coefficient, $\overline{D} = 1.8$, are very close to experimental values of $\overline{D} \sim 0(1)$ and $\phi_{rms} = (e\phi/T_e)/(\rho_s/L_n)$ 0(3) where $\rho_s/L_n \approx .3 \times 10^{-2}$ and $e\phi/T_e \approx 10^{-2}$ [6]. From Fig. 4(a) it is seen that the minimum frequency width occurs at $k_y \approx .29$ and the maximum value of the potential occurs near this at $k_y \approx .37$. This is the same feature found for the model problem that the marginally stable nonlinear modes, small frequency width modes, coincide with the maximum amplitude modes. The maximum drive, Fig. 4(b), occurs at

$k_y \approx .8$ which demonstrates, as also seen in the model problem, that there is a cascade of energy to lower wave number, which is physically understood since the undriven system would have an equilibrium centered about $k = 0$. However, the frequency width, $\langle \eta^I \rangle_{k_y}$, shown in Fig. 4(a), in contrast to the model problem, is actually quite large. The average frequency width $\langle \eta^I \rangle \approx .3$ is on the order of the average frequency $\langle \omega \rangle \approx .3$. This is in agreement with the broad drift wave frequency spectrum found from microwave scattering experiments in tokamaks [6]. The growth rate, Eq. (157), was rescaled and the spectrum equations were solved in order to determine the rescaling of the ratio of frequency width to frequency. The frequency width and the frequency were both found to exhibit roughly a linear rescaling with growth rate. Furthermore, the ratio of frequency width to frequency was found to be approximately independent of the growth rate rescaling. The assertion made at the beginning of this section was shown to be correct; the growth rate, Eq. (153), used in this analysis of the spectrum, is fundamentally different from the one used for the model problem, Eq. (111). Since all the linear eigenmodes are unstable, and many of the beat wave nonlinear modes are also unstable, there are numerous unstable triplets. The unstable triplets drive up and populate the noneigenmode frequency spectrum. In this drift wave problem, which had been reduced to wave number space, the noneigenmode frequencies are modeled by the spectral frequency widths. As was expected, the average frequency width, for the electron dissipation in the NSA, has been found to be large.

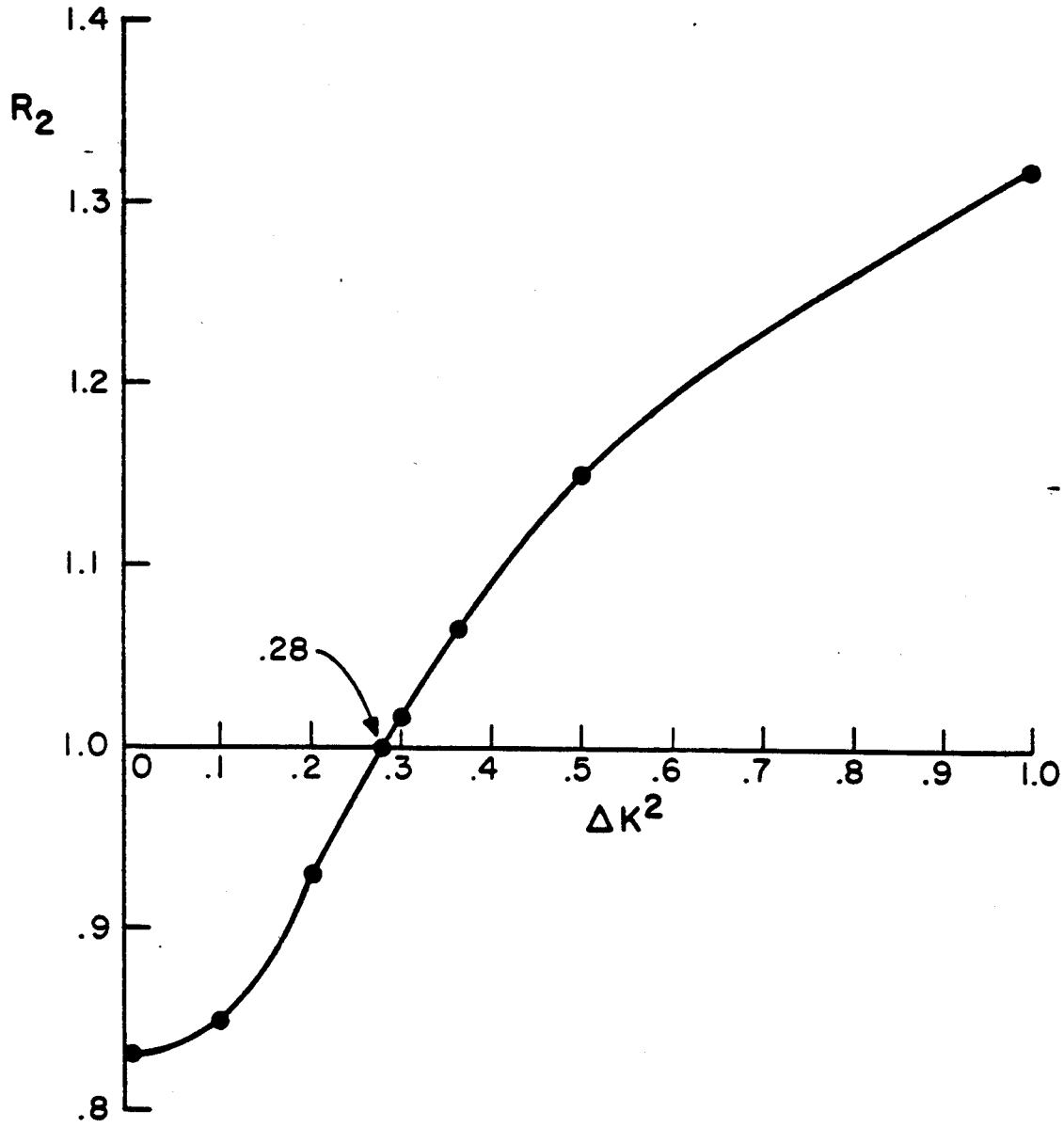

Figure 3: The spectrum solution parameters for the self-consistent drift wave problem are determined by the ratio equation, $R_2(\Delta k^2) = 1$, where the ratio, R_2, is defined by Eq. (185), and is a function of the squared wave number width parameter. A solution ($R_2 = 1$) is found at $\Delta k^2 = .28$. All the points in the above graph are from numerical computations.

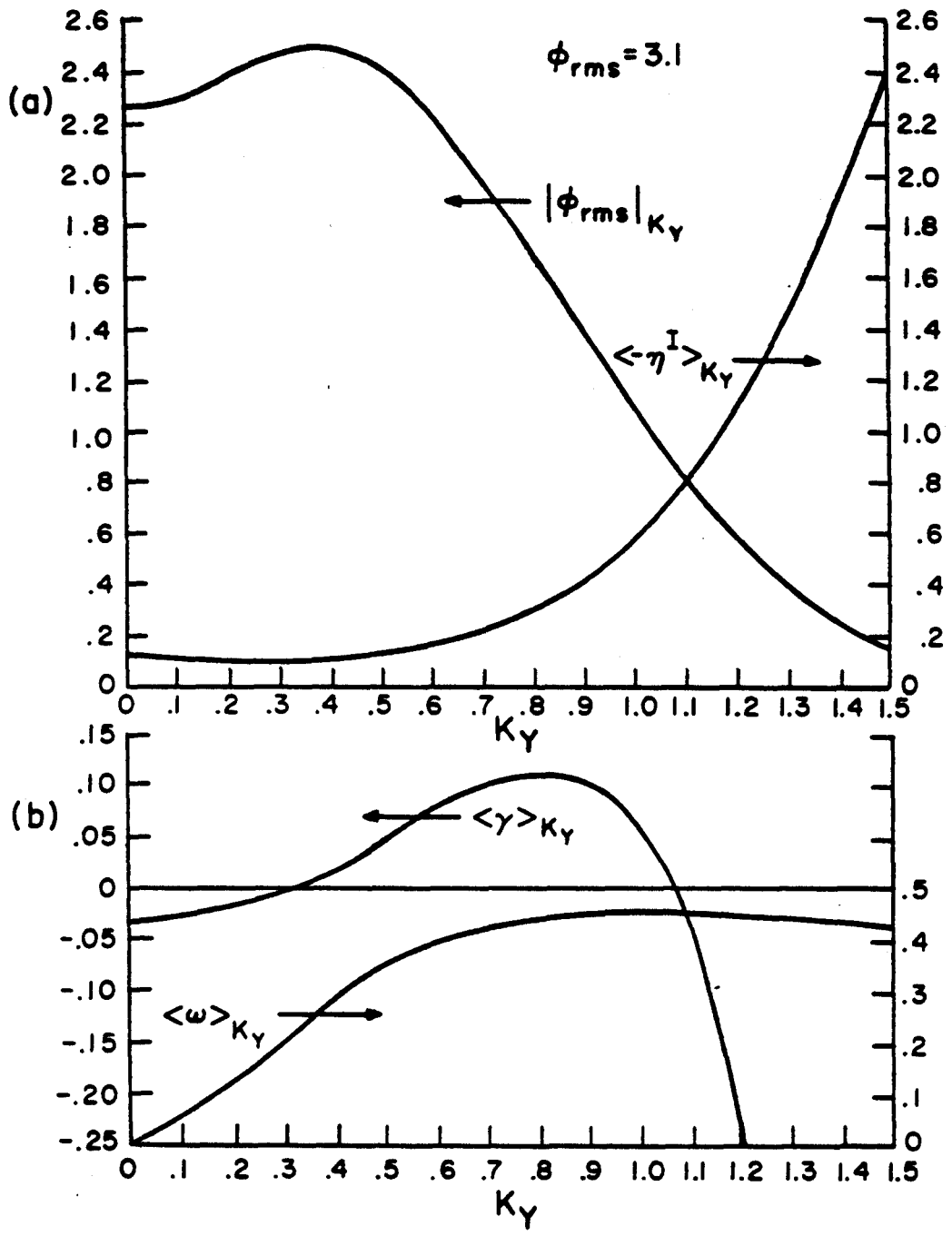

Figure 4: Spectrum results for the self-consistent drift wave problem are presented in terms of k_x-averaged quantities. (a) Root mean square potential, $|\phi_{rms}|_{k_y}$, and frequency width, $\langle -\eta^I \rangle_{k_y}$. (b) Growth rate, $\langle \gamma \rangle_{k_y}$, and frequency, $\langle \omega \rangle_{k_y}$.

IV. Summary and Conclusions

A derivation of the renormalized mode coupling spectrum equations for drift wave turbulence has been presented. The failure of a weak turbulence formulation of the spectrum equations for a system with negative dissipation was demonstrated. This failure has been shown to be directly related to the linear instability of the triplet correlation function. The nonlinear feedback effect from higher order correlations on the propagation of the triplet correlation was obtained by utilizing a renormalized theory for the spectrum equivalent to the DIA[11].

An approximate solution of the spectrum equations has been obtained first for a model dissipation proposed and numerically solved by Waltz[3], and second for the electron dissipation in the NSA[16]. The model dissipation problem was used as a check for the approximate analytic moment method. This moment method determined the first order solutions of the nonlinear integral spectrum equations, in terms of a trial function dependent on first order parameters, which correspond to physically relevant parameters of the true solution. The comparison between Waltz's numerical solution of the spectrum equations and our approximate analytic solution, indicated an excellent agreement both quantitatively and qualitatively. Using the analytic moment method, the root mean square potential in dimensionless normalized units was found to be $\phi_{rms} = 1.6$. This result is almost identical to the quoted numerical solution for the necessary set of 30×30 modes. This model dissipation problem has led to a narrow frequency spectral width, where the average frequency width was found to be $\langle -n^I \rangle \approx .02\Omega_i(\rho_s/L_n)$, while the average frequency was $\langle \omega \rangle \approx .3\Omega_i(\rho_s/L_n)$. The approximate analytic moment method solution of the self-consistent drift wave spectrum problem, with the electron dissipation in the NSA, was found to be in rough agreement with experimental observations in tokamaks[6]. The root mean square potential and the radial diffusion coefficient were found to be $e\phi_{rms}/T_e = 3.1(\rho_s/L_n)$ and $\overline{D} = 1.8\Omega_i(\rho_s/L_n)\rho_s^2$, respectively, which are on the order of experimental values. The frequency spectral width, which has been calculated using the electron dissipation in the NSA, was shown to be broad, which is also consistent with experiment. The average frequency width was approximately $\langle -n^I \rangle \approx .3\Omega_i(\rho_s/L_n)$, while the average frequency was also $\langle \omega \rangle \approx .3\Omega_i(\rho_s/L_n)$.

A comparison has been presented between the model dissipation of Waltz and the electron dissipation in the NSA, regarding the differences in the resulting spectral widths. The wave number dependent growth rate for the model problem exhibited a very narrow band of small positive growth rates. Almost any two unstable linear eigenmodes produced

a stable nonlinear mode such that the triplet growth rate was negative. Since there were very few unstable triplets to drive up the nonlinear frequency spectrum the resultant frequency spectral widths were small for the model dissipation problem. In contrast, the frequency and wave number dependent growth rate, derived from the electron dissipation in the NSA, indicated that for this model all linear eigenmodes, $\omega = \omega_{\mathbf{k}}$, were unstable. Any two linear eigenmodes, with positive y components of wave number, produced an unstable nonlinear mode, $\omega \neq \omega_{\mathbf{k}}$. These unstable triplets were driven up and populated the noneigenmode frequency spectrum. The resultant spectral widths, for the electron dissipation in the NSA, were then found to be large.

The approximate analytic moment method has been demonstrated as being a useful method for approximating the solution of the nonlinear integral equations describing the drift wave spectrum. The important feature of the approximate analytic moment method is that it can be used to extract the fundamental parameters (total integrated amplitude, wave number width, and frequency width), without actually solving the integral equations. The approximate solution is obtained from trivial numerical calculations, as compared with the lengthy computations needed to attack the spectrum solution numerically. This solution technique can then be used to readily analyze the spectrum resulting from other models of dissipation.

Acknowledgements

The authors would like to thank Dr. R.E. Waltz for numerically solving the model problem spectrum which allowed a check of the analytic moment method.

This research was supported in part by the U. S. Department of Energy Grant No. 91372.

Appendix A. Normalization Correction Factor in Model Problem

This section is in reference to the model problem where a different normalization of the spectrum is used due to the discretized approach in the numerical solution of Waltz. The numerical computation uses a discrete number of modes where the numerical root mean square potential spectrum, $|\phi_{rms}|_{i,j} \equiv S_{i,j}^{num1/2}$, utilizes indices i, j, which correspond to the k_x, k_y wave numbers of our root means square potential, $|\phi_{rms}|_{k_x,k_y}$. The correction factor needed for comparison purposes is obtained by noting that

$$\int dk_x dk_y S_{k_x,k_y} = \sum_{ij} S_{ij}^{num}, \tag{1}$$

and since the discreet interval wave number width used in the numerical study was .2, the spectrum correction factor is

$$(.2)^2 S_{k_x,k_y} = S_{ij}^{num}, \tag{2}$$

and the potential correction factor is

$$.2\,|\phi_{rms}|_{k_x k_y} = |\phi_{rms}^{num}|_{i,j} \tag{3}$$

The k_x average potential, $|\phi_{rms}|_{k_y}$, also has a different normalization than the discreet average potential, $|\phi_{rms}^{num}|_j$. The correction factor is obtained by noting that

$$.2 S_{k_y} = S_j^{num} \equiv \sum_i S_{ij}^{num}, \tag{4}$$

and using the definitions $|\phi_{rms}|_{k_y} = S_{k_y}^{1/2}$ and $|\phi_{rms}^{num}|_{k_y} = (S_j^{num})^{1/2}$, so that the following relation is obtained,

$$(.2)^{1/2}\,|\phi_{rms}|_{k_y} = |\phi_{rms}^{num}|_{k_y}\,. \tag{5}$$

Appendix B: Evaluation of T, Eq. (188)

The T parameter is found from Eq. (155),

$$T = 2.8\Omega_i \frac{\rho_s}{L_n}\left[\frac{3}{\overline{D}(\overline{k}'_{\|}v_e)^2}\right]^{1/3}, \tag{1}$$

and Eq. (156), where the inverse Fourier transform in k_x of the spectrum, $S_{k_y}(x)$, is needed. The Maxwellian velocity averaged diffusion coefficient, $\overline{D}$, is

$$\overline{D} = \int dv_{\|}\frac{1}{\sqrt{\pi}v_e}e^{-\left(\frac{v_{\|}}{v_e}\right)^2}\int dk_y \frac{\pi R}{|v_{\|}|}\left(\frac{ck_y}{B}\right)^2 S_{k_y}(x)\ \Big|_{x=\frac{L_s\overline{\omega}}{k_y v_{\|}}}, \tag{2}$$

where $\overline{\omega} = (\Omega_i/L_n)\rho_s\Delta k$, $\overline{k}'_{\|} = \Delta k/L_s$. Using the spectral ansatz, Eq. (163), $S_{k_y}(x)$, is calculated as follows,

$$\begin{aligned} S_{k_y}(x) \equiv \int_{-\infty}^{\infty} dk_x e^{ik_x x} S_{k_x,k_y} &= \int_{-\infty}^{\infty} dk_x e^{ik_x x}\frac{E}{\pi\Delta k^2}\left(\frac{k}{\Delta k}\right)^2 e^{-\left(\frac{k}{\Delta k}\right)^2} \\ &= \frac{1}{\sqrt{\pi}\Delta k}\int_{-\infty}^{\infty} dk_x e^{ik_x x}\left(\frac{k_x}{\Delta k}\right)^2 e^{-\left(\frac{k_x}{\Delta k}\right)^2}\frac{E}{\sqrt{\pi}\Delta k}e^{-\left(\frac{k_y}{\Delta k}\right)^2} \\ &+ \frac{1}{\sqrt{\pi}\Delta k}\int_{-\infty}^{\infty} dk_x e^{ik_x x}e^{-\left(\frac{k_x}{\Delta k}\right)^2}\frac{E}{\sqrt{\pi}\Delta k}\left(\frac{k_y}{\Delta k}\right)^2 e^{-\left(\frac{k_y}{\Delta k}\right)^2}. \end{aligned} \tag{3}$$

The second integral in Eq. (3) is

$$\begin{aligned} \frac{1}{\sqrt{\pi}\Delta k}\int_{-\infty}^{\infty} dk_x e^{ik_x x}e^{-\left(\frac{k_x}{\Delta k}\right)^2} &= \frac{1}{\sqrt{\pi}}\int_{-\infty}^{\infty} dt e^{ix\Delta k t}e^{-t^2} \\ &= \frac{1}{\sqrt{\pi}}\int_{-\infty}^{\infty} dt e^{-(t-i\frac{x\Delta k}{2})^2}e^{-\left(\frac{x\Delta k}{2}\right)^2} = e^{-\left(\frac{x\Delta k}{2}\right)^2}, \end{aligned} \tag{4}$$

where the contour integral was deformed from the line $[-\infty - i(x\Delta k/2), +\infty - i(x\Delta k/2)]$ to the line $[-\infty, \infty]$. The first integral in Eq. (3) is

$$\frac{1}{\sqrt{\pi}\Delta k}\int_{-\infty}^{\infty} dk_x e^{ik_x x}\left(\frac{k_x}{\Delta k}\right)^2 e^{-\left(\frac{k_x}{\Delta k}\right)^2} = \frac{1}{\sqrt{\pi}}\int_{-\infty}^{\infty} dt t^2 e^{-(t^2 - ix\Delta k t)}$$
$$= \frac{1}{\sqrt{\pi}}\int_{-\infty}^{\infty} dt t^2 e^{-\left(t - i\frac{x\Delta k}{2}\right)^2} e^{-\left(\frac{x\Delta k}{2}\right)^2},$$

and using the change of variables $z = t - i\frac{x\Delta k}{2}$,

$$= e^{-\left(\frac{x\Delta k}{2}\right)^2}\frac{1}{\sqrt{\pi}}\int_c dz\left[z^2 + ix\Delta k z - \left(\frac{x\Delta k}{2}\right)^2\right]e^{-z^2},$$

where the contour $[-\infty - i(x\Delta k/2), +\infty - i(x\Delta k/2)]$ can be deformed to $[-\infty, \infty]$,

$$= e^{-\left(\frac{x\Delta k}{2}\right)^2}\frac{1}{\sqrt{\pi}}\int_{-\infty}^{\infty} dt\left[t^2 + ix\Delta k t - \left(\frac{x\Delta k}{2}\right)^2\right]e^{-t^2}$$
$$= \frac{1}{2}\left[1 - \frac{(x\Delta k)^2}{2}\right]e^{-\frac{(x\Delta k)^2}{4}}. \qquad (5)$$

The inverse Fourier transform in k_x of the spectral ansatz is, using Eqs. (4) and (5) in Eq. (3),

$$S_{k_y}(x) = e^{-\frac{(x\Delta k)^2}{4}}\frac{E}{\sqrt{\pi}\Delta k}\left(\frac{k_y}{\Delta k}\right)^2 e^{-\left(\frac{k_y}{\Delta k}\right)^2} + \frac{1}{2}\left[1 - \frac{(x\Delta k)^2}{2}\right]e^{-\frac{(x\Delta k)^2}{4}}\frac{E}{\sqrt{\pi}\Delta k}e^{-\left(\frac{k_y}{\Delta k}\right)^2}. \qquad (6)$$

The average diffusion coefficient, Eq. (2), is then

$$\overline{D} = \int dv_{\parallel}\frac{1}{\sqrt{\pi}v_e}\frac{1}{|v_{\parallel}|}e^{-\left(\frac{v_{\parallel}}{v_e}\right)^2}\pi R\left(\frac{c}{B}\right)^2 E\int dk_y k_y^2$$
$$\cdot\left[e^{-\left(\frac{L_s\overline{\omega}\Delta k}{2k_y v_{\parallel}}\right)^2}\frac{1}{\sqrt{\pi}\Delta k}\left(\frac{k_y}{\Delta k}\right)^2 e^{-\left(\frac{k_y}{\Delta k}\right)^2} + \frac{1}{2}\left[1 - 2\left(\frac{L_s\omega\Delta k}{k_y v_{\parallel}}\right)^2\right]e^{-\left(\frac{L_s\overline{\omega}\Delta k}{2k_y v_{\parallel}}\right)^2}\frac{1}{\sqrt{\pi}\Delta k}e^{-\left(\frac{k_y}{\Delta k}\right)^2}\right]$$
$$\approx \int dv_{\parallel}\frac{1}{\sqrt{\pi}v_e}\frac{1}{|v_{\parallel}|}e^{-\left(\frac{v_{\parallel}}{v_e}\right)^2}\pi R\left(\frac{c}{B}\right)^2 E\left[\frac{3}{4} + \frac{1}{4}\right]e^{-\left(\frac{L_s\overline{\omega}}{2v_{\parallel}}\right)^2},$$

since $M \equiv \overline{\omega}L_s/2v_e \ll 1$, so that the result is

$$\overline{D} = \frac{\pi R}{v_e}\left(\frac{c}{B}\right)^2 I \Delta k^2 E, \tag{7}$$

where

$$I \equiv \frac{2}{\sqrt{\pi}} \int_0^\infty dx \frac{1}{x} e^{-\left(\frac{M^2}{x^2}+x^2\right)}. \tag{8}$$

The integral I can be approximated as follows,

$$I = \frac{1}{\sqrt{\pi}} \int_0^\infty dz \frac{1}{z} e^{-\left(\frac{M^2}{z}+z\right)},$$

where the change of variables $x^2 = z$ was made,

$$= \frac{1}{\sqrt{\pi}} \int_{-\infty}^\infty dt e^{-2M\cosh t} = \frac{2}{\sqrt{\pi}} \int_0^\infty dt e^{-2M\cosh t},$$

where the additional change of variables $z = Me^t$ was made, so that the result is

$$I = \frac{2}{\sqrt{\pi}} K_0(2M), \tag{9}$$

where

$$K_0(x) = \int_0^\infty dt e^{-x\cosh t} \tag{10}$$

is the modified Bessel function. The Bessel function K_0 can be approximated as

$$K_0(x) \approx -\left[\ln\left(\frac{x}{2}\right) + \gamma\right],$$

where γ is the Euler constant which is $\gamma \approx .577$, so that Eq. (9) is approximately given by

$$I \approx -\frac{2}{\sqrt{\pi}}[.577 + \ln(M)]. \tag{11}$$

The expression for T, Eq. (1), can be written in terms of familiar quantities by using the transformation to dimensionless variables,

$$\Delta k \rho_s \to \Delta k \quad \text{and} \quad \frac{\left(\frac{e}{T_e}\right)^2}{\left(\frac{\rho_s}{L_n}\right)^2} E \to E,$$

as follows,

$$T = 2.8\left[\frac{3\Omega_i^2\rho_s^3}{L_n^3\overline{Dk}_{||}'^2 v_e^2}\right]^{1/3}$$

$$= 2.8\left[\left(\frac{3\Omega_i^3\rho_s^3 v_e B^2 L_s^2}{L_n^3\pi R c^2 I v_e^2}\right)\cdot\left(\frac{\rho_s^4 e^2 L_n^2}{T_e^2\rho_s^2}\right)\right]^{1/3}\frac{1}{(\Delta k^4 E)^{1/3}}$$

$$= 2.8\left[\frac{3\Omega_i^5\rho_s^5 L_s^2}{\pi I v_e c_s^4 L_n R}\right]^{1/3}\frac{1}{(\Delta k^4 E)^{1/3}} = 2.8\left[\frac{3c_s L_s^2}{\pi I v_e L_n R}\right]^{1/3}\frac{1}{(\Delta k^4 E)^{1/3}},$$

or

$$T = 2.8\left[\frac{3}{\pi I}\left(\frac{L_s}{L_n}\right)\left(\frac{L_s}{R}\right)\sqrt{\frac{m_e}{2m_i}}\right]^{1/3}\frac{1}{(\Delta k^4 E)^{1/3}}. \tag{12}$$

In a similar manner the diffusion coefficient can be obtained by using Eq. (7),

$$\overline{D} = \left[\frac{\pi}{\sqrt{2}}\left(\frac{m_e}{m_i}\right)^{1/2}\left(\frac{R}{L_s}\right)\left(\frac{L_s}{L_n}\right)(I\Delta k^2 E)\right]\Omega_i\frac{\rho_s}{L_n}\rho_s^2. \tag{13}$$

The value of T, Eq. (12), can be approximated by using

$$M = \frac{\overline{\omega}L_s}{2v_e} = \frac{\Omega_i L_s\rho_s}{2v_e L_n}\Delta k = \frac{c_s L_s}{2v_e L_n}\Delta k = \frac{1}{2}\sqrt{\frac{m_e}{2m_i}}\left(\frac{L_s}{L_n}\right)\Delta k, \tag{14}$$

where

$$\frac{m_e}{m_i} \approx \frac{1}{1836}, \quad \frac{L_s}{L_n} \approx 16, \quad \frac{L_s}{R} \approx 3, \quad \Delta k \approx .6, \tag{15}$$

so that

$$M \approx .08 \quad \text{and} \quad I \approx 2, \tag{16}$$

and finally the dissipation parameter is

$$T \approx \frac{2}{(\Delta k^4 E)^{1/3}}. \tag{17}$$

References

1. A. Hasegawa and K. Mima, Phys. Rev. Lett. **39**, 205(1977).

2. R.H. Kraichnan, J. Fluid Mech. **5**, 497(1959).

3. R.E. Waltz, Phys. Fluids **26**, 169(1983).

4. S.P. Hirshman, and K. Molvig, Phys. Rev. Lett. **42**, 648(1979).

5. R.C. Davidson, *Methods in Nonlinear Plasma Theory* (Academic Press, New York, 1972), pp. 107-115.

6. E. Mazzucato, and A. Semet, Bull. Am. Phys. Soc. **26** 6P4, 981(1981).

7. R.C. Davidson, *Methods in Nonlinear Plasma Theory* (Academic Press, New York, 1972), pp. 243-273.

   B.B. Kadomtsev, *Plasma Turbulence* (Academic Press, New York, 1965), pp. 31-34.

8. R.C. Davidson, *Methods in Nonlinear Plasma Theory* (Academic Press, New York, 1972), p. 135.

9. D.C. Leslie, *Developments in the Theory of Turbulence* (Clarendon Press, Oxford, 1973), pp. 47-59.

10. D.C. Leslie, *Developments in the Theory of Turbulence* (Clarendon Press, Oxford, 1973), pp. 72-81.

    H.W. Wild, Ann. Phys. **14**, 143(1961).

11. B.B. Kadomtsev, *Plasma Turbulence* (Academic Press, New York, 1965), pp. 49-53.

12. E. Gerjuoy, A.R.P. Rau and L. Spruch, Reviews of Modern Physics **55**, 725(1983).

13. R.H. Kraichnan, Phys. Fluids **7**, 1164(1964).

14. S.F. Edwards, J. Fluid Mech. **18** 239(1964).

15. R.H. Kraichnan, J. Fluid Mech. **47** 513(1971).

16. C.O. Beasley, K. Molvig and W.I. van Rij, Phys. Fluids **26**, 678(1983).

17. P.W. Terry, and W. Horton, Phys. Fluids **26**, 106(1983).

18. T.W. Seyler, Y. Salu, D. Montgomery and G. Knorr, Phys. Fluids **18** 803(1975).

R.H. Kraichnan, and D. Montgomery, Rep. Progr. Phys. **43**, 547(1980)